SPRAY COMBUSTION OF RESIDUAL FUEL OIL: PARTICULATE AND GASEOUS EMISSION IN A TWO STAGE SYSTEM - D. Rodriguez Polanco.

ERRATA

Page	line	reads	should read
1	2	uses	use
20	14	sylphur	sulphur
41	16	oins	ions
49	18	(2000°K)	(>2000°K)
60	23	aprts	parts
73	11	chemiluminescen	chemiluminescent
77	9	than separate	then separate
78	15	higroscopic	hygroscopic
85	Fig 4.8	3.37, 3.50....	3.50, 3.37....
86	Fig 4.9	3.37, 3.48....	3.48, 3.37....
96	diagram	$\beta_4 CH_4$	$\beta_6 CH_4$
103	5	Net molar...	Wet molar...
108	eq(5.33)	$(A_{VO_2})^{-\frac{1}{2}}$	$(A_{O_2})^{-\frac{1}{2}}$
108	last equation	$A_{VO_2} = \ldots$	$A_{O_2} = \ldots$
116	4	runs discusses...	runs discussed...
122	9	Kenetic	Kinetic
122	16	For $\phi = 1.0$	For $\phi_1 = 1.0$
127	16	expiric equation	empiric equation
127	21	equartion	equation
133	1	oxides on...	oxides in...
151	1	1, 2 and 3	5.6, 5.7 and 5.8
156	S-13	$\phi_2 = 2.00$	$\phi_2 = 1.00$
168	1	for hoth air...	for both air...
169	13	minimution in...	disminution in...
176	4	summarozed	summarized

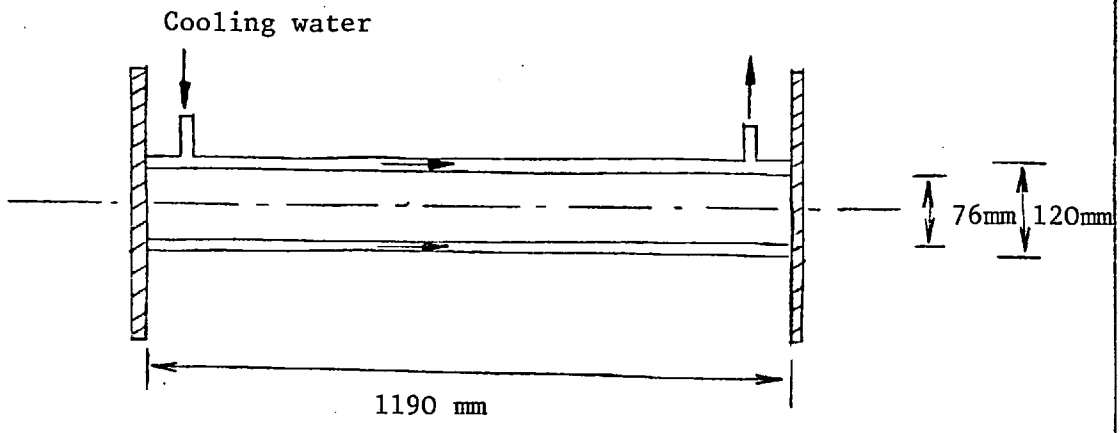

Diagram of Interstage cooling section

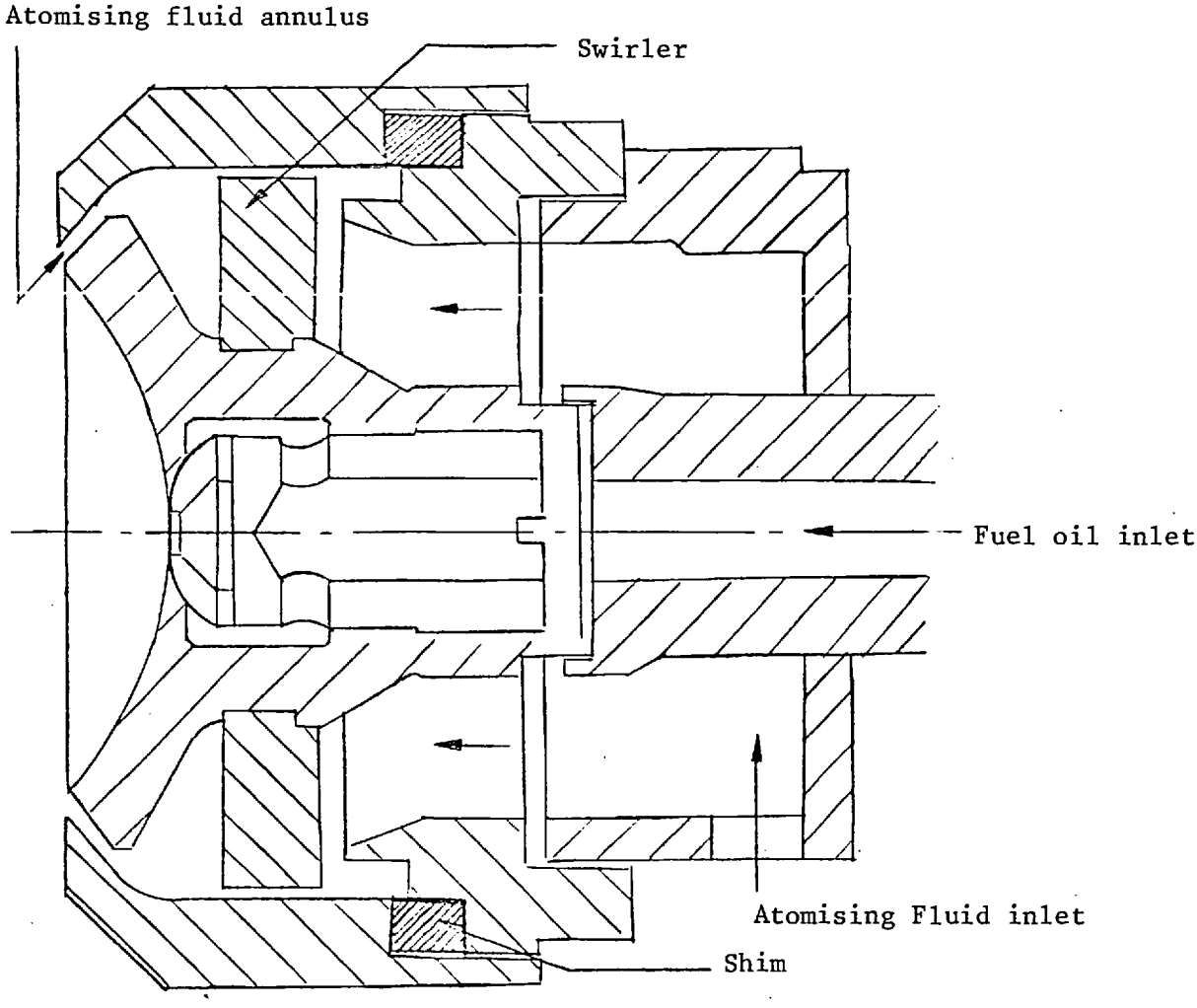

Sectional view of the Twin fluid atomiser

SPRAY COMBUSTION OF RESIDUAL FUEL-OIL :

PARTICULATE AND GASEOUS EMISSION IN A TWO STAGE SYSTEM

A thesis submitted for the

Doctor of Philosophy

University of London

by

DOMINGO J. RODRIGUEZ POLANCO, Ing. Quimico (Venezuela)

Combustion Engineering Laboratory,
Department of Chemical Engineering and Chemical Technology,
Imperial College of Science and Technology
London S.W.7.

November, 1975.

ABSTRACT

The most widely recognised difficulties in combustion processes that uses residual fuel oil are deposition and corrosion (high and low temperature) of heat receiving surfaces as well as the emission of the gaseous pollutants oxides of sulphur and nitrogen.

Stoichiometric two-stage combustion constitutes a means of lowering temperature and oxygen levels in a combustion process. A reduction in peak temperatures combined with a lack of excess oxygen leads to avoiding formation of highly reactive V_2O_5 and SO_3 as well as kinetic limitation of thermal NO_x.

This work is concerned with the stoichiometric spray combustion of residual fuel oil in a two-stage combustion pilot plant. An investigation of the history of the compounds comprising the main impurities in the fuel during two-stage combustion was undertaken. It also includes the major gaseous compounds emission particularly the pollutants NO_x and SO_x as well as the particulates ones.

In the first stage chamber (or gasifier) the fuel is injected by a twin fluid atomiser using air or steam as atomising medium. Gasification was obtained working with first stage equivalence ratios up to 1.55 and the products, after interstage heat removal are passed to the second stage combustion chamber (or converter) where air is added to complete over all stoichiometric conditions.

It has been proved that steam atomised stoichiometric two stage combustion can provide an effective method of reducing NO_x and particulate emissions as well as avoiding formation of deposit forming agent V_2O_5 and corrosive complex 1:1:5 sodium vanadyl vanadate ($Na_2O.V_2O_4.5V_2O_5$).

Particulate emission reached 0.4% of fuel input which constitutes a reduction of 60% compared with single stage operation. NO_x emission was reduced in 92% whereas SO_2 levels were found practically unaffected by staged combustion.

Major non carbonaceous compounds found in the solid products wet-collected were V_2O_4, Na_2SO_4, $NiSO_4$ and NiS. This finding appears unaffected by the atomising mode.

LIST OF CONTENTS

LIST OF FIGURES

CHAPTER 2. PAGE

CHAPTER 3

CHAPTER 4

CHAPTER 5

LIST OF TABLES

ACKNOWLEDGEMENTS

The author wishes to thank Dr. Paul Eisenklam who supervised the work for introducing him to the study of residual fuel oil combustion, for his advice and continuous encouragement throughout the duration of the research and also for his constructive criticisms to the draft thesis.

The author also wishes to acknowledge Dr. D.A. Pantony and Mr. P.L. Bird, Director and Manager of the Analytical Services Laboratory for their great contribution on the solid samples analysis.

The practical assistance in Instrument Techniques given by Dr. F. Carleton (Analytical Lab.) and the assistance with the X-ray diffraction analysis by Dr. G.S. Parry are appreciated.

The author also wishes to thank his colleagues in the laboratory, C. Davies and N. Munz, without whom this work would have not been made possible.

To the memory of my parents.

NOMENCLATURE

SYMBOL	SIGNIFICANCE	UNITS
A	Air mass flow rate	g/s
Ai	Activity of species i	dimensionless
C	Number of components of a reacting mixture	
Cpi	Constant pressure heat capacity of species i	KJ/g.mol ^{o}K
F	Fuel mass flow rate	g/s
G	Total Gibbs free energy	KJ
$\overline{G}_i$	Gibbs free energy of component i	KJ/g mol
$\underline{G}_i^o$	Gibbs free energy of component i at standard state	KJ/g mol
$\Delta\underline{G}^o$	Gibbs free energy of reaction	KJ/g mol
H	Total enthalpy	KJ
ΔH_{fi}^o	Standard Enthalpy of formation of species i	KJ/g mol
I	Radiation Intensity	einsteins/cm^3s
Ja_i	Activity ratio for reaction i	dimensionless
$(Ja)_{in}$	Activity ratio based on inlet conditions	dimensionless
Ka	Thermodynamic equilibrium constant based on activities	dimensionless
Kp	Equilibrium constant based on partial pressures	dimensionless
K_{eq}	Equilibrium constant based on concentrations	dimensionless
Ms	Soot formation	dimensionless
Ni	Number of moles of component i	g moles
P	Total pressure	bar

p_A^o	Partial pressure of component A	bar
R	Universal gas constant	8.314 KJ/Kmol ^oK
S	Solid loading	dimensionless
T	Absolute temperature	^oK
d	interplanar spacing	A^o
fi	fugacity of component i in a mixture	dimensionless
h	Planck's constant	6.626×10^{-34} Js
hi,T	specific enthalpy of component i at temperature T	KJ/g mol
r_{af}	atomising air to fuel ratio	dimensionless
r_{sf}	atomising steam to fuel ratio	dimensionless
α	number of moles of O_2 in combustion air per atom-mol of carbon burnt.	
α_i	stoichiometric coefficient of species i	
α_{ij}	stoichiometric coefficient of the ith species in the jth reaction	
θ	angle between the incident X-ray beam and the atomic planes	
λ	wavelength of radiation	A^o (= 10^{-8} m)
ϕ	Equivalence ratio	dimensionless
ϕ_1	First stage equivalence ratio	dimensionless
ϕ_2	Second stage equivalence ratio	dimensionless
X_i	Yield of the i th reaction	dimensionless

CHAPTER 1

INTRODUCTION

The bottom residual product of refined crude oil, commonly named residual fuel oil although it contains appreciable amounts of non-combustible substances referred as impurities is commercially a major source of thermal energy. These impurities are notable amounts of vanadium, iron, sodium, nickel, sulphur, calcium, chlorine and silicon which are associated to complex organic and inorganic compounds. It is understood that vanadium, nickel, sodium and sulphur are the major impurities since they are responsible for many problems in central station power plants. The most serious of these difficulties are corrosion (high and low temperature corrosion) of heat receiving surfaces as well as the unpredictable decrease in heat transfer caused by deposits and the emission of gaseous compounds referred to as pollutants (NO_x and SO_x).

A well established approach to avoid high temperature corrosion is the use of controlled combustion, which involves aerodynamic design of the combustion chamber and carefulcontrol of fuel and air. Stoichiometric two-stage combustion is one of those controlled combustion systems and constitutes a means of lowering temperature and oxygen levels in the system. This technique involves firing all the fuel in the first stage with substoichiometric quantities of combustion air and injecting the remainder of the air in the second stage after interstage heat removal. Reduction in peak temperatures combined with lack of excess oxygen in the system leads to avoiding formation of highly reactive V_2O_5 and SO_3, as well as kinetic limitation of gaseous pollutant NO. Nevertheless, in

practical systems the distriburion of the main impurities vanadium, nickel, sodium, and sulphur in the particulate emission as well as the gaseous pollutants NO_x and SO_x levels have not yet been assessed.

In the present work a qualitative and quantitative investigation was carried out of the history of the compounds comprising the main impurities in the fuel during two stage combustion of a residual fuel-oil. It includes the major gaseous compounds and the emission of pollutants NO_x and SO_x as well as the particulate ones. The experimental work was based upon two atomising modes, namely steam and air. The work has been conveniently divided into 8 chapters: The Introduction, The Literature Survey, The Equipment and Experimental Programme, Measurement Techniques, Theoretical Results, The Experimental Results and Discussion and finally the Conclusions. In the Literature Survey an up-to-date review is presented on the open literature of spray combustion of residual fuel oil. It comprises: the impurities present in fuel oil, the gaseous emission particularly NO_x and SO_x, the particulate emission and the effect of the impurities on combustion equipment. The mechanism of formation of SO_x and NO_x have also been included. In chapter 3 the two-stage combustion pilot plant is described as well as the experimental programme. Then follows the measurement techniques that enable us to carry out the experimental investigation. In the next chapter, theoretical results on the particular operating conditions were obtained, in this way a multi reaction equilibrium model involving major gaseous compounds as well as NO_x and SO_x was developed. These results were used to determine the operational regions where V_2O_5 was likely to be formed. Calculations were also performed on second stage stream temperature as a function of interstage heat removal. The experimental results are presented in Chapter 6 and discussed in relation to the literature survey and the theoretical results.

CHAPTER 2

LITERATURE SURVEY

As a part of the investigation on spray combustion of residual fuel oil an up-to-date literature survey has been carried out. It comprises the main following topics: impurities present in residual fuel oil, the gaseous emission particularly the pollutants NO_x and SO_x, the particulate emission and the effect of the impurities present in fuel oil on combustion equipment. The mechanism of formation of SO_x and NO_x have also been included.

2.1 Occurrence of Inorganic Matter in Fuel-oil.

All fossil fuels contain appreciable amounts of non-combustible substances. In fuel oil these major impurities are associated to complex organic compounds originating in the life forms that become petroleum, plus minor inorganic material unavoidable included during transportation and refining. However, fuel oil contains traces of a considerable number of elements. Notable amounts of Vanadium, Iron, Sodium, Nickel, Sulphur, Calcium, Chlorine and Silicon are present in the bottom residual product (commonly named residual fuel oil) of refining crude oil.

The relative amounts of the impurities varies widely with the type of fule oil, although it is understood that Sulphur, Vanadium, Nickel and Sodium are the major impurities. Vanadium is present in crude oils as a thermally stable porphirin which is not removed during refining so that all Vanadium present initially in the crude appears in the residual fuel oil.

In Figure 2.1 the Vanadium content of crudes from some important producing regions of the world is graphed (4).

Extensive analysis on the nature of Vanadium in crudes has been carried out (5, 6, 7, 8). Dunning et al (6) found definitive evidence of Vanadium and Nickel porphyrin complexes. Beach and Shewmaker (7)

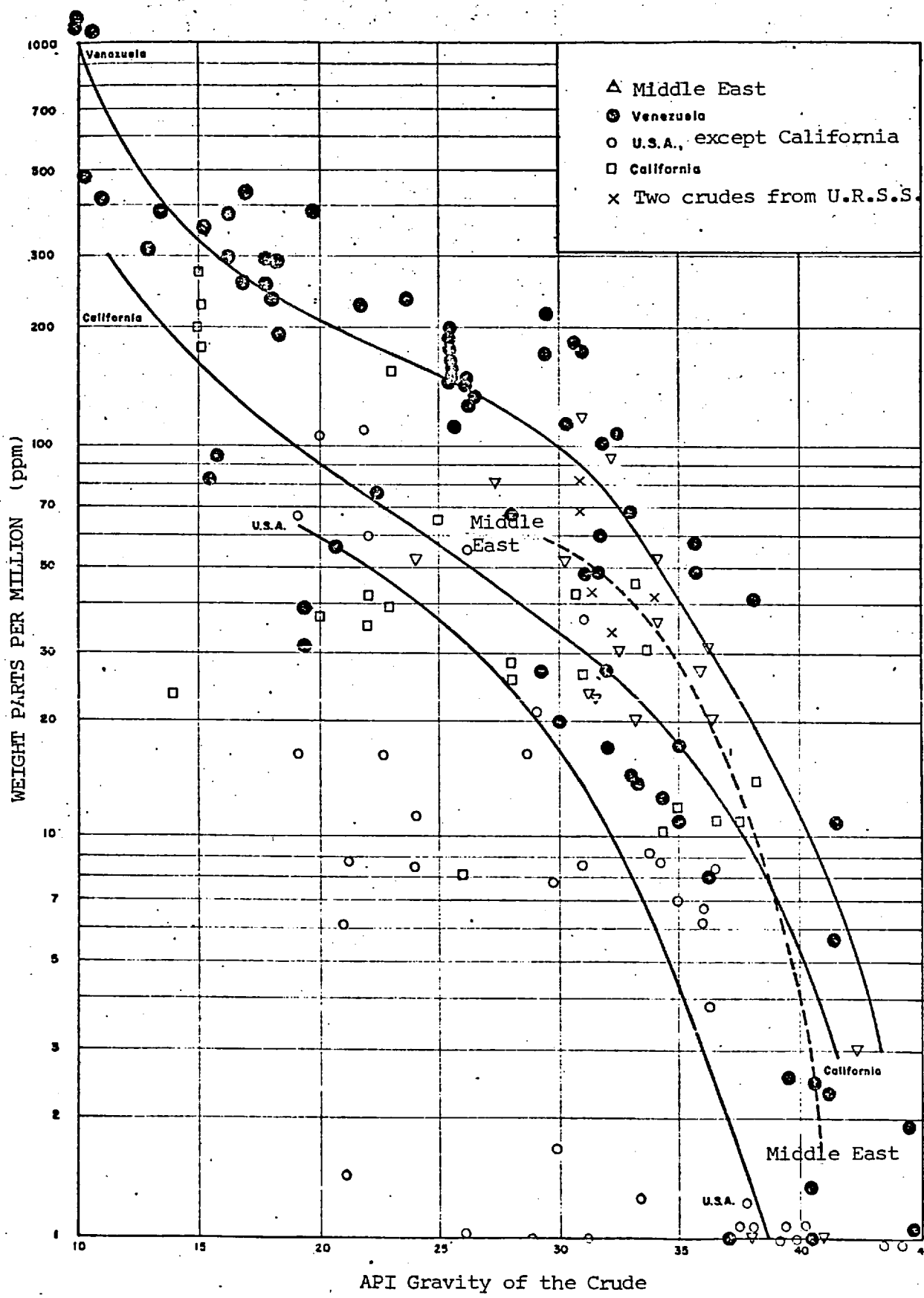

FIG. 2.1 VANADIUM CONTENT OF SOME IMPORTANT PRODUCING REGIONS. Ref(4)

TABLE 2.1 METALLIC CONTENT OF SOME VENEZUELAN CRUDES ref. (9, 10)

	MELONES I (LIGHT)	MELONES II (HEAVY)	MORICHAL I (LIGHT)	MORICHAL II (HEAVY)	BOSCAN
VANADIUM, ppm	197	342	176	388	1200
NICKEL, ppm	49	82	57	80	150
TITANIUM, ppm	-	-	-	-	50
IRON, ppm	3	4	1	4	60
SILICON, ppm	-	-	-	-	70
MAGNESIUM, ppm	-	-	-	-	4
ALUMINIUM, ppm	-	-	-	-	150
COPPER, ppm	.05	.05	-	0.4	3
CALCIUM, ppm	-	-	-	-	10
MOLYBDENUM, ppm	-	-	-	-	50
SODIUM, ppm	45	754	250	879	-
ZINC, ppm	1	1.3	3.4	42	-
GRAVITY ^{o}API	20.1	9.9	12.4	9.6	10.1
SULPHUR % Wt	2.10	3.32	2.12	4.13	5.5

concluded that Vanadium-porphyrin complexes in petroleum can be divided into two categories: all class I Vanadium probably exists in a group of monomeric porphyrins and all class II Vanadium compounds apparently of higher molecular weight probably porphyrins whose side chains are several folded larger than the central molecule and are of polymeric nature. Wolski and Chapman (8) working with Boscan asphaltenes reported less than 10% of Vanadium found was in porphyrinic form.

Laboratory analysis results of the metal content of several Orinoco heavy oil (9) as well as Boscan crude is presented in Table 2.1 (10). These include two samples of Melones and Morichal crudes, one each of typical light and heavy crudes. The designation of a light crude here is a relative measure meaning only that it is lighter than the other crude. Boscan crude also of Venezuelan origin, represents a quite remarkable crude both in Sulphur and metallic content.

A typical feedstocks properties of a pilot plant for hydrodesulphurization of high metal content middle eastern residues is presented in table 2.2.

Sodium in residual fuel-oil is usually present in the form of simple inorganic salts such as sodium chloride (11).

2.2 Gaseous Emission from Combustion Systems

During combustion of residual fuel oil a wide variety of gaseous compounds are expected to be found in the flue gases, these include major amounts of CO_2, H_2O, CO, SO_2, CH_4, NO and considerable traces of unburnt Hydrocarbons. In the present work stress is laid particularly on formation and emission of SO_x and NO_x considered to be gaseous pollutants, and finally on measurement methods of the major gaseous combustion products.

2.2.1 SO_x Formation and Emission. Sulphur in the form of organic and inorganic compounds commonly accounts for several percent by weight of

TABLE 2.2 METALLIC CONTENT OF SOME MIDDLE-EAST RESIDUES ref.(77)

	KUWAIT LONG RESIDUE	QATAR MARINE LONG RESIDUE	IRANIAN HEAVY LONG RESIDUE	ARABIAN HEAVY LONG RESIDUE
VANADIUM, ppm	53	26	145	88
NICKEL, ppm	12.7	9.7	33.6	26.9
SODIUM, ppm	7.7	7.4	7.2	25
SULPHUR, % W	4.21	2.77	2.73	4.31
SPECIFIC GRAVITY	.9336	.9027	.9254	.9514

the fuel burnt in power stations and other large industrial plants. Most common effects of its combustion are pollution by Sulphur oxides emitted and corrosion of plants by Sulphuric acid and alkali sulphates formed during combustion.

I. Principal Species in Final Products of Combustion. The predominant Sulphur containing product formed by the combustion of Sulphur compounds is undoubtedly sulphur dioxide (SO_2). Even when oxygen is largely in excess, sulphur trioxide (SO_3) is hardly found in amounts greater than a few percent of SO_2.

The equilibrium of the reaction:

$$SO_2\ (g) + \tfrac{1}{2}\ O_2\ (g) \rightleftharpoons SO_3\ (g) \quad \ldots\ldots\ldots\ldots\ldots\ldots \quad (2.1)$$

is well established and lies well to the right at ambient temperatures but in absence of a suitable catalyst the reaction is remarkably slow below 1100°C.

Although SO_3 concentrations are relatively small compared to that of SO_2, its presence has profound effects on fuel technology. In most circumstances SO_3 appears in combustion products at room temperatures as sulphuric acid.

II. The System $SO_2/O_2/SO_3$.

II.1 Thermodynamics. The equilibrium of the reaction

$$SO_2 + \tfrac{1}{2} O_2 \rightleftharpoons SO_3 \quad \ldots\ldots\ldots\ldots\ldots\ldots\ldots\ldots \quad (2.1)$$

has been extensively estudied (14,15).

The thermodynamic equilibrium constant Kp at atmospheric pressure in terms of the partial pressures of the reactants is given by:

$$Kp = \frac{P^o_{SO_3}}{P^o_{SO_2}} \times \frac{1}{(P^o_{O_2})^{\frac{1}{2}}} \quad \ldots\ldots\ldots\ldots\ldots\ldots\ldots\ldots \quad (2.2)$$

where $P^o_{SO_3}$, $P^o_{SO_2}$, and $P^o_{O_2}$ are the partial pressures of SO_3, SO_2 and O_2 respectively.

Its dependence on temperature has been correlated (15):

$$\text{Log}_e\, Kp = \frac{22600}{RT} - 10.68 \quad \ldots\ldots\ldots\ldots\ldots\ldots\ldots\ldots \quad (2.3)$$

where R is the perfect gas constant in cal/gr. mol ^oC

T Temperature in degrees Kelvin (^oK)

The Yield Y of the reaction 2.1 is

$$Y = \frac{SO_3}{SO_2 + SO_3} = \frac{Kp}{Kp + \frac{1}{(P_{O_2})^{\frac{1}{2}}}} \quad \ldots\ldots\ldots\ldots\ldots\ldots\ldots\ldots \quad (2.4)$$

The percentage of conversion of SO_2 to SO_3 plotted against temperature for a range of equilibrium oxygen concentrations is presented in Fig. 2.2.

II.2 Kinetics of the System. $SO_2/O_2/SO_3$. As it will be seen later (Section III.1) the most likely reaction to be the major source of sulphur trioxide in practical combustion systems is reaction 2.1. As shown in Fig. 2.2, the equilibrium compositions favour SO_2 at high temperatures and SO_3 at low temperatures. Hedley (17) showed that in flame gases the SO_3 concentration normally exceeds the level given by theoretical thermodynamic considerations, while in the cooled gases the SO_3 levels are below equilibrium. The explanation given (18) for SO_3 behaviour during its formation was based upon a mechanism by which SO_3 was formed by the

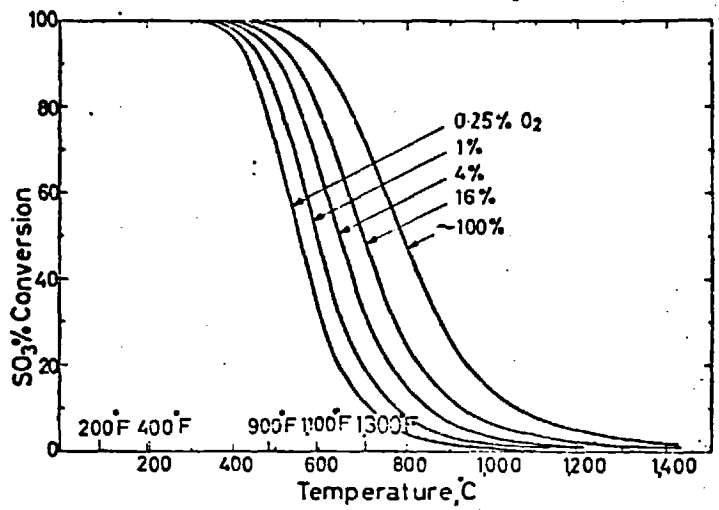

FIG. 2.2 RELATION BETWEEN SO_3 AND TEMPERATURE (0-1,400°C) FOR VARIOUS O_2 LEVELS. Ref. (16)

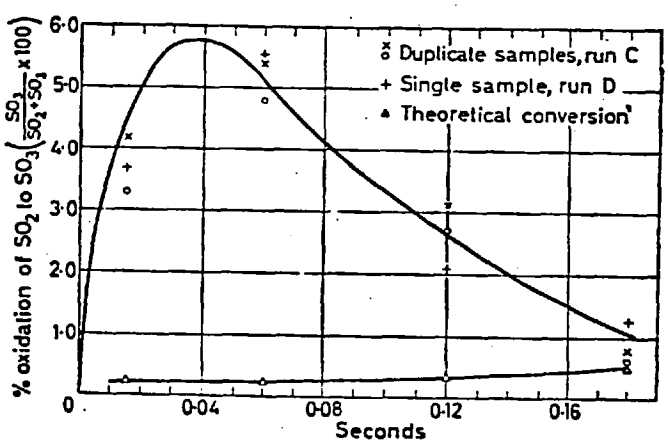

FIG. 2.3 VARIATION OF HOMOGENEOUS OXIDATION OF SO_2 TO SO_3 WITH TIME. ref(18)

collision between an SO_2 molecule and atomic oxygen. When an SO_2 molecule and an oxygen atom collide in absence of a third body M, it is possible that an activated molecule of SO_3 could be formed; the excess of energy being absorbed could be released by radiation or by later molecular collision, thus:

i) $SO_2 + O \longrightarrow SO_3^*$

ii) $SO_3^* \longrightarrow SO_3 + h\nu$

or $SO_3^* + M \longrightarrow SO_3 + M$

Fig 2.3 presents both experimental and theoretical concentrations of SO_3. It can be seen the actual yield is greater than the maximum theoretical yield calculated from thermodynamic considerations; however as the gases passed along the chamber the actual yield tended towards the theoretical.

As can be seen from experimental data published elsewhere (19) and plotted in Fig. 2.4, SO_3 is formed only when there is excess oxygen present. This would suggest that SO_2 does not combine with oxygen atoms produced in combustion mechanism chain reaction such as:

$CO + O_2 \longrightarrow CO_2 + O$

$CO + O_3 \longrightarrow CO_2 + 2O$

These oxygen atoms would react with the existing hydrocarbons in the flame. The SO_2 oxidation seemed to be carried out by the oxygen atoms originated from the pyrolisis of excess oxygen molecules. Since SO_2 is an easily oxidizable substance at flame conditions one could expect SO_2 to react rapidly with the oxygen atoms to form SO_3. The SO_3 thus formed is of transient nature and is well above equilibrium and therefore dissociation begins.

The theory was then represented (18) by the consecutive reaction theory:

$$SO_2 + O \xrightarrow{K_1} SO_3 \xrightarrow{K_2} SO_2 + \tfrac{1}{2} O_2$$

where K_1 and K_2 are the specific reaction rate constants for the individual reactions.

Assuming two consecutive first order reactions, the kinetics of SO_3 formation is given by:

$$[SO_3] = a\frac{K_1}{K_2 - K_1}\left[e^{-K_1 t} - e^{-K_2 t} \right] \qquad \ldots\ldots\ldots\ldots (2.5)$$

where $[SO_3]$: conc. of SO_3 after a time t.

a : initial concentration of atomic oxygen.

A very extensive review on sulphur containing compounds in combustion system has been published by Cullis and Mulcahy (20).

III. Effects of Sulphur in Practical Combustion Systems.

The presence of sulphur in the fossil fuel creates a wide variety of industrial problems, which can be classified into two categories:

A. The plant may corrode or the passage of the combustion gases fouled by solid or liquid sulphur compounds.

B. The atmosphere may be polluted by gaseous sulphur compounds emitted by combustion plants. These are known to be SO_2 and smaller amounts of SO_3.

The general facts concerning the occurrence of corrosion and deposit formation have been extensively investigated (21, 22, 23). Briefly can be said that metallic surfaces can be overlaid and attacked by two types of sulphur compounds: firstly the molten alkali sulphates deposited in association with other solid or molten materials from combustion products at temperature above 1000°C and secondly by aqueous sulphuric acid precipitated on cooler parts of the equipment where surfaces temperature can fall to about 130°C and lower. Vapour pressure data for sulphuric acid aqueous solutions with applications to flue gas dew point are comprehensively presented by Banchero and Verhoff (24).

Two mechanisms have been proposed to explain the formation of sulphur trioxide in large combustion systems (20):

A. Reaction of SO_2 with atomic oxygen in the high temperature flame zone.

B. The heterogenereous catalysis of the SO_2/SO_3 oxidation by molecular oxygen on steel surfaces at lower temperatures where the SO_3 equilibrium is favoured.

Oil fuels frequently contain vanadium compounds, which in many cases is found deposited as V_2O_5 is a well known catalyst for the oxidation of SO_2 to SO_3 and may be acting as a heterogeneous catalyst. This possibility as well as homogeneous catalysis at temperatures below 600°C via nitrogen dioxide has received some support from laboratory experiments (25, 26) but its importance under large system conditions has not yet been assessed. Ferric oxide, like vanadium pentoxide, is well known as a catalyst for oxidation of SO_2 and it has been suggested (19) that the oxide surface produced by exposing steel to combustion gases is capable of catalyzing oxidation of SO_2 in combustion gases at temperatures ranging 600 - 650°C. The other question is whether all SO_3 formed during the early flame stages can survive and reach the cooler parts of the plant. Hedley (18) found in flames with excess of oxygen, concentrations of SO_3 considerable in excess of those predicted from normal thermodynamic considerations (see Section II.2) involving molecular oxygen. However as the gases passed along the combustion chamber, the actual yield tended towards the theoretical. He concluded that the majority of sulphur trioxide found in boiler combustion gases originates in the combustion chamber and that relatively small amounts is produced by heterogeneous catalysis later in the system. Glaubitz (27) from a study of the effect of adding extra air to an oil-burning furnace at different positions between the burner mouth and a bank of superheater tubes, found that SO_3 detected

downstream was entirely formed within the flame region. Laxton (28) gives supporting views and has concluded that for the alleviation of low temperature corrosion and acid stack emission the most important measure is to reduce air excess to a minimum.

Production of SO_3 is largely determined by the first few percent (see Fig 2.4) excess of oxygen. The observation that oxygen entering the combustion gases downstream from the flame does not oxidize sulphur dioxide represents a strong evidence against heterogeneous catalysis at steel surfaces as a significant source of SO_3. The effects of sulphur content in the fuel on SO_3 emission operating with excess combustion air (28) is shown in Fig. 2.5. An increase in fuel sulphur brings about increase in SO_3 emitted from the system. This has been corroborated in Fig 2.6, where dew-point temperatures of the burnt gas with excess air were measured. The dew-point is related approximately linearly to the sulphur trioxide concentration in the range 40 - 120°C (27).

TABLE 2.3 NO_x EMISSION FROM VARIOUS TYPES OF CONVENTIONAL COMBUSTION PLANTS. ref (29).

Approximate Temperature of Flue Gas (°C)	Fuel	Nitrogen chemically combined in fuel (% W)	Type of Plant	NO_x reported in flue gas ppm dry basis
1500 - 1700	Oil	Not disclosed	Oil fired power station plant	110-800
1500 - 1700	Natural Gas	Negligible	Natural fired power station boilers	50-1500
1500 - 1700	cracked residual fuel-oil	1.0%	Oil fired power station boiler	425
1500 - 1700	paraffinic fuel oil	.2%	"	215

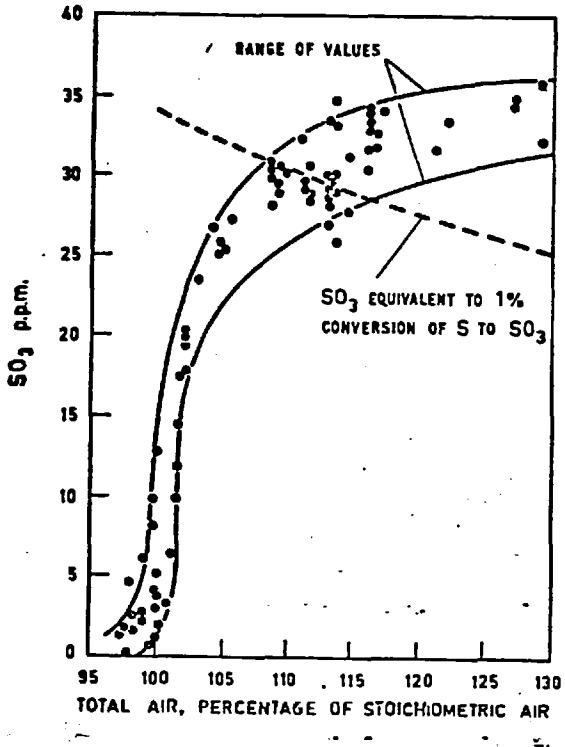

FIG. 2.4 MEASUREMENTS OF THE EFFECT OF EXCESS AIR ON THE FORMATION OF SULPHUR TRIOXIDE IN A HYDROCARBON FLAME. ref (19)

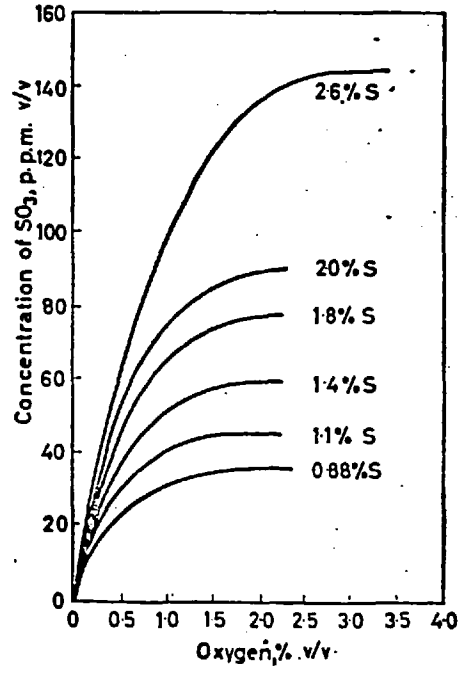

FIG. 2.5 MEASUREMENTS ON THE VARIATION OF SO_3 IN FLUE GAS WITH OXYGEN LEVEL AND SULPHUR IN THE FUEL. ref(28)

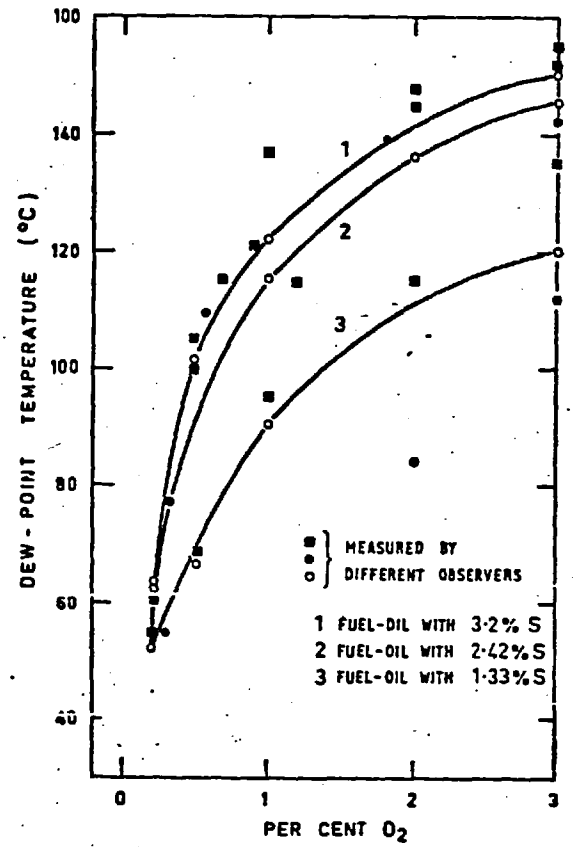

FIG. 2.6. EFFECT OF EXCESS AIR ON THE FORMATION OF SULPHUR TRIOXIDE IN AN OIL FIRED BOILER ref(27)

2.2.2 NO_x Formation and Emission. One of the most important causes of the notorious photochemical smogs that affect large areas of the west coast of the U.S.A. is the emission of nitrogen oxides to the air. There are several oxides of nitrogen but in air pollution arising from combustion, only two, nitric oxide and nitrogen dioxide, are formed in sufficien quantity to be very important. Throughout this work the term NO_x is used to denote the sum of the NO + NO_2 without specifying the relative amount of each. Thus not considering the other oxides of nitrogen.

When fuel is burnt in air, oxides of nitrogen are formed partly by the combination of atmospheric nitrogen and oxygen at high temperatures, and partly by the oxidation of chemical held nitrogen in the fuel. The formation and level emission of NO_x depend on combustion conditions such as the temperature profile of the flame, the supply of oxygen, combustion intensity and the rate of quenching. Reported emission from various types of large boiler with fossil fuel range from 50 to 1500 ppm. See Table 2.3.

I Reaction Mechanism of NO_x Formation. Generally speaking, the reaction mechanism of NO formation depends on the nature of the reactant; the nitrogen containing compound (which may be either molecular nitrogen or organic molecules containing N-H, N-C, N=C or N≡C bonds) and on the nature of the available coreactants; the latter may be very different in the flame front and in the combustion products. According to the diversity of the nitrogen sources and of the characteristics of the reaction medium, the following main NO_x mechanism can be distinguished.

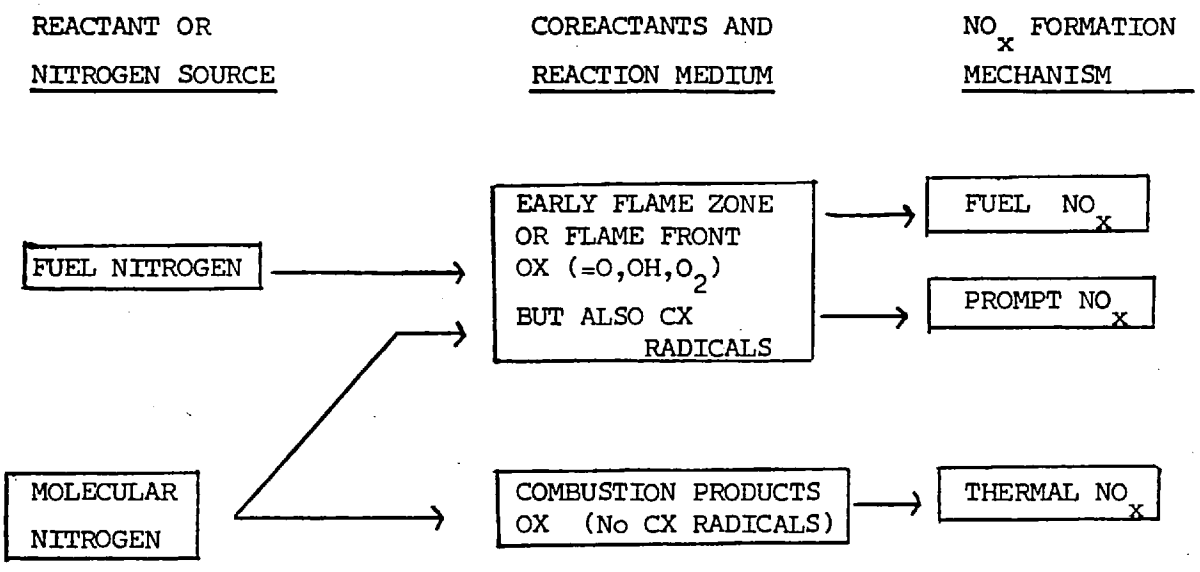

I.1 The Thermal NO_x Formation Mechanism. There has been much work carried out to develop a comprehensive mechanism on thermal NO formation according to the stoichiometric equation.

$$N_2 + O_2 \rightleftharpoons 2NO \quad \ldots\ldots\ldots\ldots\ldots\ldots\ldots\ldots\ldots\ldots \quad (2.6)$$

However there seem to be a general agreement (30) that in practical flame conditions those proposed by Zeldovich (31) and Kaufman (32) contain the main factors of the kinetic process. Table 2.4 presents a guide to the reaction proposed by those two mechanisms.

TABLE 2.4 THERMAL NO FORMATION MECHANISMS

REACTION	MECHANISM	
	ZELDOVICH	KAUFMAN
1. $N_2 + O \rightleftharpoons N + NO$	✓	✓
2. $NO + O \rightleftharpoons N + O_2$	✓	✓
3. $NO + NO \rightleftharpoons N_2 + O_2$		✓
4. $O_2 + M \rightleftharpoons O + O + M$	✓	✓

The Zeldovich mechanism considers the elementary steps 1, -1, 2 and -2. Introduction of the steady state conditions for nitrogen atoms,

i.e. $\frac{d(N)}{dt} = 0$, (quasi-steady state hypothesis), the admittance of existing equilibrium between O and O_2 molecules (Zeldovich supplementary hypothesis) as stated in Reaction 4 (see Table 2.3), Bartok (33) presents the net rate of NO formation based on the best available kinetic information, and valid only in presence of excess air as:

$$\frac{d(NO)}{dt} = 9 \times 10^{14} \exp(-135000/_{RT}) \ (N_2) \ (O_2)^{\frac{1}{2}} - 4.1 \times 10^{13} \exp(-91600/_{RT}) \ (NO)^2 \ (O_2)^{-\frac{1}{2}} \quad \ldots\ldots\ldots (2.7)$$

where $\frac{d(NO)}{dt}$ is the net rate of NO formation in gmol /cc/sec

R is the gas constant, 1.988 cal/g mol ^{o}K

T is the absolute temperature (^{o}K).

The thermodynamic equilibrium of eq. 2.6 is given by:

$$Keq = \frac{(NO)^2}{(N_2) \ (O_2)} = 21.9 \exp(-43400/RT) \quad \ldots\ldots\ldots\ldots (2.8)$$

T in ^{o}K and R = 1.988 cal/g mol ^{o}K

The mechanism proposed by Kaufman adds to the Zeldovich elementary steps 1, -1, 2 and -2, the molecular reaction:

$$2 \ NO \underset{-3}{\overset{3}{\rightleftharpoons}} N_2 + O_2 \quad \ldots\ldots\ldots\ldots\ldots\ldots\ldots\ldots\ldots\ldots (2.9)$$

The addition of the molecular steps 3 and -3 to the Zeldovich mechanism leads to consider two new terms in the net rate of NO formation, namely:

NO formation : $K_{-3} \ (N_2) \ (O_2) \quad \ldots\ldots\ldots\ldots\ldots\ldots (2.10)$

NO decomposition : $K_3 \ (NO)^2 \quad \ldots\ldots\ldots\ldots\ldots\ldots (2.11)$

Therefore:

$$\begin{bmatrix}\text{KAUFMAN NET} \\ \text{RATE OF NO} \\ \text{FORMATION}\end{bmatrix} = \begin{bmatrix}\text{ZELDOVICH NET} \\ \text{RATE OF NO} \\ \text{FORMATION}\end{bmatrix} + K_{-3} \ (N_2) \ (O_2) - K_3 \ (NO)^2 \quad \ldots (2.12)$$

As far as thermal NO_x formation is concerned the important parameter

to be controlled is in the first place temperature and in the second place the oxygen atom concentration (or equivalent ratio of the mixture).

1.2 The Fuel NO_x Formation Mechanism.

In the case where organic nitrogen compounds constitute the nitrogen source, the NO formation presents some typical characteristics (30).

a) The formation rate of NO from fuel nitrogen compounds is much faster than the thermal NO formation rate.

b) The formation of NO mainly takes place in the flame front and the very early flame zone.

c) During the NO formation some other nitrogen compounds are formed (C_2N_2, HCN, CN) as transient intermediate products; HCN is the most commonly reported.

d) The relative value of the maximum NO concentration i.e. The NO yield (R) depends on the initial fuel nitrogen content and decreases with increasing equivalence ratio. (see Fig 2.7).

I.3 The Prompt NO_x Formation Mechanism. Prompt-NO_x was designed (34) in order to explain a very fast NO formation in the visible flame zone of fuel rich hydrocarbon flames, originating from molecular nitrogen. The suggested mechanism for prompt-NO_x after the breaking of the $N \equiv N$ bond is:

$$N_2 + C_2 \longrightarrow 2CN \quad \ldots\ldots\ldots\ldots\ldots\ldots\ldots\ldots (2.13)$$

$$N_2 + CH \longrightarrow N + HCN \quad \ldots\ldots\ldots\ldots\ldots\ldots\ldots\ldots (2.14)$$

Owing to the fact that nitrogen molecules need some carbon containing radicals as coreactants, their existence is evidently restricted to the early flame zone. Some calculations done by Fenimore (34) to determine how significant is Prompt-NO_x compared with thermal-NO_x indicates that for a combustor of mean residence time of 2 ms with adiabatic stoichiometric flame using kerosene and air, the combustor would emitt 178 ppm NO of which 27% is prompt-NO_x. Burning with steam injection, would emit 106 ppm NO of which 37% is prompt-NO_x. The calculations suggest that the

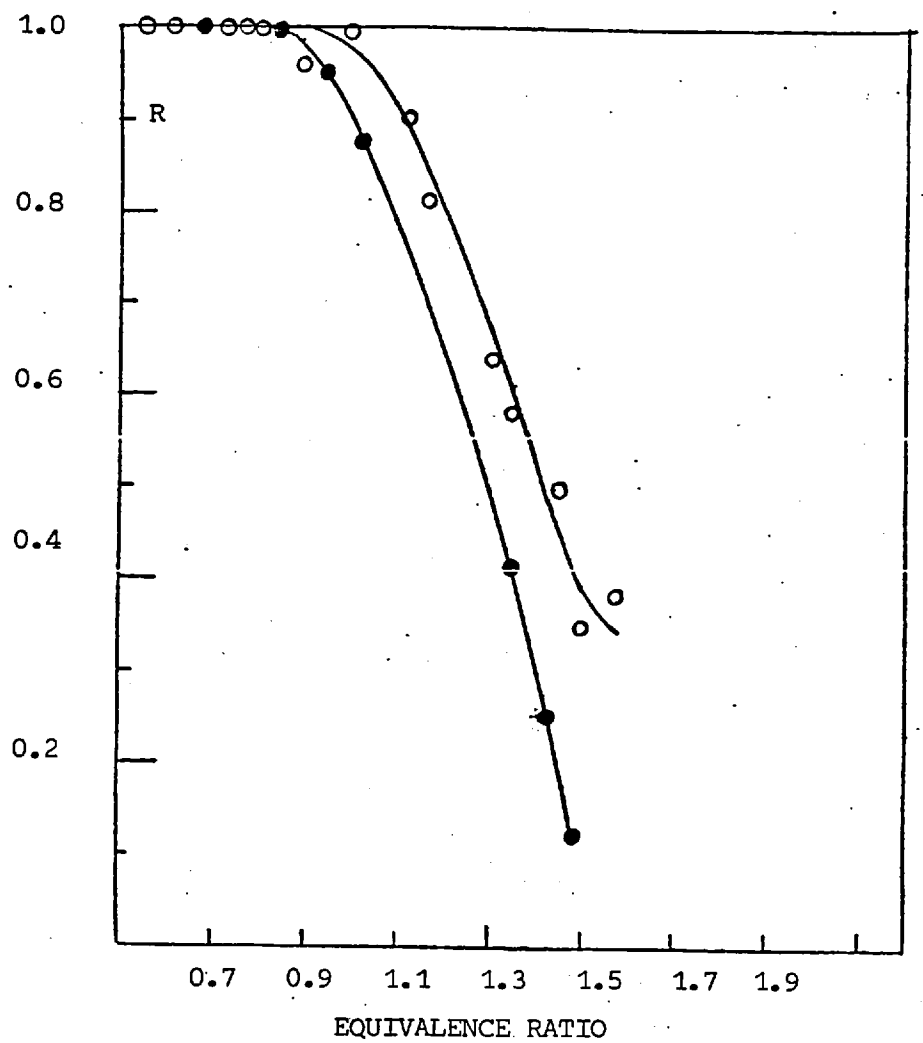

FIG. 2.7 VARIATION OF THE NO YIELD (R) AS A FUNCTION OF EQUIVALENCE RATIO. $C_2H_4/O_2/A_r$ MIXTURE DOPED WITH ETHANE-DIAMINE.
Ref. (30)

quickly formed NO (prompt-NO) might be a significant part of the total, though not the major part.

II. Control of NO_x Emission by Control of NO_x Formation. The formation of No is encouraged by the following factors:

a) High flame temperature.

b) Long residence time at high temperature.

c) High oxygen concentration

d) High nitrogen content of the fuel.

While surviving of NO is encouraged by the rapid quenching of the flue-gas, NO will be oxidised to NO_2 by oxygen present in the cooled flue-gas. The effect of fuel-nitrogen in NO_x emission can be seen in Fig 2.8 and appears to be dominantly as predicted by Fuel-NO_x mechanism.

Reports indicate that an increase of the oxygen level in the flue gas (29) is related to an increase in NO_x emission from oil fired boilers, this observation is presented in Fig 2.9.

Limitation of NO formation due to unavailability of oxygen and lowering temperature profiles can be achieved by TWO-STAGE COMBUSTION. This technique involves firing all the fuel in the first stage with sub-stoichoimetric quantities of primary air and injecting the remainder air in the second stage after heat removal between stages is performed. Reduction in peak temperatures leads to a kinetical limitation of NO formation. Bartok et al (33) postulates a model to assess the effects of the major combustion parameters on the NO_x formation, i.e. low excess air firing, two-stage combustion and water injection. The model is based on Zeldovich type NO formation in natural gas combustion by using premixed, gaseous hydrocarbon fuel/air feed. Provision of multiple point injection of fuel or air makes possible simulation of two stage combustion. Results obtained by Bartok are plotted in Figs 2.10 and 2.11 which can be summarised as follows:

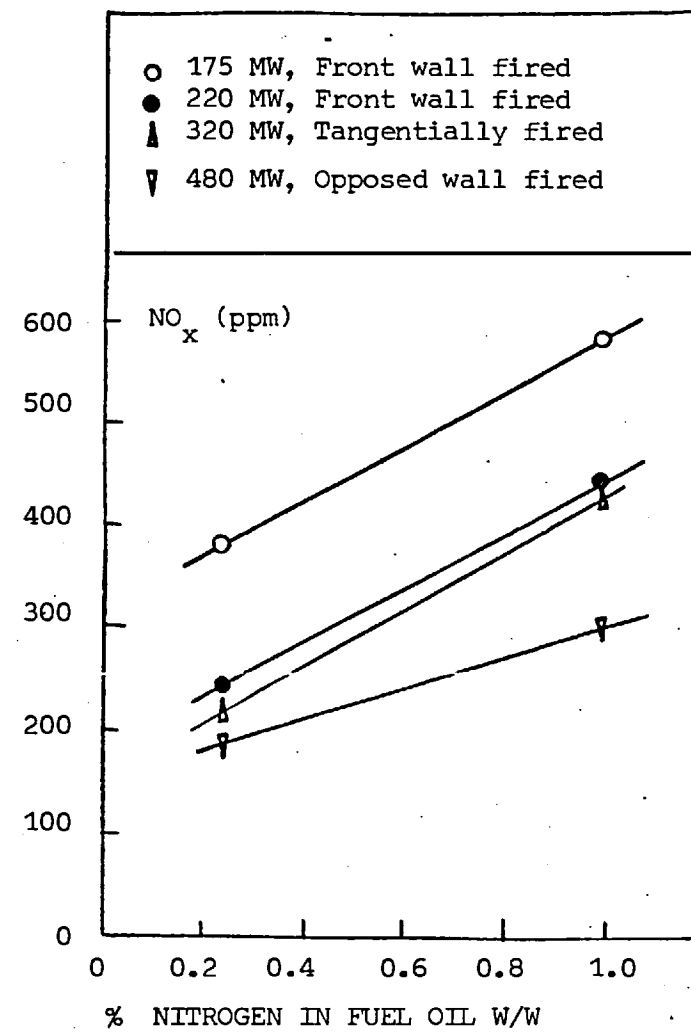

FIG. 2.8 EFFECT OF FUEL NITROGEN IN NO_x EMISSIONS.ref(33)

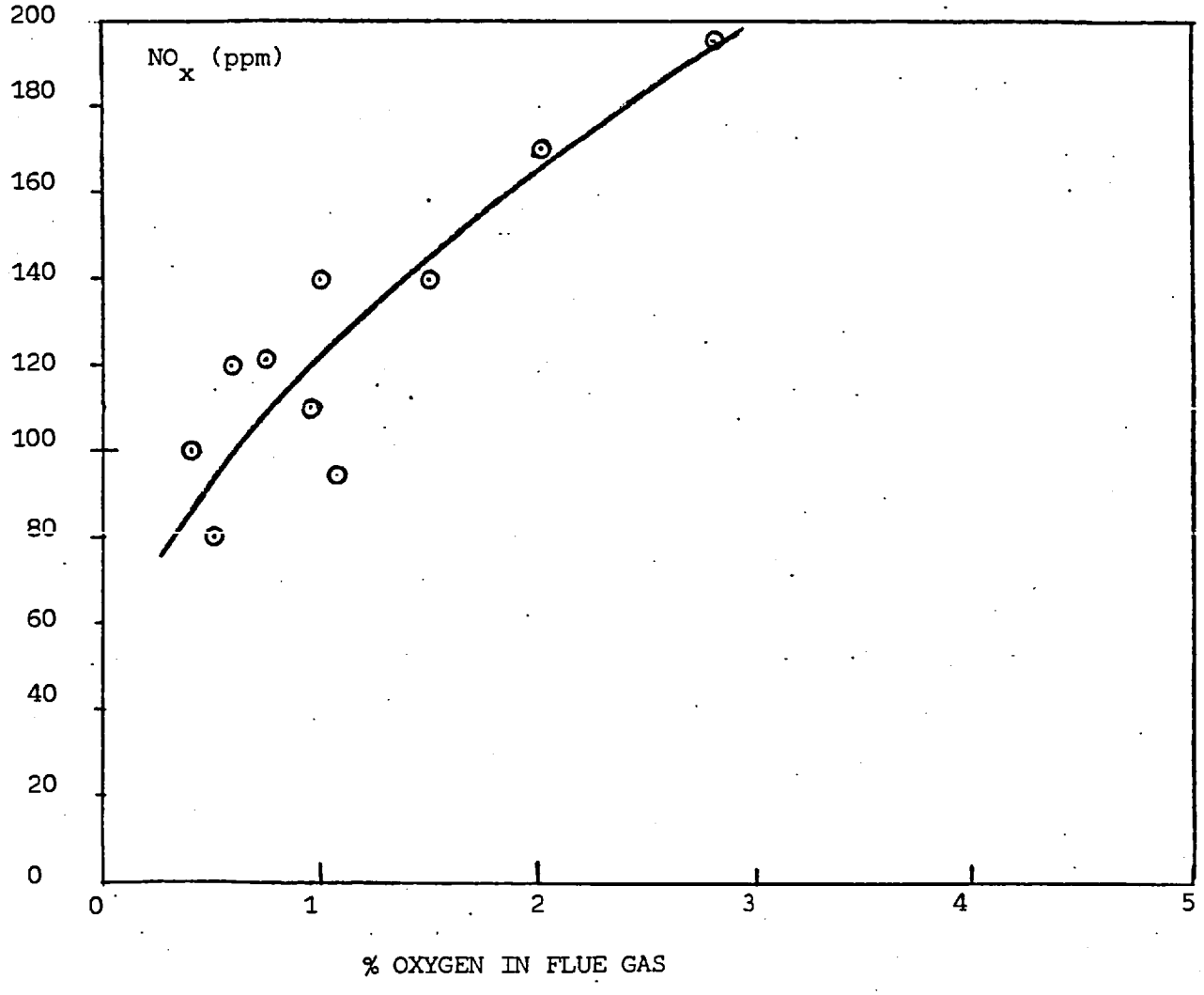

FIG. 2.9 NO_x EMISSIONS FROM OIL-FIRED BOILERS AT VERY LOW EXCESS AIR.

Ref. (29)

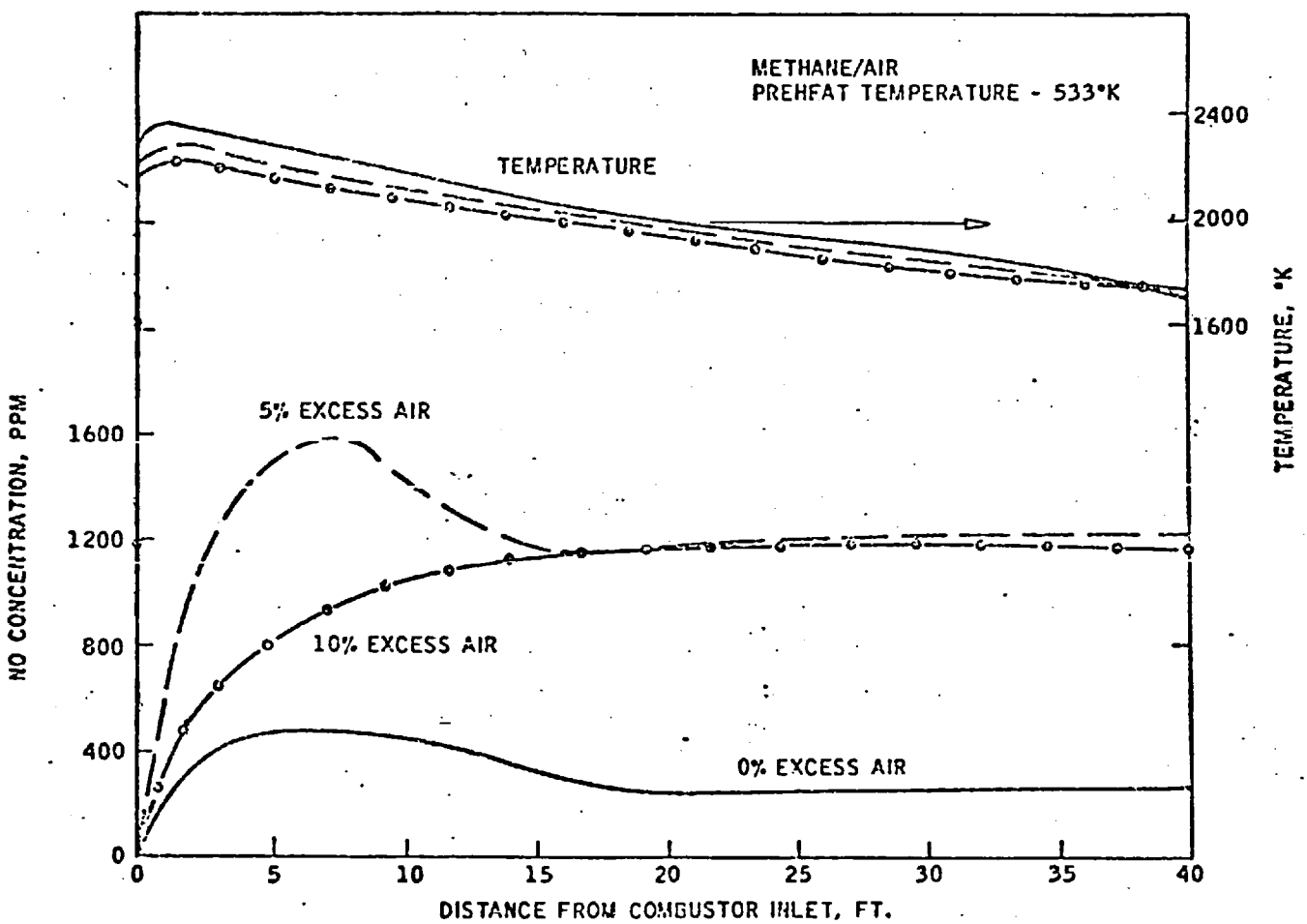

FIG. 2.10. EFFECT OF EXCESS AIR ON NO AND TEMPERATURE PROFILES AS PREDICTED BY BARTOK (33).

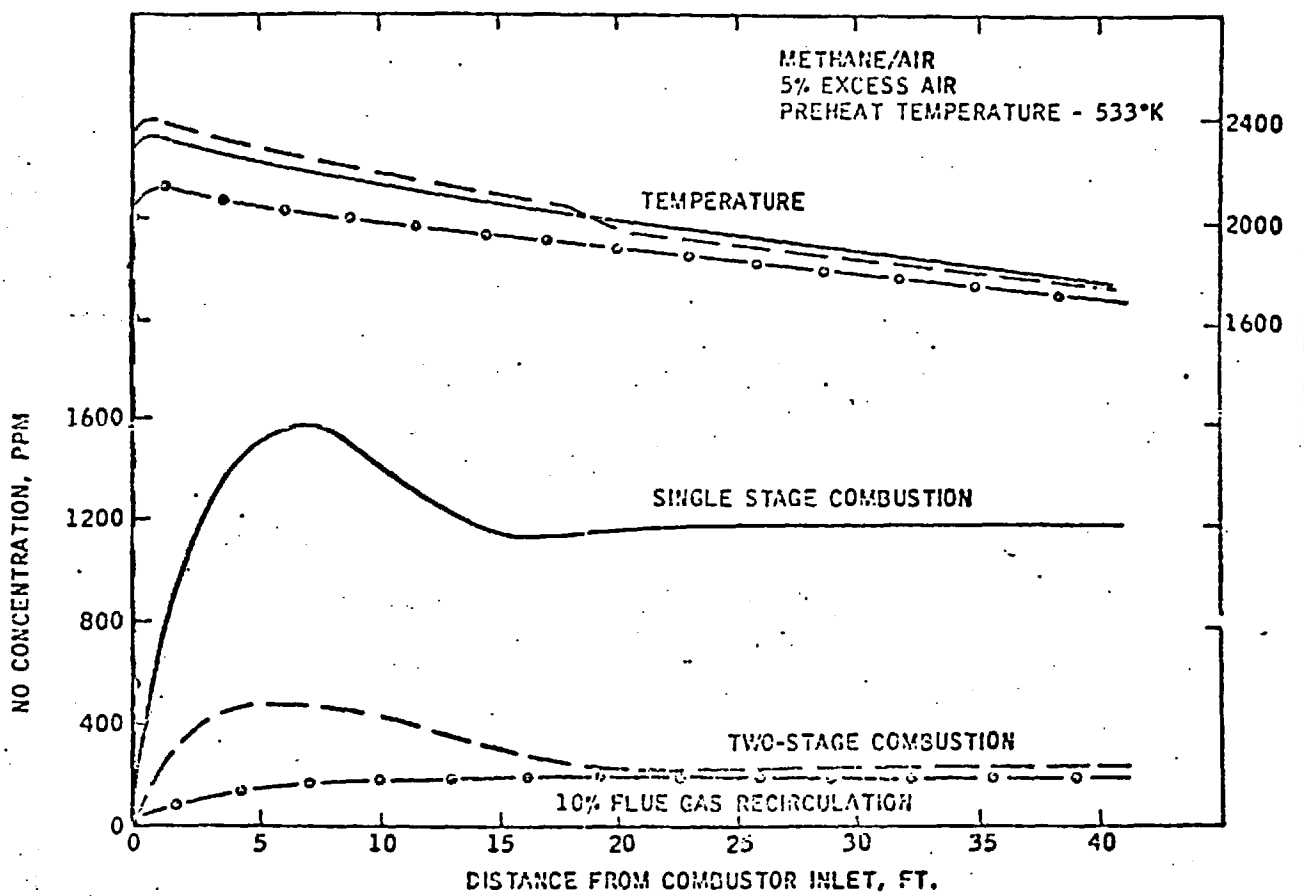

FIG. 2.11 EFFECTS OF TWO-STAGE COMBUSTION AND FLUE GAS RECIRCULATION ON NO AND TEMPERATURE PROFILES AS PREDICTED BY BARTOK (33)

a) Lower excess of air in the combustor leads to lower NO emission.

b) Two-stage combustion reduces drastically the emission of NO.

c) Flue-gas recirculation by lowering temperature profile also brings a considerable reduction in NO emission.

2.2.3. Monitoring of Major Gaseous Compounds in Combustion Systems. As part of the investigation of gaseous and particulate emission from fuel oil fired combustion system, it becomes necessary to determine the concentration of SO_2 and SO_3, NO and NO_2 and basic components of gaseous products of combustion. Archer (35) using a combustion system similar to the one the present work is based on, developed an on-line analysis of wet combustion gases by gas chromatography. He used a 4m x 0,475 cm diameter "Poropak Q" column and a 2m x 0.475 cm diameter molecular sieve 5A. Both columns graded between 80 and 100 BSS Mesh. The carrier gas was helium and the operation temperature 50°C. A specially designed Biotron Valve was located between the columns to allow by-passing. The following components of a single sample were successfully separated: carbon dioxide, carbon monoxide, oxygen, nitrogen, hydrogen, water, methane, ethylene and ethane. For a carrier gas flow of 0.688 cm^3/s the analysis took just above 1 hour.

I SO_x (= SO_2 + SO_3) Determination in Stack Gases. Many data from both boiler plants and gas turbines show that concentration of SO_3 rarely exceeds 50 ppm. Typical values for conversion of SO_2 to SO_3 are around 3.5 %v when operating with large excesses of air. Presence of SO_2 in stack gases slightly differs to that of SO_3 in the way that SO_2 can occur in concentrations up to 0.3 %v . The large excess of SO_2 to SO_3 in flue gases is the main difficulty in determining SO_3 concentrations. If some small additional oxidation is allowed to take place during the early stages of sampling or analysis, a large positive error can occur in the value of SO_3 concentration. Another characteristic is the fact that small traces of SO_3 in gases raise significantly the dew point of the mixture compared with that containing water vapour alone.

The method most commonly used when determining concentration of SO_2 and SO_3 each in the presence of the other was originally developed by Flint (36) and is based on absorption of SO_2 and SO_3 in an 80%v isopropyl alcohol in water. SO_x absorbed in the solution is in the form of sulphate ions, which are subsequently precipitated and determined as barium sulphate. Improvements on the barium sulphate determinations were carried out by Corbett (37,38) and Fielder (39) who introduced a phototurbidimetric method and Seidman (40) who completed determination of sulphate ions in the isopropyl alcohol solution by titration. Although these improvements have been achieved, the techniques involve tedious manipulations and are time consuming. A more recent and important achievement was obtained by introducing the Central Electricity Research Lab. SO_3 monitor which is based on the work of Bertolecini (41).

The CERL-SO_3 monitor's new feature is the introduction of a new reagent, solid barium chloranilate. This reacts with sulphate ions producing acid chloranilate oins which give to the solution a reddish colour, whose intensity is determined colorimetrically and gives a measure of the original SO_x absorbed as sulphate ions.

The simplest method developed yet (42) is based on the condensation of SO_3 as H_2SO_4 droplets on cooled surfaces between 60 and 90°C. This method gives quantitative determination of SO_3 and allows measurement of SO_2. It involves an apparatus easy to make and to manipulate. Differences up to 6% were found measuring SO_3 in flue-gas by this technique when comparing with techniques based on SO_3 absorption in isopropanol solution.

SO_2 determination by Gas Chromatography has been reported by Leibrand (43) using a 80/100 mesh silica gel column maintained at 100°C.

"Poropak Q" columns are widely known to produce SO_2 separation. Determination of SO_2 by different authors (44, 45, 46, 47, 48) using

"Poropak Q" columns, was achieved with operating temperatures ranging between 75°C and 100°C. Packing graded between 50 and 100 mesh and the use of helium as a carrier gas.

II. NO_x (=NO + NO_2) Determination in Stack Gases. The specific problems in determining NO_x are the facts that the equipment should be able to defect very low amounts (5 ppm is the maximum safe allowable in the air).

The measuring techniques for NO_x determination most widely known are the wet chemical batch process, which although now standardized, is generally cumbersome.

A recent apparatus based on the chemiluminescent reaction of nitric oxide with ozone has been developed (49); (see Section 4.1.3).

$$NO + O_3 \longrightarrow NO_2^* + O_2 \quad \ldots\ldots\ldots\ldots\ldots\ldots \quad (2.15)$$

$$NO_2^* \longrightarrow NO_2 + h\nu \quad \ldots\ldots\ldots\ldots\ldots\ldots \quad (2.16)$$

An extensive and comprehensive review of NO_x methods of analysis has been carried out by Allen (50), who concluded that the chemiluminescence monitor offered great possibilities in NO_x measurements due to its high sensitivity and reliability. In a latter publication (51) he evaluated the chemiluminescent method and found that it can provide an extremely stable, accurate, sensitive and fast response method in measuring NO in combustion exhaust gases.

2.3 Solid Emission in Combustion Process.

The solids contained in the waste flue gases from fossil fuel fired combustion appliances consist of three types of material, derived in different ways and found in different proportions, according to the kind of appliance and the type of fuel, viz.

(i) fly-ash, consisting of incombustible particles derived from minerals associated with the fuel.

(ii) chars, consisting of partially burnt or carbonised particles of fuel.

(iii) carbon particles or soot, formed in the course of gas-phase combustion of volatile hydrocarbons resulting from the pyrolisis of the fuel.

The individual particles are normally less than 50 μm diameter, but their distribution of particles size depends largely on the combustion conditions.

Gills (52) discusses the general parameter which could lead to a substancial influence on the solid emission from liquid fuel flames. Solid emission can be defined as the amount of solid discharged per unit of time by the appliance. However, throughout this work it is defined as the mass of solid discharged per unit mass of fuel fed expressed as per centage. The quality of atomization with particular reference to the maximum drop size, the excess of oxygen and the combustion intensity are correlated to the solid emission and plotted in Figs 2.12 and 2.13 (52). As it can be seem excess oxygen brings about a reduction in solid emission; similar results are obtained by the improving quality of atomization. He also found that low values of swirl produce large quantities of carbon due to slow mixing. Increasing swirl reduces the emission of solids; nevertheless there is an indication of a high swirl value beyond which solid burden increases.

2.3.1 Solid Emission from Residual Fuel-oil Gasification in a Single Stage. Archer and Eisenklam (53) using a gasifier described in detail in Section 3.1.1 found the solid formed originated from two sources:

a) Chars, i.e. incompletly evaporated drop which have undergone gasification, of size range 0.5 to 1.5 μm.

b) Soot from light hydrocarbon cracking reactions of size less than 0.1 μm.

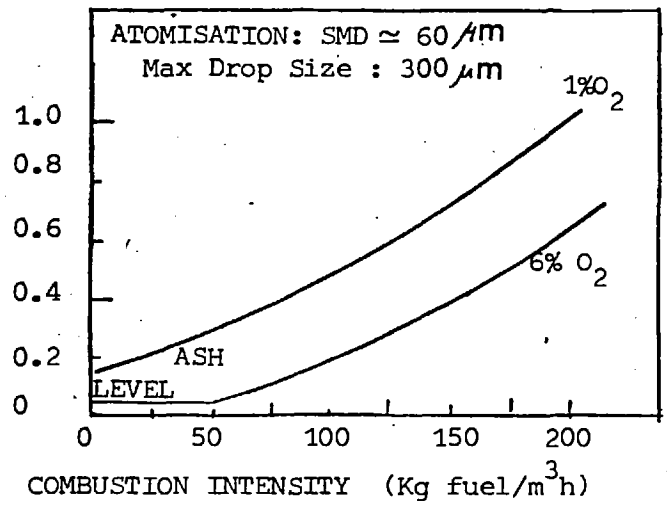

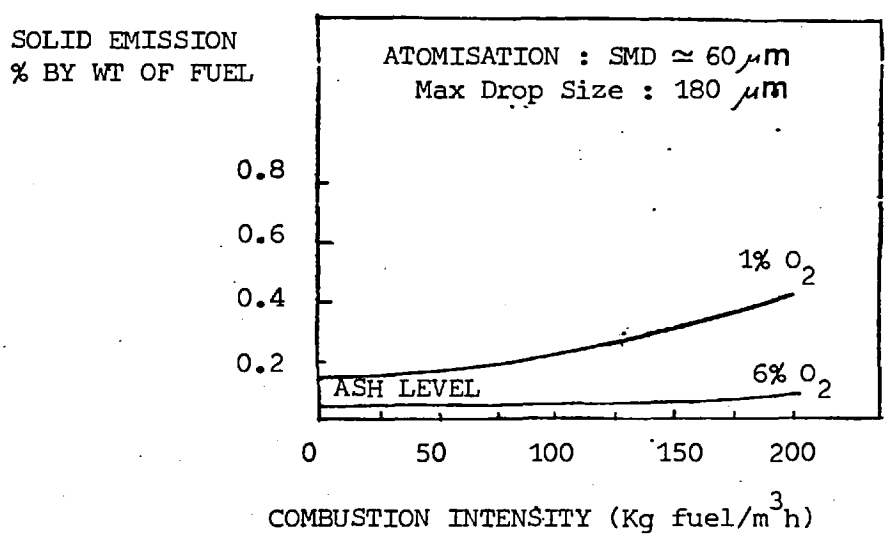

FIG. 2.12 and 2.13. INFLUENCE OF SPRAY CHARACTERISTICS ON SOLIDS EMISSION RELATED TO COMBUSTION INTENSITY AND OXYGEN LEVEL. Ref. (52)

Solid emission from the gasifier was measured to be considerably lowered by using steam as an atomising fluid instead of air. The results are plotted in Figs 2.14 and 2.15, where it can be seen the general effect of increasing the equivalence ratio* is to increase the amount of solid emitted from the gasifier. The effect of injecting steam as an atomising fluid was to increase the concentration of [OH] in the flame and thus lowering soot formation.

2.3.2 Solid Emission from Residual Fuel-oil Combustion in a Two-stage System. Three groups of particles were found (54) by using electron photomiscroscopy on solid collected from a two-stage system which involves the first and second stage described in Chapter 3. Steam was used as atomising fluid.

Group A. Cenospheres - Diameter range 5-10 μm. hollow particles produced by swelling during devolatilization.

Group B. Char - Carbonised fuel drops. Diameter range : 0.25 - 1.5 μm

Group C. Soot - Carbon particles formed from cracking reactions.

The results obtained with such systems concerning solid emission show the general decrease of solids emitted from the second stage with an increase of the first stage equivalence ratio. Needless to say that the overall operation was carried out at stoichiometric condition, thus $\phi_2 = 1.0$. Solid emission's results are plotted in Fig 2.16 against first stage equivalence ratio and using atomising steam to fuel ratio as a parameter. The increase of the atomising steam to fuel ratio

---

* Equivalence ratio ϕ is defined as the operating fuel-air ratio divided by the stoichiometric fuel-air ratio. i.e. $\phi = \dfrac{\frac{F}{A}}{\frac{F_s}{A_s}}$

For "vanilla" fuel this is $\phi = 13.99 \times (\frac{F}{A})$

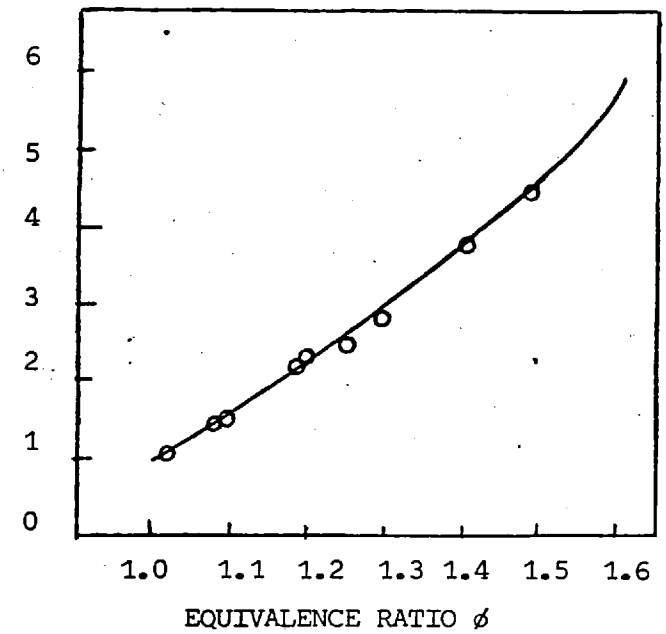

FIG. 2.14. SOLID BURDEN FROM GASIFIER WITH AIR ATOMIZATION Ref(53)

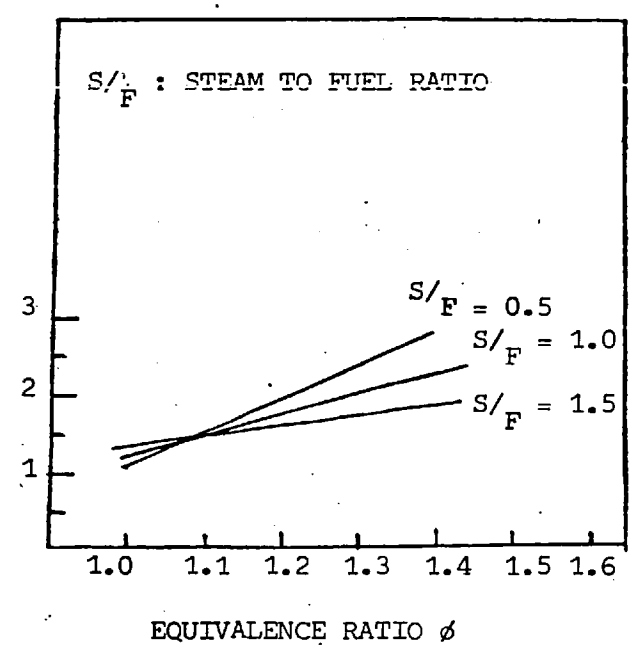

FIG. 2.15 SOLID BURDEN FROM GASIFIER WITH STEAM ATOMISATION Ref.(53)

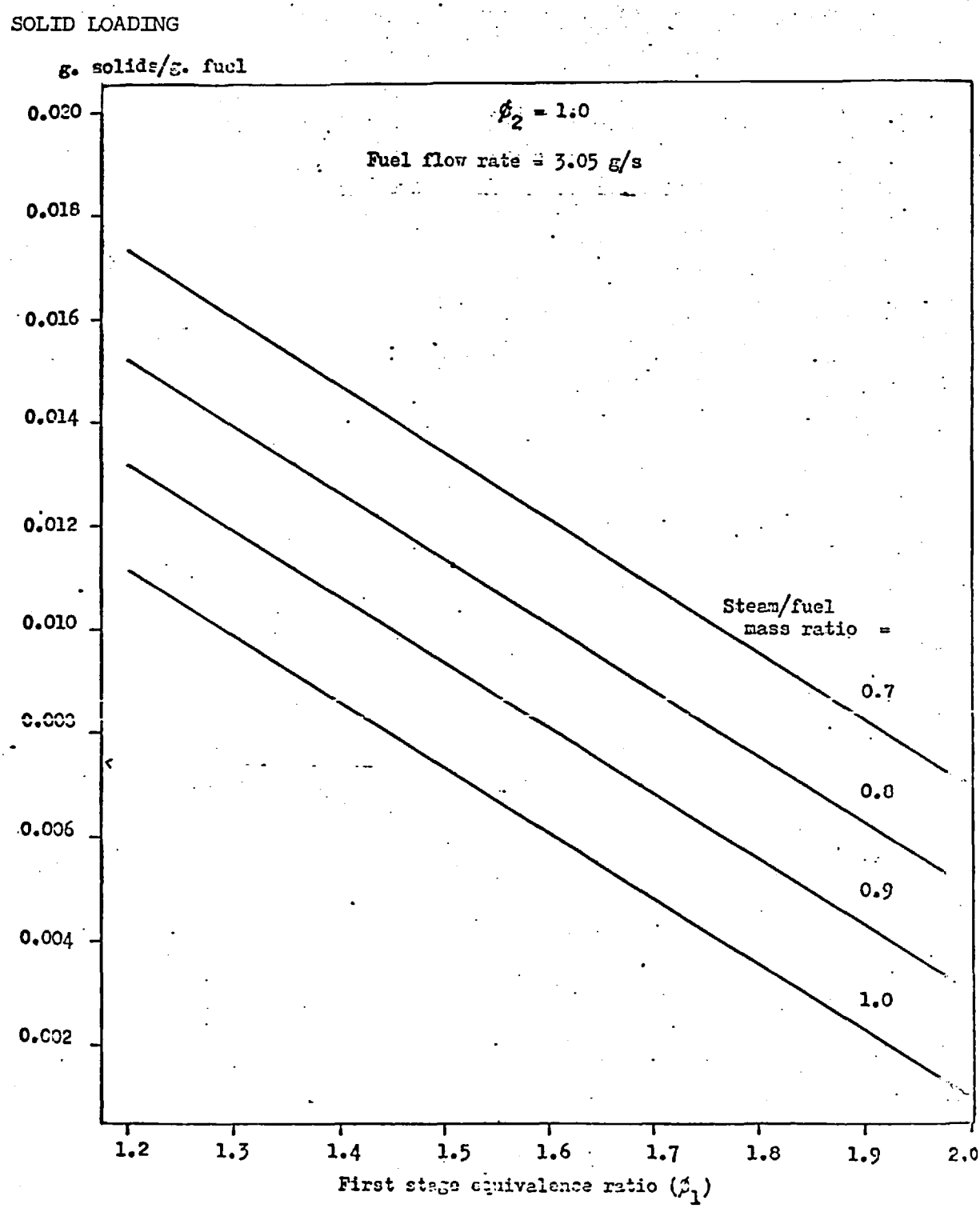

FIG. 2.16 EFFECT OF FIRST STAGE EQUIVALENCE RATIO ON SOLID PRODUCT FORMATION IN SECOND STAGE Ref.(2)

reduces the solid emission levels, since it brings about a reduction in fuel drops diameter.

2.4 Behaviour of Vanadium Nickel, Sodium and Sulphur During Combustion.

A well accepted mechanism for combustion of single drops of residual fuel-oil is:

1. Evaporation and Combustion of lighter hydrocarbons.
2. Thermal cracking of heavier hydrocarbons and combustion of lighter fractions leaving a tarry residue.
3. The combustion of residual carbon.

During these processes the main impurities in the fuel (V, Ni, Na and S) are released into the bulk of the chamber and, as it will be seen later, produce a series of different effects on the equipment, The initial stages followed by these elements are different in each case so each of one will be dealt with separately and at the end their interaction will be considered.

2.4.1 Vanadium During the early stages of combustion, the vanadium-porphyrin complexes are oxidised and vanadium is released. Vanadium can exist in six different valency states, namely 0 to 5; thus vanadium released by combustion of the metal-organic complex can remain either in its original 2-valent state or oxidise to the 3, 4 or 5 valency states.

On the grounds of thermodynamics, it can be shown (see Section 5.3.1) at temperatures existing in combustion chambers, vanadium will oxidise first to its lower oxides : VO, V_2O_3, or V_2O_4; and if reactions come to equilibrium and there is not excess oxygen present,but as long as there is any carbon or hydrogen from the organic compounds, these lower oxides will not yield V_2O_5. Although the affinity of oxygen is to react with carbon and hydrogen in preference to V_2O_3 or V_2O_4, the facility of oxygen to reach any of those reactants comes to play an important role.

During combustion of fuel oil drops, after vanadium-porphyrin molecule has been oxidised, vanadium would most probably remain in the carbonaceous residue as VO (melt.pt.= 2077°C ,b.p.= 3130°C). Having high boiling point it will remain part of the combusting particles, along with other metallic oxides.

$$V^{II} + \tfrac{1}{2}\, O_2\ (gas) \longrightarrow VO\ (sol.) \quad \ldots\ldots\ldots\ldots\ (2.17)$$

From the oxidation potential diagram (see Fig 5.7), it can be seen that in the range 1200°C to 2000°C the following oxidation reaction may be expected:

$$VO\ (s) + \tfrac{1}{2}\, O_2\ (g) \longrightarrow VO_2\ (s \text{ or } l) \quad \ldots\ldots\ldots\ldots\ (2.18)$$

$$2VO\ (s) + \tfrac{1}{2}\, O_2 (g) \longrightarrow V_2O_3\ (s) \quad \ldots\ldots\ldots\ldots\ (2.19)$$

or $$V_2O_3 (s) + \tfrac{1}{2} O_2\ (g) \longrightarrow V_2O_4 (s) \quad \ldots\ldots\ldots\ldots\ (2.20)$$

Formation of V_2O_3 via equation 2.19 and V_2O_4 via eq. 2.19 does not involve corrosion in the system, corrosive deposit-forming agent V_2O_5 is not formed as long as low partial oxidising conditions prevail. Thus, when oxygen is nowhere in excess in the system and reactions are assumed to come to equilibrium, V_2O_3 and V_2O_4 are theoretically the final products to be formed, and having high melting points (2000°K), there is the strong possibility of finding them in the stack fly-ash.

On the other hand, high oxygen partial pressure i.e. air rich conditions, formation of V_2O_5 could well be expected by simply further oxidation of V_2O_3 and V_2O_4:

$$V_2O_3\ (s) + O_2\ (g) \longrightarrow V_2O_5\ (l) \quad \ldots\ldots\ldots\ldots\ (2.21)$$

$$V_2O_4\ (s) + \tfrac{1}{2} O_2\ (g) \longrightarrow V_2O_5\ (l) \quad \ldots\ldots\ldots\ldots\ (2.22)$$

V_2O_5 formation in the combustion system would probably lead to deposition by impaction (55) rather than by vapour diffusion on the interior surfaces and therefore interacting with other compounds (For V_2O_5 vapour pressure, see Fig 2.17)

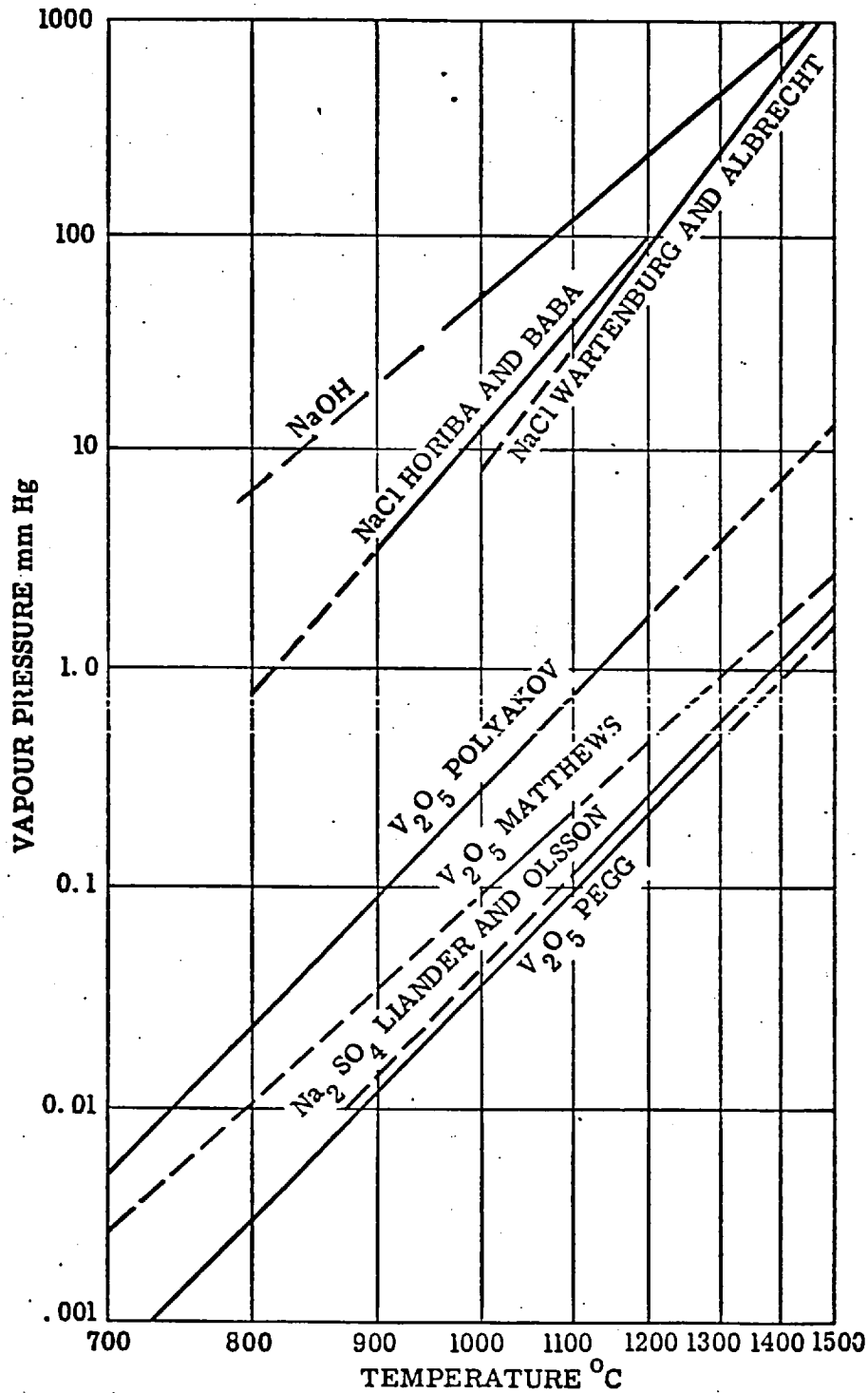

FIG.2.17 VAPOUR PRESSURE OF FUEL OIL ASH CONSTITUENTS Ref. (77)

Halstead (56) also proposes V_2O_3 and V_2O_4 formation via condensation of VO_2 (g) as:

$$2VO_2\ (g) \longrightarrow V_2O_3\ (\text{condensed}) + \tfrac{1}{2}O_2 \quad \ldots\ldots\ldots\ (2.23)$$

$$2VO_2\ (g) \longrightarrow V_2O_4\ (\text{condensed}) \quad \ldots\ldots\ldots\ (2.24)$$

at temperature of 1750 and 1830°K respectively.

2.4.2 Sodium. Sodium usually occurs in fuel oil mostly in the form of NaCl, which is incorporated into the droplets and subjected to evaporation at combustion temperatures. The nature of sodium in the vapour phase is mainly determined by the NaCl hydrolisis (56):

$$NaCl\ (g) + H_2O\ (g) \longrightarrow NaOH\ (g) + HCl\ (g) \quad \ldots\ldots\ldots\ (2.25)$$

or when in excess of oxygen by its interaction with sulphur dioxide:

$$2NaCl(g) + SO_2(g) + H_2O(g) + \tfrac{1}{2}O_2 \longrightarrow Na_2SO_4(g) + 2HCl(g) \quad \ldots\ (2.26)$$

2.4.3 Sulphur. During the combustion process the sulphur present in the fuel is oxidised to form gaseous SO_2 or SO_3. SO_3 formation has been discussed in detail in Section 2.2.1.

2.4.4 Nickel. During the early stages of combustion nickel exists in the vapour phase as metallic atoms (57) which are subsequently oxidised following:

$$2Ni + O_2 \longrightarrow 2NiO \quad \ldots\ldots\ldots\ (2.27)$$

2.4.5 Interaction Between These Impurities. Of the compounds formed by combustion of residual fuel oil, V_2O_5 and Na_2SO_4 are the two most reactive species which can further combine and interact with one another to form highly corrosive complex compounds.

NaOH having a high vapour pressure (see Fig 2.17) will probably initiate reaction within the vapour phase as well as the molten layer of V_2O_5, following (58):

with SO_3 to form Na_2SO_4

$$2NaOH + SO_2 + \tfrac{1}{2}O_2 \longrightarrow Na_2SO_4 + H_2O \quad \ldots\ldots\ldots\ (2.28)$$

or with V_2O_5 to form sodium vanadates:

$$2NaOH + V_2O_5 \longrightarrow 2NaVO_3 + H_2O \quad \ldots\ldots\ldots\ldots (2.29)$$

The system Na_2SO_4/V_2O_5 has been extensively studied both in air (60) and more recently in an $SO_2/SO_3/O_2$ atmosphere (61). On the basis of laboratory experiments it was concluded that sodium sulphate and V_2O_5 reacted on heating to form metavanadates and complex vanadates as follows:

$$\begin{matrix} Na_2SO_4 \\ + \\ V_2O_5 \end{matrix} \xrightarrow{\text{HEATING}} \begin{matrix} NaVO_3 \\ Na_2O.3V_2O_5 \\ Na_2O.6V_2O_5 \end{matrix} + SO_3 \quad \ldots\ldots\ldots (2.30)$$

According to the initial molar ratio of Na_2SO_4 and V_2O_5 in the original mixture the listed compounds in the products were appearing. Apart from SO_3 only metavanadates and complex vanadates were the products of reaction at different molar ratios of Na_2SO_4 and V_2O_5.

When $Na_2O.6V_2O_5$ was formed a "breathing" phenomena was observed upon crystallization and was atributed to oxygen evolving from the molten state, well represented by:

$$Na_2SO_4 + 6V_2O_5 \longrightarrow Na_2O.6V_2O_5 + SO_3 \quad \ldots\ldots\ldots\ldots (2.31)$$

$$Na_2O.6V_2O_5 \text{ (molten)} \longrightarrow Na_2O.V_2O_4.5V_2O_5 \text{ (cryst.)} + O \quad \ldots (2.32)$$

Thus forming the complex 1.1.5 Sodium vanadyl vanadate, that, as it will be seen later, in Section 2.5, is largely responsible for corrosive effects in equipment (high temperature corrosion) and commonly found in deposits in combustion systems.

2.5 Effect of Impurities on Combustion Equipment.

The impurities in residual fuel oil released during combustion lead to many problems in central stations power plants. One of the most serious of these difficulties is the external corrosion of heat receiving surfaces in boiler furnaces. Another is the unpredictable decrease in heat transfer caused by deposits formed from the inorganic constituents of the fuel.

Vanadate deposits are the most common in oil fired boiler systems (62). Such deposits consist of mixed vanadates and vanadyl-vanadates, normally the reaction products of sodium sulphate and vanadium oxides.

Table 2.5 (22, 63, 64) presents melting and some boiling points of relevant compounds that might occur associated to the solids formed from the combustion of residual fuel-oil.

2.5.1 High Temperature Corrosion. As it is shown in Table 2.4, several vanadates are molten at the temperature of superheater elements. For boiler furnaces sodium vanadates particularly $Na_2O.V_2O_4.5V_2O_5$ and $Na_2O.3V_2O_5$ are the most corrosive.

No assured mechanism has been derived dealing with the way in which vanadium leads to corrosion; proposed mechanisms published elsewhere (21, 23, 65) include:

1. Vanadates serving as oxygen carriers
2. Vanadates distorting the normal crystal lattice of the protective oxide-film of the metal
3. Molten vanadates dissolving the protective film.

2.5.2 Low Temperature Corrosion. Low temperature corrosion takes place in the relatively cool surfaces (100 - 200°C) of air heaters and economizers, where low temperatures can reach the dew point of the flue gas and a liquid film of sulphuric acid forms on the metal. This H_2SO_4 results when vapour SO_3 combines with water vapour both present in flue gas. (see Section 2.2.1)

Hydrochloric acid formed from chlorides in the fuel latter converted in the furnace are also known (58) to produce corrosion in cool surfaces.

TABLE 2.5

MELTING AND SOME BOILING POINTS OF RELEVANT COMPOUNDS THAT MIGHT OCCUR IN SOLID FORM DURING COMBUSTION OF RESIDUAL FUEL OIL.

COMPOUND	FORMULAE	MELT. PT. °C	BOIL. PT. °C
Vanadium Oxide	VO	2077	3130
Vanadium Dioxide	VO_2	1545	dec.3030
Vanadium Trioxide	V_2O_3	1970	3027
Vanadium Tetroxide	V_2O_4	1970	
Vanadium Pentoxide	V_2O_5	690	2052
Sodium Metavanadate	$Na_2O.V_2O_5$	630	
Sodium Pyrovanadate	$2Na_2O.V_2O_5$	640	
Sodium Orthovanadate	$3Na_2O.V_2O_5$	850	
Sodium Vanadyl-Vanadates (1:1:5)	$Na_2O.V_2O_4.5V_2O_5$	625	
Sodium Vanadyl-Vanadates	$Na_2O.V_2O_4.11V_2O_5$	535	
Sodium Sulphate	Na_2SO_4	884	
Sodium Chloride	NaCl	800	1413
Sodium Hydroxide	NaOH	318	1387
Nickel Pyrovanadate	$2NiO.V_2O_5$	900	
Nickel Orthovanadate	$3NiO.V_2O_5$	900	
Ferric Metavanadate	$Fe_2O_5.V_2O_5$	860	
Ferric Vanadate	$Fe_3O_4.2V_2O_5$	855	

CHAPTER 3

THE EQUIPMENT AND EXPERIMENTAL PROGRAMME

A schematic flow diagram of the two stage combustion plant is shown in Fig. 3.1. In a brief description of this system the main points are:

Liquid fuel is injected into the gasifier (First stage) in the form of a spray which is produced by either air or superheated steam as the second fluid in a twin fluid sonic atomiser. The air required for the gasification process was injected through jets located in the inner wall of the chamber. Initial ignition of the mixture air-fuel was made possible by the use of a pyrotechnic device after which combustion was selfsustained. The hot combustion gases passed through a sampling device called a cross-piece, enabling us to sample gasification products. After the cross-piece, the hot gases passed through a water cooled heat exchanger into the converted (Second stage) where a carefully rated amount of air is injected in order to achieve further combustion. After a few minutes of running, a spontaneous flame in the converter is obtained. A second sampling section (T-piece) is coupled to the end of the second stage. The resulting flue gas is passed through the T-piece and a short-length quenching section. Quenching was obtained by means of evaporating radially arranged jets of water. The quenched products are scrubbed before being pulled into a cyclone. Scrubbing was performed by a set of 6-3-jets water nozzles, designed to produce water drops with which the solid particle carried in the gas agglomerated.

Particulates were separated from the gaseous phase in the cyclone and collected in a tank located at the bottom of it. The solid in the slurry was prevented from settling down by continuous recycling. This

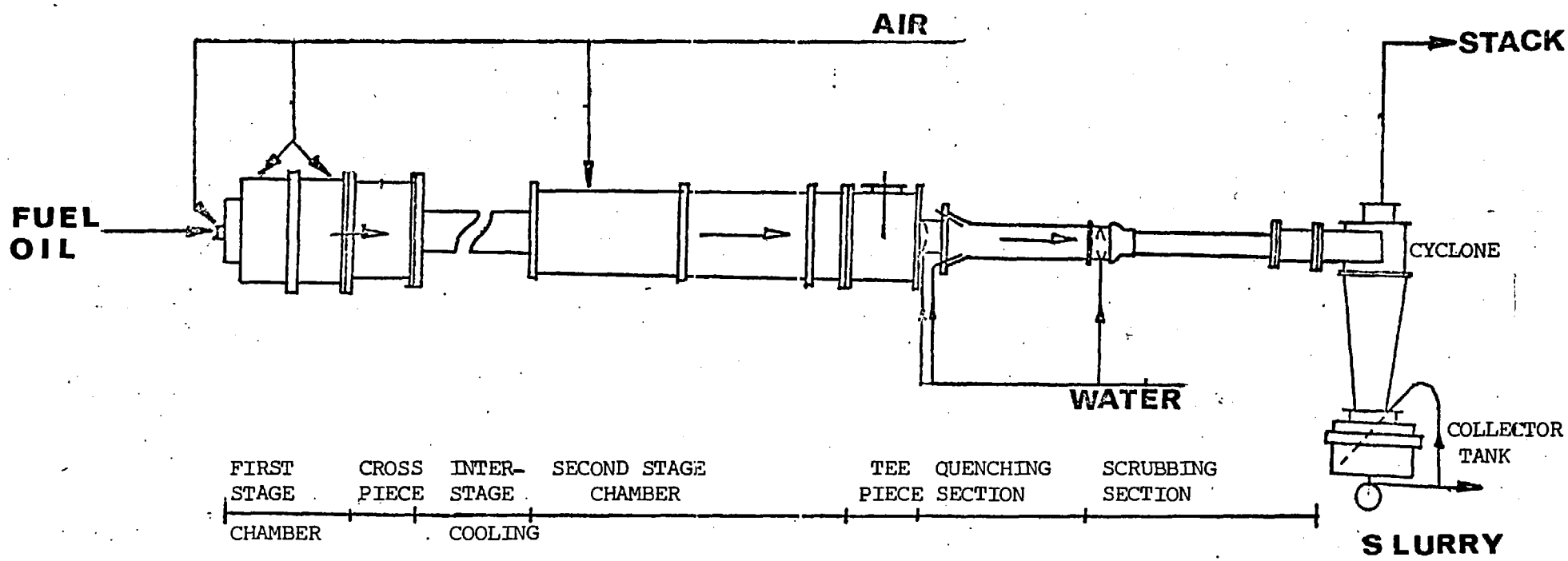

FIG. 3.1. SCHEMATIC DIAGRAM OF THE TWO-STAGE COMBUSTION PLANT

well mixed slurry was then pumped out either to waste or to a large vacuum filter. The solids thus separated were subsequently dried and prepared for weighing and analysis.

3.1. The Experimental System.

Description of the two-stage combustion plant could be focused by dividing it into three parts; the first stage and atomiser, the second stage and the solid collecting system.

3.1.1 First Stage Combustion Chamber and Atomiser. The combustion chamber known as the first stage combustion chamber used as gasifier was an Urquhart High Duty chamber with a combustion volume of 0.0115 m^3 (nominally 0.33 ft^3), exit diameter of 76 mm (3 in) and combustion intensities of 10 MW/m^3. Fig. 3.2 presents a schematic diagram of the chamber, whose simplified description can be summarized as follows:

The chamber where the actual gasification reactions take place, was formed by two co-axial refractory lined cones joined at their bases. This design being mounted into a cylindrical casting. The shape of the gasification space was specially designed for an atomised fuel cloud.

The atomiser which reduced the liquid fuel to a cloud of drops of a mean initial dropsize of about 100 μm was a twin fluid design where the liquid issues from an orifice and the gas from an annulus surrounding it. The width of this annulus is adjustable by means of a shim. The shim simply consists of a cylindric short length.

In case of air atomised combustion, the atomising air was known as primary air. The remainder of air required for the gasification reactions was known as secondary air and was injected into the gasification space through a set of nozzles arranged radially in both refractory cones. Most of the heat loss through the cone walls was taken up by the secondary

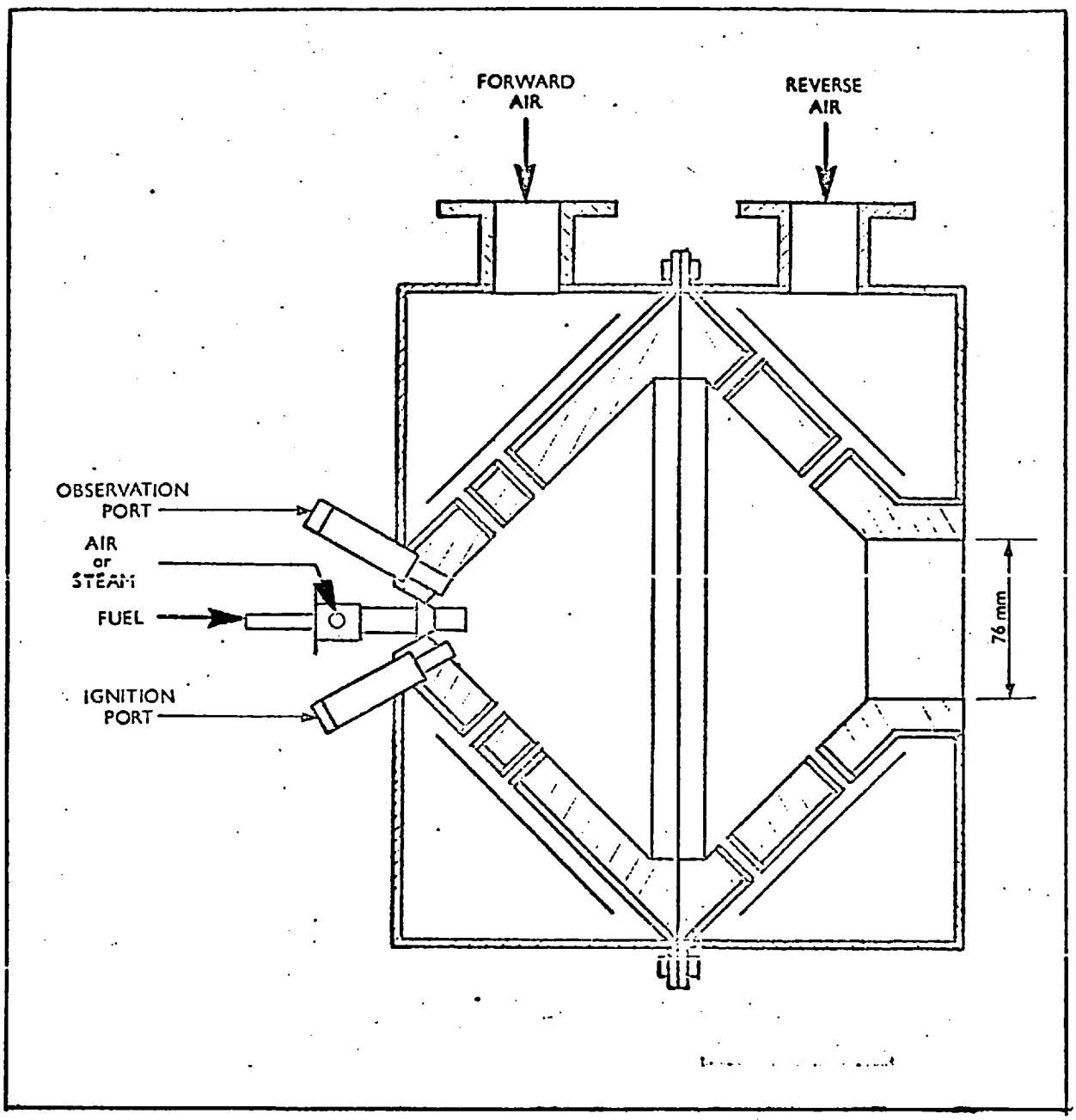

FIG. 3.2 FIRST STAGE COMBUSTION CHAMBER Ref(3)

air as sensible heat and brought back into the chamber, thus allowing only small losses. During the experimental runs, the gasifier outer surface temperature was kept as low as 40°C due to air cooling.

The primary air to the atomiser was supplied by a hydrovane compressor, and the atomising pressure was kept just above 1 bar (15 psig) thus ensuring sonic conditions.

The secondary air was supplied by a centrifugal fan at differential pressure of 0.1 bar and a capacity of 38 g/s.

During steam atomised runs, steam from the main was used. The wet steam was passed through a constant pressure reducing valve and a condensate trap. Between the reducing valve and the atomiser the steam was superheated by a 2KW heating tape. The degree of superheating was controlled by a Variac Variable transformer. In such a system atomising steam temperatures as high as 200°C were achieved. Steam mass flow rate was determined by temperature and pressure measurements and from calibration data for air. Atomiser calibration for a particular shim size is a correlation between atomising pressure and the correspondent mass flow rate of atomising fluid at one temperature. Atomiser calibration curves for air at 50°C and superheated steam at 200°C and for a shim size of 7.27 mm can be found in Appendix 8.3.

The fuel supply to the gasifier consisted in two storage drums kept outside the laboratory and containing gas oil and residual "Vanilla" fuel oil. In the present work gas oil was only used for start-up and shut-down operations. Ignition of the fuel-air mixture was achieved by an electrically triggered pyrotechnic ignitor. A stable flame was rapidly formed at various fuel flow rates. After a reasonable period (1 - 2 hrs) when temperature indicators and strategically located thermocouples throughout the plant revealed stable thermic conditions, the fuel supply

was switched from gas oil to residual fuel oil. Either fuel injections were obtained by a fuel metering pump of a variable throughput of 0 to 6 g/s.

3.1.2. Second Stage Combustion Chamber. Combustion products from the gasifier passed through the interstage cooling section and then to the second stage combustion chamber and were mixed with air flowing counter-current through four radially disposed tangential nozzles (70).

The second stage combustion chamber is illustrated in Fig. 3.3. It has a combustion volume of 0.012 m^3 and was 1.32 metres long, and combustion intensities of 6.34 MW/m^3 have been reported (2). Heat was transferred from the refractories to preheat the air intake to the chamber by tubes along the chamber length. A greater quantity of air than the required amount for combustion was fanned to the second stage, which kept the refractories cool. The excess of air required was then vented by an air return line. The air entering the combustion chamber for combustion was the difference between the total air supplied and the air in the return line.

The air supplied to the second stage was known as tertiary air and was delivered by a Blackman Cast Iron Blower rated at 0.0258 m^3/s at 15°C and pressure of 0.1 bar.

3.1.3. The Solid Collecting System. After the hot gases pass the sampling T-piece they reach the solid collecting system which can be divided into four major aprts as can be seen in Fig. 3.4. They are: the quenching section, the scrubber section, the cyclone and the collecting tank.

The quenching section function was to quench the hot combustion products to about 130°C. Quenching water was pumped to a ring of 6 nozzles. Each nozzle has three orifices, thus forming 18 jets perpendicular to the hot gas stream. The hot gases were cooled down by evaporation of

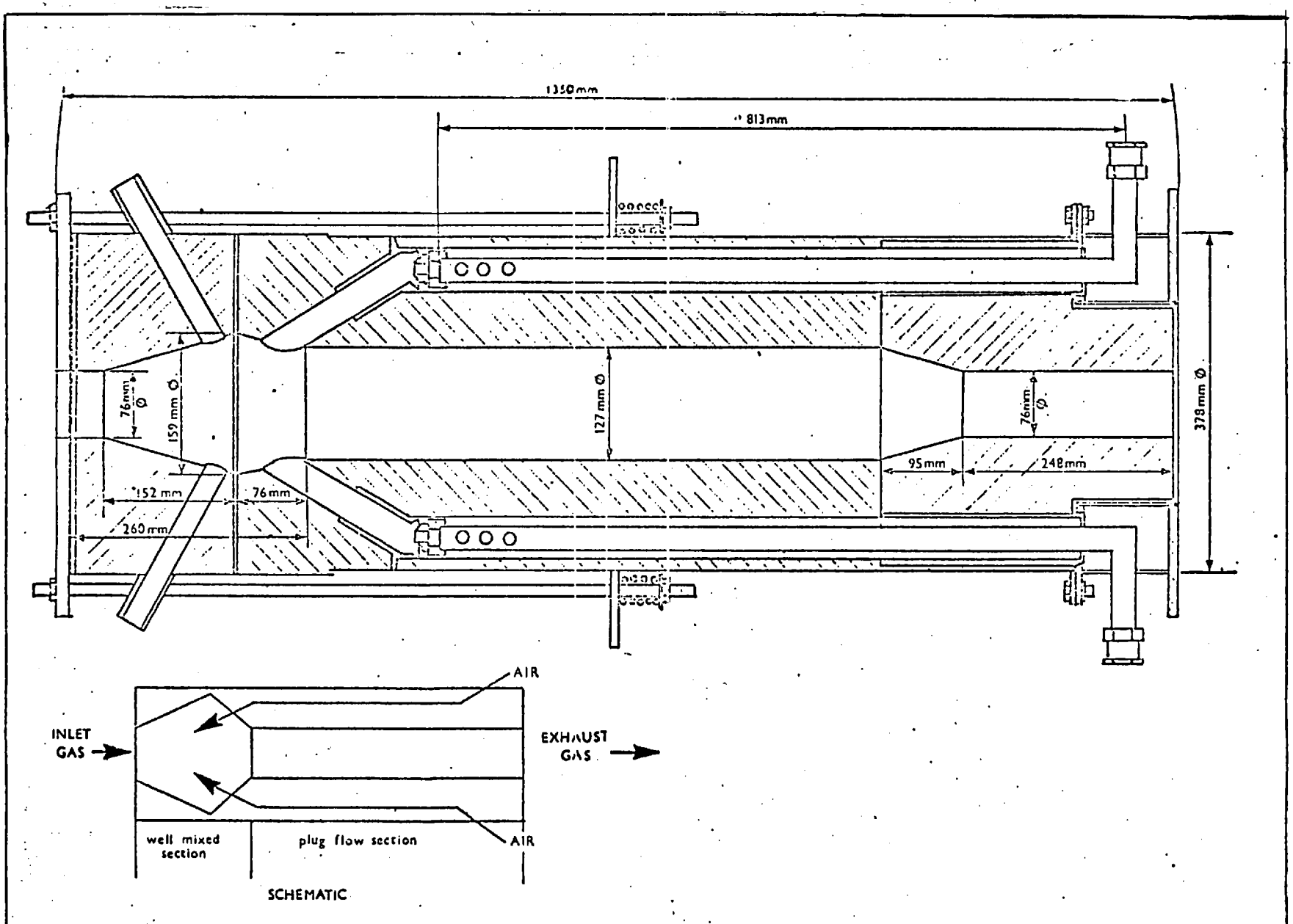

FIG. 3-3 SECOND STAGE CHAMBER Ref(3).

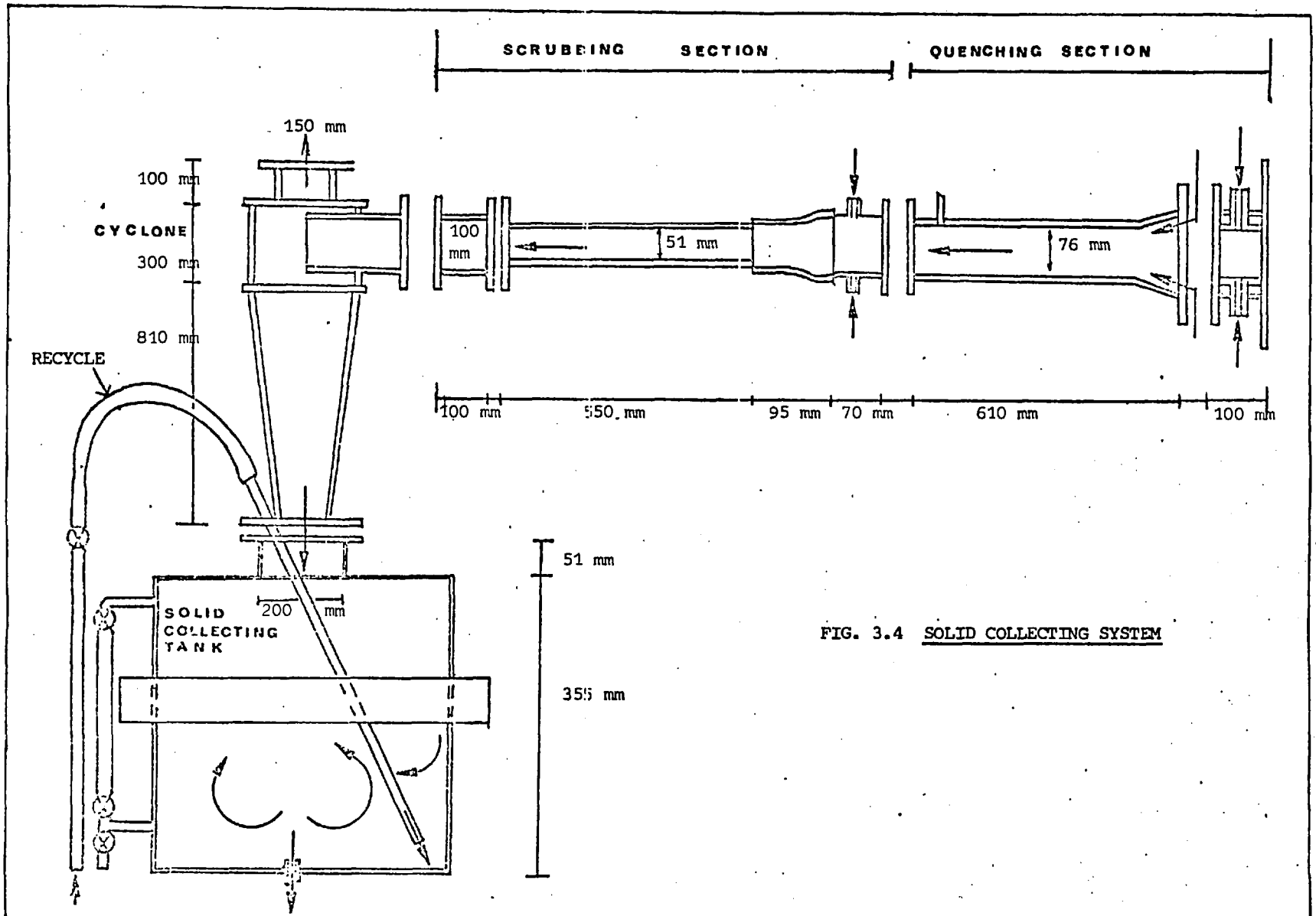

FIG. 3.4 SOLID COLLECTING SYSTEM

the drops provided by the jets. Water supply to the six quenching nozzles totalled 20 g/s at a differential pressure of 0.136 bar (2 psig).

In order to avoid solid deposition on the inner surfaces of the region immediatley after the quenching nozzles wall nozzles were used. They constitute a set of six ceramic fan spray nozzles radially arranged directed along the wall and inpinging on it. The water mass flow rate through this set of nozzles was 13 g/s and a differential pressure of 1.13 bar (17 psig).

The scrubber section consists of a set of six three-orifice nozzles located around the throat of a venturi type short length. The jets were directed perpendicular to the gas stream, forming clouds of water drops. The total water mass flow rate through the scrubber nozzles was of 70 g/s at a differential pressure of 0.65 bar (10 psig). Small solid particles passing through the scrubber section were retained by impaction on the large drops., coagulation follows with a consequent slurry formation. No evaporation of the scrubber section drops should take place since the hot gases were quenched down to around 130°C.

Flue gases from the scrubber section then passed to a cyclone at velocity of about 25 m/s, where the solid containing drops were separated from the gaseous phase. Clean gases were vented to the stack and the slurry went down to the collector tank. Suction was provided by a Sturtavent Seven Stage Centrifugal Extractor rated at 37.8 g/s and a pressure of 0.7 bar.

The collector tank was located at the bottom of the cyclone serving as a slurry reservoir. Operating under steady state conditions its liquid level was effectively controlled by the use of the recycle and the outlet line valve, and the mixture kept in a high degree of mixing. The slurry was pumped out of the tank by a Mono pump type M25 rated at 330 g/s

either to a vacuum filter or to waste. After certain period of operation (60-70 hrs) the inlet of the mono-pump was found to tend to get blocked by heavy insoluble solids, thus a similar alternative pump (named Emergency pump) was fitted to the tank ensuring continuity of the operation (see Fig. 3.5). Temperature measurements of the slurry in the collecting tank indicated values around $80^{o}C$.

Details of the quenching and scrubber nozzles as well as a cross sectional view of the quenching and scrubber nozzles arrangements are given in Figs. 3.6 and 3.7.

3.2 Experimental Programme.

A series of runs was devised in order to fullfill the experimental investigation of three main areas in spray combustion of residual fuel oil in a two stage system. These areas comprise : a) Solid loading from the second stage using both air or superheated steam as atomising fluid. b) Distribution of the main impurities (vanadium, nickel, sodium and sulphur) in the solid products of combustion as a function of combustion parameters to enable an investigation of the behaviour of these impurities during two stage combustion to be undertaken. c) Gaseous emission from the combustion plant particularly those referred to as pollutants such as NO_x and SO_2.

Thus, according to the objectives two series of runs were devised, namely series A and series S. The former constituted air atomised runs and the latter steam atomised ones. In each case the combustion parameters were given by the mass fuel flow rate, atomising fluid to fuel mass ratio and the first stage equivalence ratio (ϕ_1). Overall equivalence ratio was maintained at one ($\phi_2 = 1.0$). The aero-dynamic configuration of the first stage as determined by the forward to reverse air ratio was kept constant and equal to one throughout the runs. The shim size of the

atomiser was also kept constant at 7.27 mm (0.2865 in). The air atomised runs actually totalled 21 compared with 15 steam atomised ones. The settings and the obtained results are tabulated in appendix 8.1.

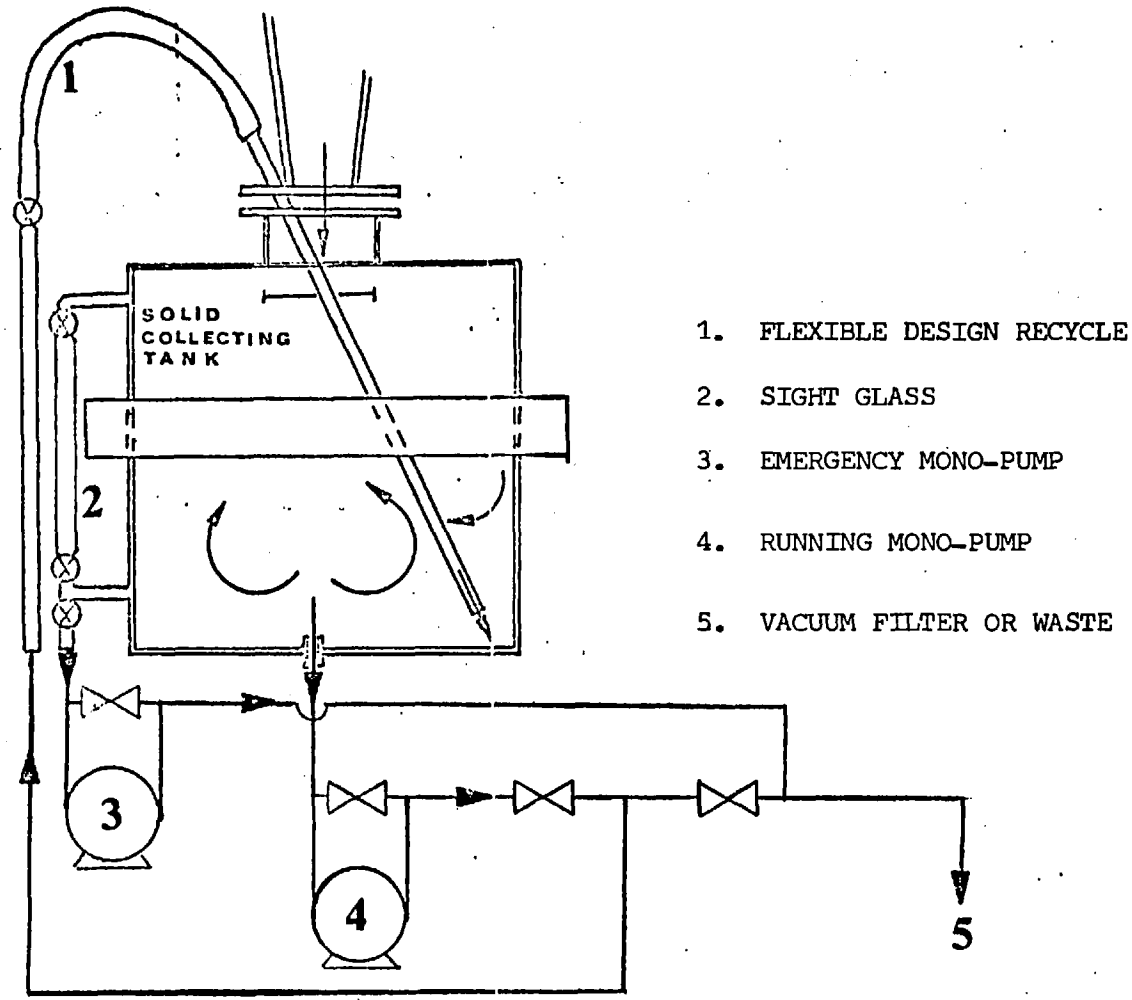

FIG. 3.5 FLOW DIAGRAM OF THE SOLID COLLECTING TANK.

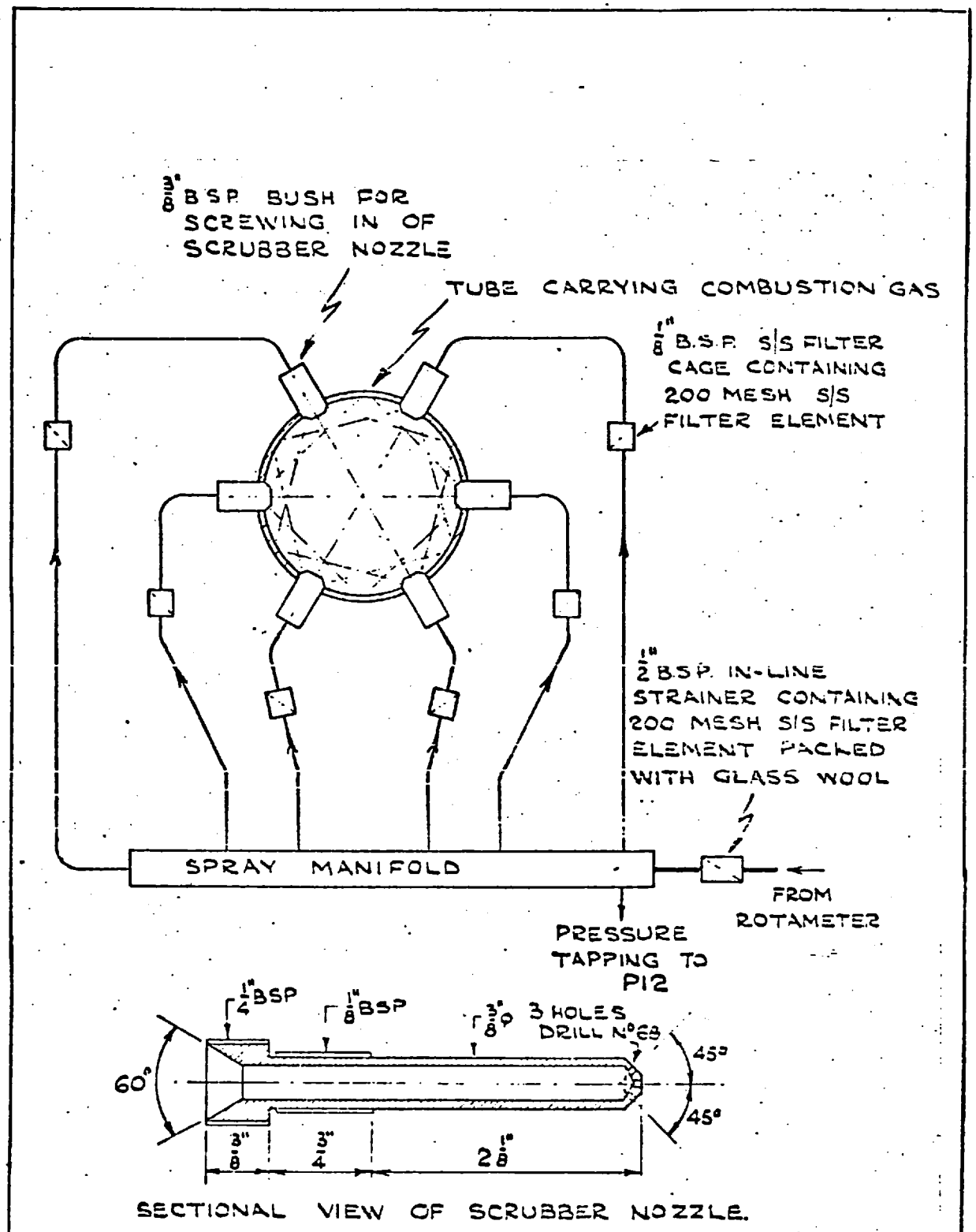

FIG. 3.6 CROSS SECTIONAL VIEW OF QUENCHING SECTION Ref.(1)

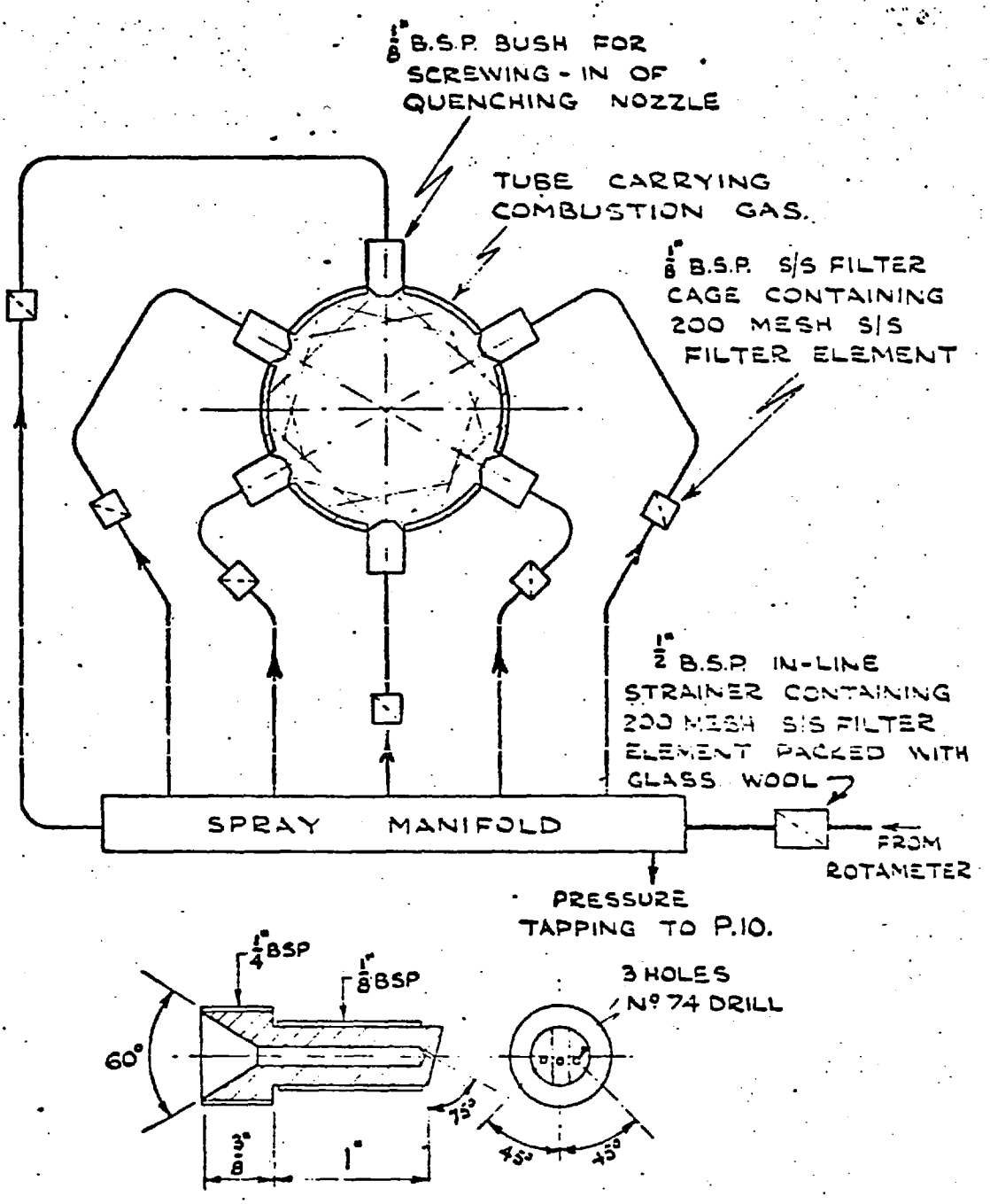

FIG. 3.7 CROSS SECTIONAL VIEW OF SCRUBBING SECTION Ref.(1)

CHAPTER 4

MEASUREMENT TECHNIQUES

A variety of techniques were employed in the investigation of gaseous and particulate emission from the two-stage combustion plant burning "Vanilla" residual fuel oil.

Measurements were made on the gaseous products of combustion and on the solids collected by the collector tank. Determination of the major components of the gaseous phase was made. NO_x and SO_2 concentrations were also obtained.

Fig. 4.1 shows the points in the experimental system where measurements were made.

Gas composition from first and second stage of the system was possible by means of specially designed steam cooled probes inserted through sampling ports in the X-piece and T-piece (1).

The solid products were collected using the scrubber-cyclon-collector tank described in Chapter 3.

Separation was carried out by using a vacuum filter attached to the outlet of the collector tank. After drying and weighing, the samples were analysed in order to obtaincomposition of vanadium, sodium, nickel and sulphur. To this end X-ray fluorescence and flame fotometry was used. An X-ray diffraction analysis was carried out in order to identify the major non-carbonaceous compounds. Lastly, a novel method for determining carbon and hydrogen composition of the solid was used, which includes both total combustion and chromatographic determination of its products.

A multi-point temperature recorder was utilized linking a 16 thermocouple system located at strategic points over the combustion plant. The

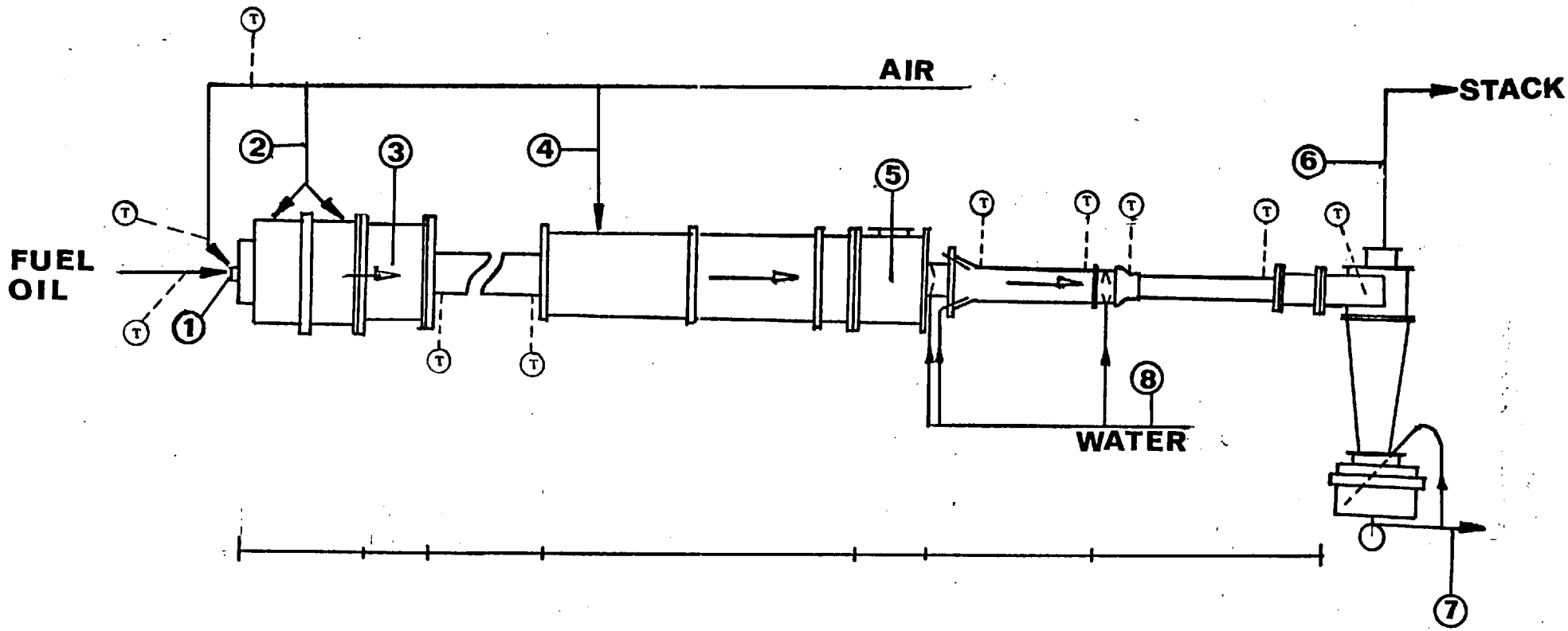

1 Air or steam mass flow rate
Fuel oil mass flow rate

2 Secondary air mass flow rate

3 Gas Composition: a) Gas chromatography Unit
b) Chemiluminescence Unit

4. Tertiary air mass flow rate

5 Gas Composition: a) Gas Chromatography Unit
b) Chemiluminescence Unit

6 Check-up for solids

7 Solid collecting point;
leading to: a) Solid loading
b) Elemental Analysis of solid for V, Ni, Na, S,C, and H

8 Quenching, wall and scrubber nozzles water flow rates,

T Temperature Measurement

Fig. 4.1 Measurements in the Two-stage Combustion Plant

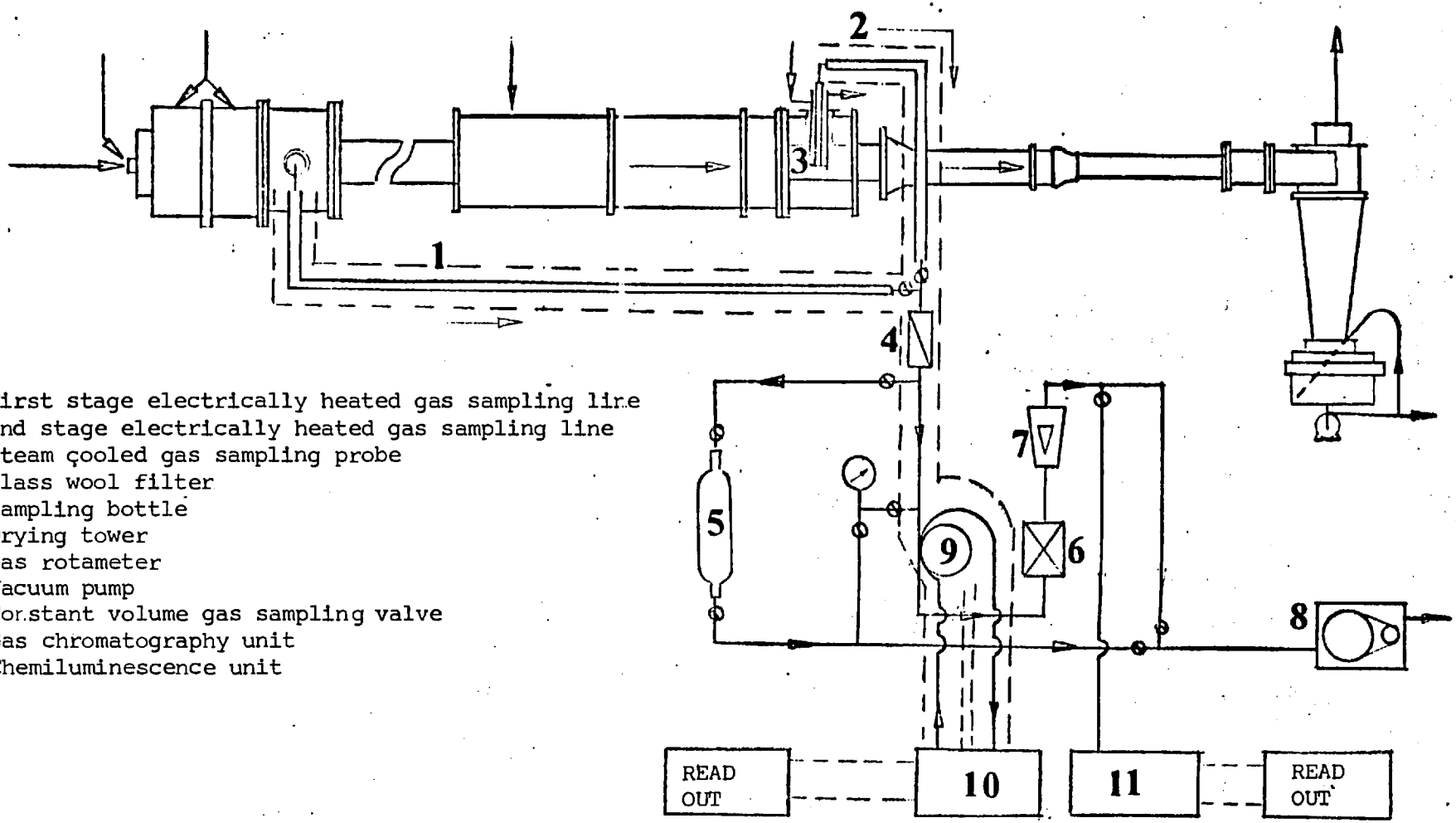

1. First stage electrically heated gas sampling line
2. 2nd stage electrically heated gas sampling line
3. Steam cooled gas sampling probe
4. Glass wool filter
5. Sampling bottle
6. Drying tower
7. Gas rotameter
8. Vacuum pump
9. Constant volume gas sampling valve
10. Gas chromatography unit
11. Chemiluminescence unit

Fig. 4.2 Gas Sampling and Analysis Arrangement

continuous recording of temperature was found very useful when trying to identify stable operational conditions.

4.1. Gas Composition.

The gas sampling system diagram is presented in Fig. 4.2. As it can be seen the set up provides sampling facilities for both the gasifier (X-piece) and the converter (T-piece). The sample to be analysed was sucked through a 6.25 mm x 0.65 m steam cooled stainless steel probe along an electrically heated line into the actual analyser. The heated line was kept at about 120°C so no condensation of the components would occur. The analyser could be a gas chromatography unit or a chemilumicescence unit.

The gas sampling system was also provided with a section designed for bottling samples. This arrangement was devised for measuring SO_2 by mass spectrometry and also as a check for other methods.

4.1.1 Gas Chromatography. Determination of CO_2, CO, O_2, N_2, H_2, CH_4 and SO_2 was made possible by using gas chromatography. The arrangement was devised by Archer (35) and it was originally designed for determination of CO_2, C_2H_4, H_2, O_2, N_2, H_2O, CH_4, CO, and C_2H_6 in flue gases.

The set-up basically comprises a Perkin-Elmer Model 452 Hot-wire gas chromatography unit, fitted with a constant volume (0.25 cm^3) gas sampling valve, a Biotron four-part column switching valve, a 4 m x 0.475 cm diameter "Poropak Q" column and a 2 m x 0.475 cm diameter P.T.F.E. tube molecular sieve 5A column. Both column packings were graded between 80 and 100 BSS Mesh. Helium was used as sample carrier.

During the actual analysis the columns and the detector were kept at oven temperature of 80°C, thus allowing SO_2 separation in the Poropak Q column (44, 45, 46, 47). A Helium inlet pressure of 2 bars (25 psig) was used.

In Fig. 4.3 a diagram of the arrangement of the columns is presented. The Poropak Column function was to separate CO_2, H_2O, and SO_2, whereas the molecular sieve column was to separate CO, H_2, O_2, N_2 and CH_4. By switching the Biotron valve H_2O, CO_2 and SO_2 passed directly into the detector and were prevented from reaching the molecular sieve column thus avoiding irreversible absorption of these polar compounds.

4.1.2. Chemiluminescence. Reaction of common air pollutants such as NO and NO_2 with certain second reactants such as ozone or oxygen are known to result in light emission. Chemiluminescent gas phase reactions of nitric oxide with ozone have been used for the determination of nitric oxide (49). The method is based on the light generated by the chemiluminescen reaction of NO and O_3;

$$NO + O_3 \longrightarrow NO_2 + O_2 + h\nu \quad \ldots\ldots\ldots\ldots\ldots\ldots \quad (4.1)$$

whose intensity is monitored through an optical filter by a high sensitivity photomultiplier. In an evaluation of this technique in measuring oxides of nitrogen in combustion products the response of the instrument has been found (51) to be linear over the range 0 to 1000 ppm.

NO and NO_x concentrations were measured in both sampling ports, viz. X-piece and T-piece by using a thermo-electrons model 12A chemiluminescent analyser, based on the above reaction 4.1 of nitric oxide and ozone. This instrument provided a fast response and accurate technique for monitoring NO and NO_2 in combustion gases ranging from 0.01 ppm to 1000 ppm.

To measure NO concentrations, the gas sample to be analysed is blended with O_3 in a flow reactor. The resulting chemiluminescence is monitored through an optical filter by a high sensitivity photomultiplier.

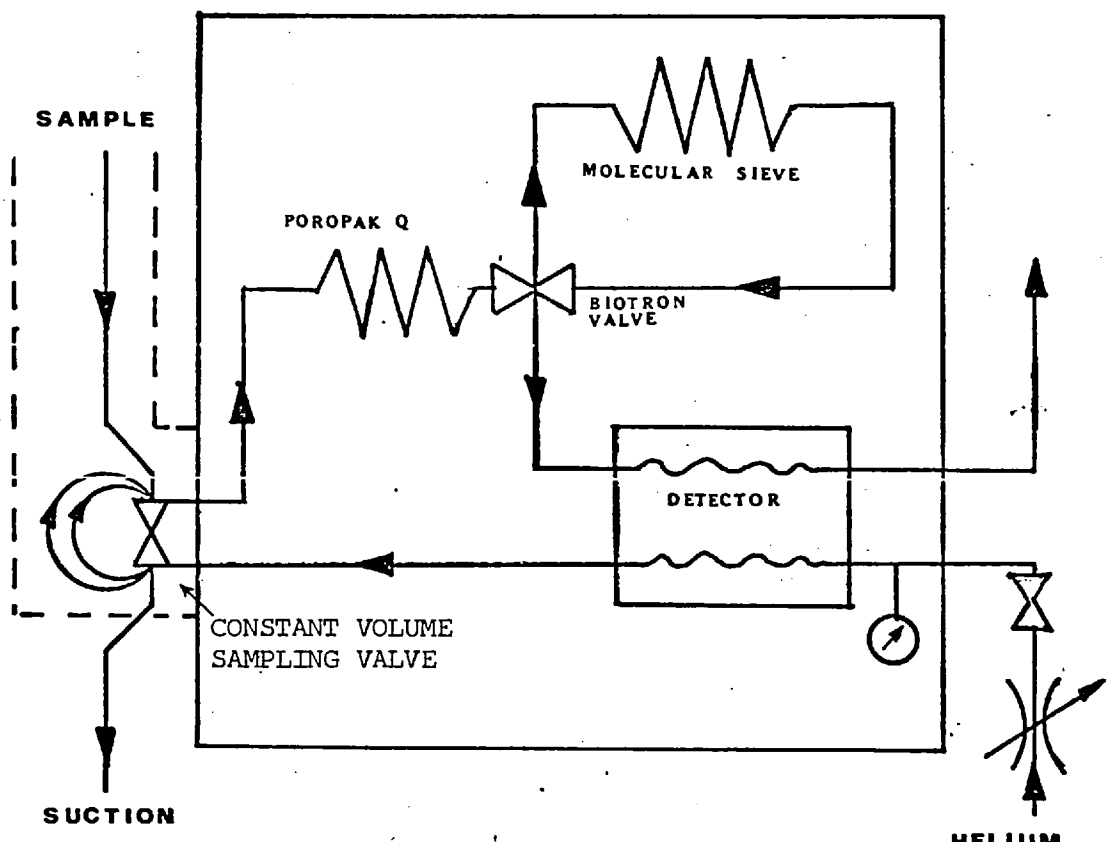

FIG. 4.3 FLOW DIAGRAM OF THE GAS CHROMATOGRAPHY UNIT

The filter-photomultiplier combination responds to light in a narrow wavelength band, unique to the reaction 4.1, hence no interference is expected.

The light intensity of the NO/O_3 reaction is given by (49):

$$I = 12 \left\{\exp(-4180 \pm 300)/RT\right\} \left\{ [NO]\,[O_3] / [M] \right\} \quad \ldots . \quad (4.2)$$

for the 6000 to 8750 A° region for M ≡ Air. Where I is radiation intensity, einsteins/cm^3S and the concentrations of NO, O_3 and Air in g-mol/cm^3.

The flow parameters of the reaction chamber can be adjusted ($[O_3]$, $[M] \gg [NO]$) in such a way that output from the photmultiplier is approximately linear to the NO concentrations.

To measure NO_x (=NO + NO_2) concentrations the sample gas is diverted into a NO_2 - to - NO converter, therefore the photomultiplier output will be linearly proportional to the NO_x concentration in the gas.

A schematic flow diagram of the analyser unit is presented in Fig. 4.4.

The reaction chamber was maintained at a pressure within the range of 400 to 1333 N/m^2 (3-10 mm Hg).

The ozone is obtained from oxygen that is introduced through the oxygen regulator to the ozone generator. At air flow rate of about 1.1 cm^3/s a conversion of about 0.2 of the oxygen to ozone was obtained. The sample whose NO_x concentration is to be determined is introduced by the sampling port and to the NO_2-to-NO converter or bypassing the converter. In the first case NO_x will be determined whereas the latter the NO content of the sample is obtained. The network of capillaries and pressure regulators was designed to provide a highly constant flow into

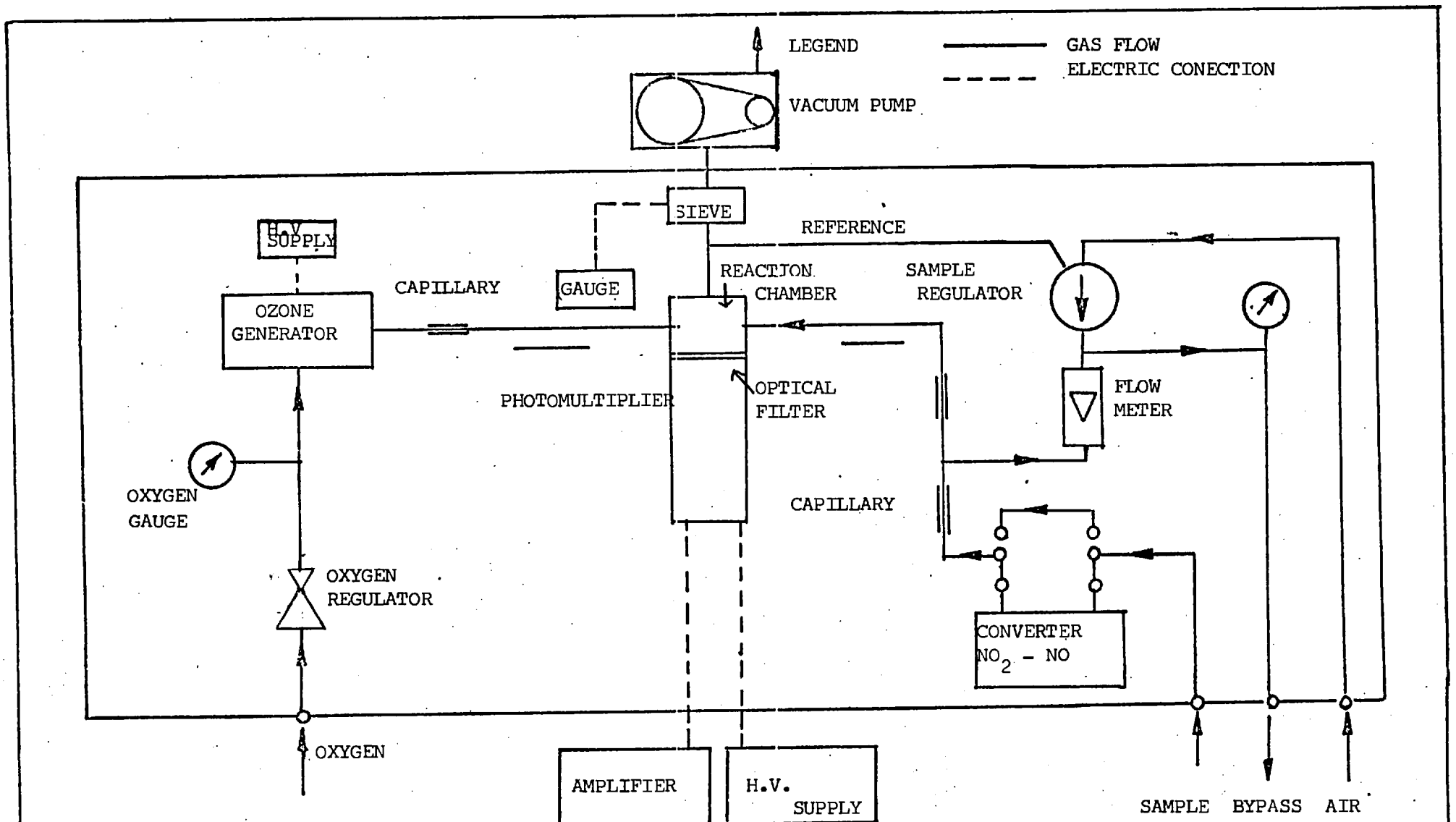

FIG. 4.4 CHEMILUMINESCENT UNIT FLOW DIAGRAM

the reaction chamber, over a wide range of sample source pressures and flow rates.

The high sensitivity photomultiplier is positioned at the end of the reactor; the filter limits the optical bandwidth to a narrow range specific to the chemiluminescent reaction of nitric oxide and ozone. The anode current from the photmultiplier is proportional to the NO concentrations up to 1000 ppm.

4.1.3 Mass Spectrometry. The basic function of the mass spectrometer is to produce ions from a sample, than separate them according to their mass to charge ratio (m/e). Ions travelling through a magnetic field experience a force that is perpendicular to the magnetic field and to their direction of travel. The magnitude of this force depends on the velocity of the ion, which in turn depends on the mass and charge of the ion. All ions follow essentially the same path through the field-free region, but immediately begin to disperse on entering the magnetic field. For a given magnetic field strength and accelerating voltage, the light ion will be deflected most and the heavy ion least, making their path leading to an ion detector placed at the end of the analyser tube. A record of masses and abundances of the various ions produced from the sample constitutes a mass spectrum.

General comprehensive discussion of the Instrumentation of Mass Spectrometry can be found in Kiser (72). Bottled samples were analysed in order to determine sulphur dioxide concentrations and these were estimated directly from the heights of the mass peaks. The calculations were based on the relative heights of the peaks for sulphur dioxide and nitrogen and comparing to a standard known composition sample.

4.2 Solid Loading Measurements.

The solid collecting system was described in detail in Section 3.1.3. and a diagram is presented in Fig. 3.4.

Solid loading measurements were based on the slurry collected in the collector tank situated at the bottom of the cyclone. Sampling was done from the collector tank outlet during periods of 10 minutes, into a large vacuum filter using filter paper of 320 mm diameter (Whatman No.1). In order to obtain representative samples two factors had to be fulfilled: Good mixing and steady state flow conditions. The former was attained by using the recycle specially designed to obtain tank in-flow recirculation. The latter was attained after a warm-up period of about one hour for every setting. A glass level fitted to the tank was used to identify this condition. During the actual runs the stack gases were checked for solids which gives an indication of the performance of the scrubbing section spray system. Solids collected in the filter were dried and weighed. Drying was done for periods of 10 - 15 hours in an oven at about 100^{o}C. After drying, the samples were placed in air-tight bottles since a higroscopic tendency was noted.

4.3 Elemental Analysis of Solids.

Solids collected in the system were subjected to elemental analysis in order to determine contents of carbon, hydrogen, vanadium, nickel, sodium and sulphur. The final scheme for solid sample analysis is illustrated in Fig. 4.5.

Carbon and hydrogen content were determined by the use of an elemental analyser Model 1102 which is an instrument specifically designed for the determination of carbon, hydrogen, nitrogen and oxygen content in organic materials.

The basic principles for CHN determination employed by the Elemental Analyser can be summarized as follows:

The organic material whose CHN composition is to be determined is weighed in a tin container. The container is loaded into an automatic sampler which drops it into an oxidation tube where the organic

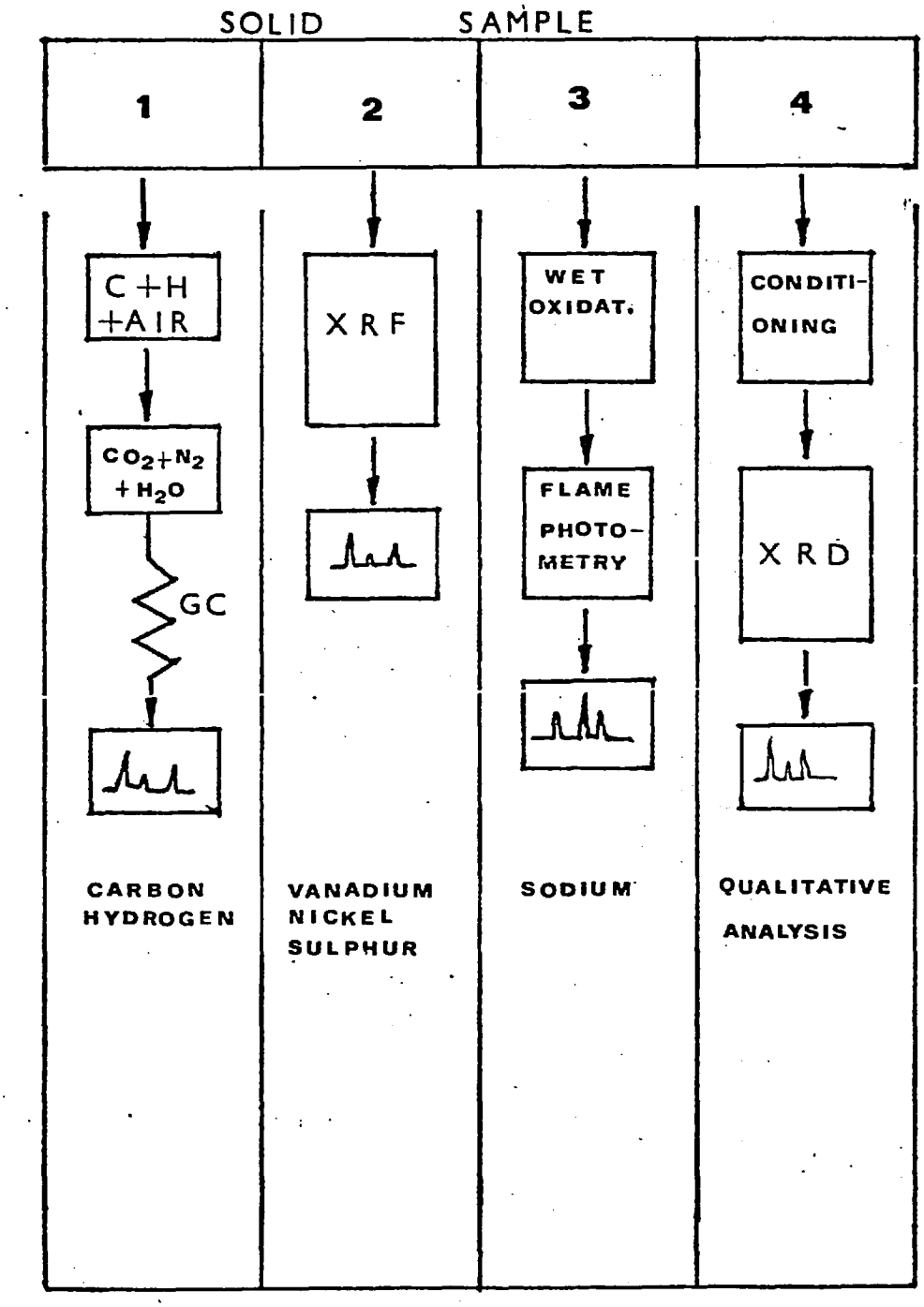

GC : GAS CHROMATOGRAPHY
XRF : X-RAY FLUORESCENCE
XRD : X-RAY DIFFRACTION

FIG. 4.5 SOLID SAMPLE ANALYSIS

substance is pyrolised in an oxygen-rich atmosphere. The decomposition products are carried away by a constant stream of helium through a reactor filled with Cr_2O_3 amd Co_3O_4 and converted to the desired state of oxidation namely CO_2,H_2O and NO_x. This mixture passes through a tube packed with reduced copper to reduce nitrogen oxides to elemental nitrogen. The products are carried by helium into a chromatographic 3 metres long column packed with Poropak 80/100, where N_2, CO_2 and H_2O are separated. As each component elutes from the column, it enters a thermal conductivity detector which develops a signal. The signal is then sent to a potentiometric recorder where it is recorded as a peak. Either peak-area or peak-height measurement is used to determine the CHN content of the sample by referring to the values given by a standard sample, run using same conditions. Appendix 8.5 presents the basic equations and procedure in carbon and hydrogen determination by this method.

The amounts of vanadium, nickel and sulphur were determined by X-ray fluorescence (XRF). Unfortunately main impurities Fe and Zn present in the sample absorbed sodium radiation so strongly that at the level of the latter (less than 0.5% w) in the samples it was completly obscured. However, sodium determination was made possible by "wet oxidation" in nitric and sulphuric acids. After eliminating nitric acid and as much as possible sulphuric acid, sodium was determined in the resultant aqueous solution by flame photometry.

4.4 Qualitative Analysis of Chemical Compounds in the Ash.

Solids collected from the collector tank were carefully prepared to be subjected to a qualitative analysis. This analysis was aimed at determining major compounds existing in the solid such as vanadium oxides, sodium sulphate, nickel oxides and sulphates, complexes of vanadium and sodium etc. One of the most succesful methods for detecting compounds

present in a solid sample is X-ray diffraction (XRD). Original samples were pelletized and taken to X-ray analysis. Because carbon was the major constituent of the sample (80 - 85% W) they appeared amorphous to the X-ray beam. Attempts were made to concentrate the relevant matter of the sample. A method was devised to condition the solid samples so the inorganic matter was concentrated enough to be picked up by the resolution of the apparatus. To this end solid samples were placed at 450°C in reducing conditions in a furnace for a period of time sufficiently long to burn off the carbon. It was found 8 hours a convenient period of time.

Standard samples of known constituents placed at similar conditions for over 12 hours showed that conditioning had no effect on the relative amounts of the original constituents.

4.4.1 X-ray Diffraction (XRD). X-rays are electromagnetic waves of wavelength ranging from several hundredths of Angstrom Units to a few Angstrom Units and are produced in X-ray tubes. The fundamental principle of X-ray structural analysis is based on the interaction of X-rays with atoms of the irradiated crystals. The result of this interaction is the reflection of X-rays by the crystal. The resultant reflection is the result of interference of rays that are reflected on neighbouring atomic planes of the crystal, following Bragg's law:

$$n\lambda = 2d \sin\theta \qquad \ldots\ldots\ldots\ldots\ldots\ldots\ldots\ldots \quad (4.3)$$

where, n is an integer

λ : wavelength of the radiation

d : distance between atomic planes

θ : angle between the incident rays and atomic planes.

The registered X-ray reflected constitutes an X-ray diffraction pattern.

Figs. 4.6 and 4.7 present the patterns that were obtained with nickel filtered copper radiation for standard samples of V_2O_5 and V_2O_3 respectively,

whereas Figs. 4.8 an 4.9 present typical X-ray diffraction patterns of the samples under analysis.

On the patterns every radiation intensity peak is located by 2θ , then its corresponding Interplanar spacing "d" is calculated for the particular wavelength for nickel filtered copper radiation by the equation 4.3. The interplanar spacing "d" for the major reflected radiations and its relative intensity is given in Appendix 8.4 (A.S.T.M. index) for relevant compounds.

The X-ray diffraction pattern analysis of the samples was done partly by comparation with known standard samples and partly by using the A.S.T.M. index. In this way comparing interplanar spacings "d" in Figs. 4.6 and 4.7 with Figs. 4.8 and 4.9 it can be seen that the latters contain no V_2O_5 and V_2O_3. Same procedure was followed by patterns of standard samples of Na_2SO_4 and α-$NaVO_3$.

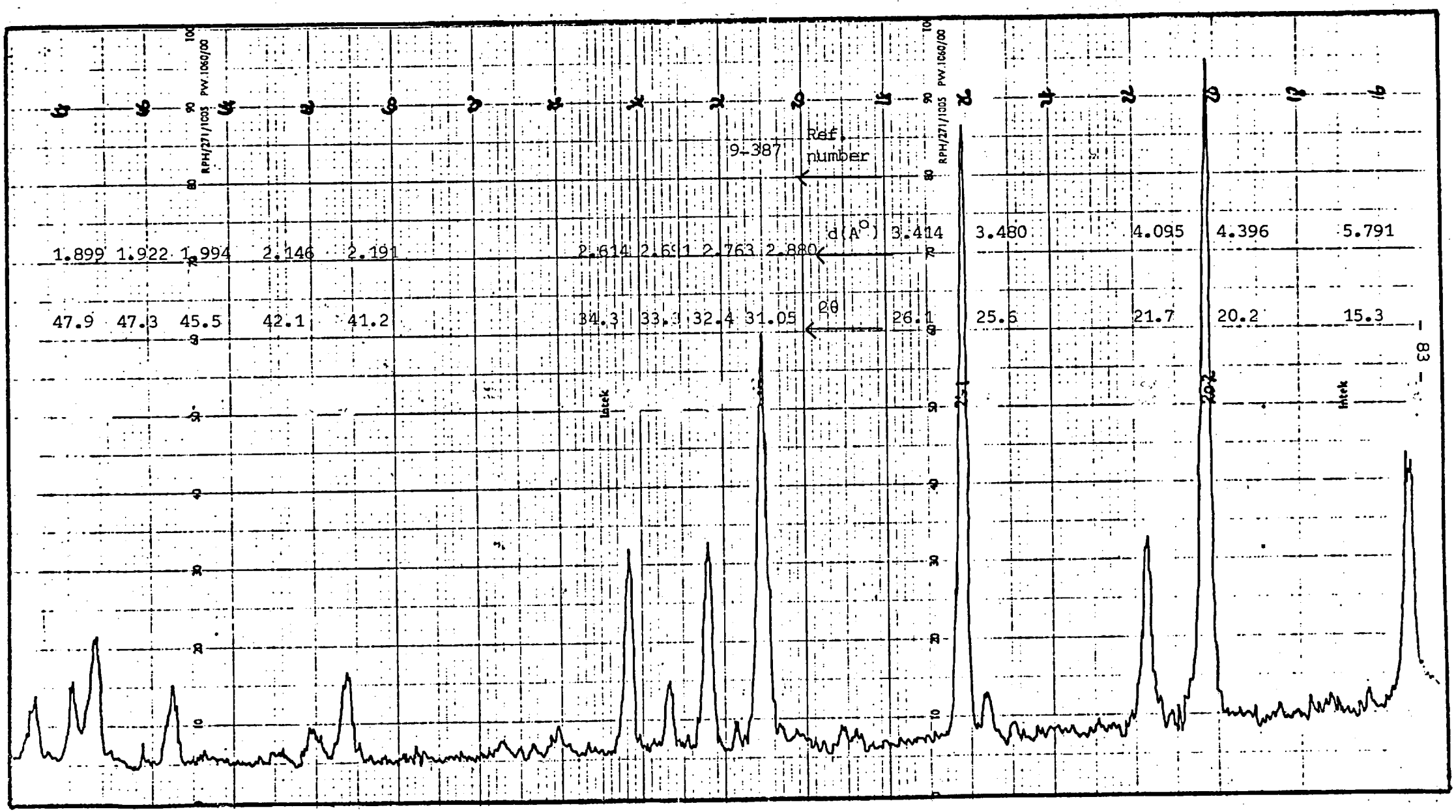

FIG. 4.6 X-RAY DIFFRACTION PATTERN FOR PURE V_2O_5. NICKEL FILTERED COPPER RADIATION

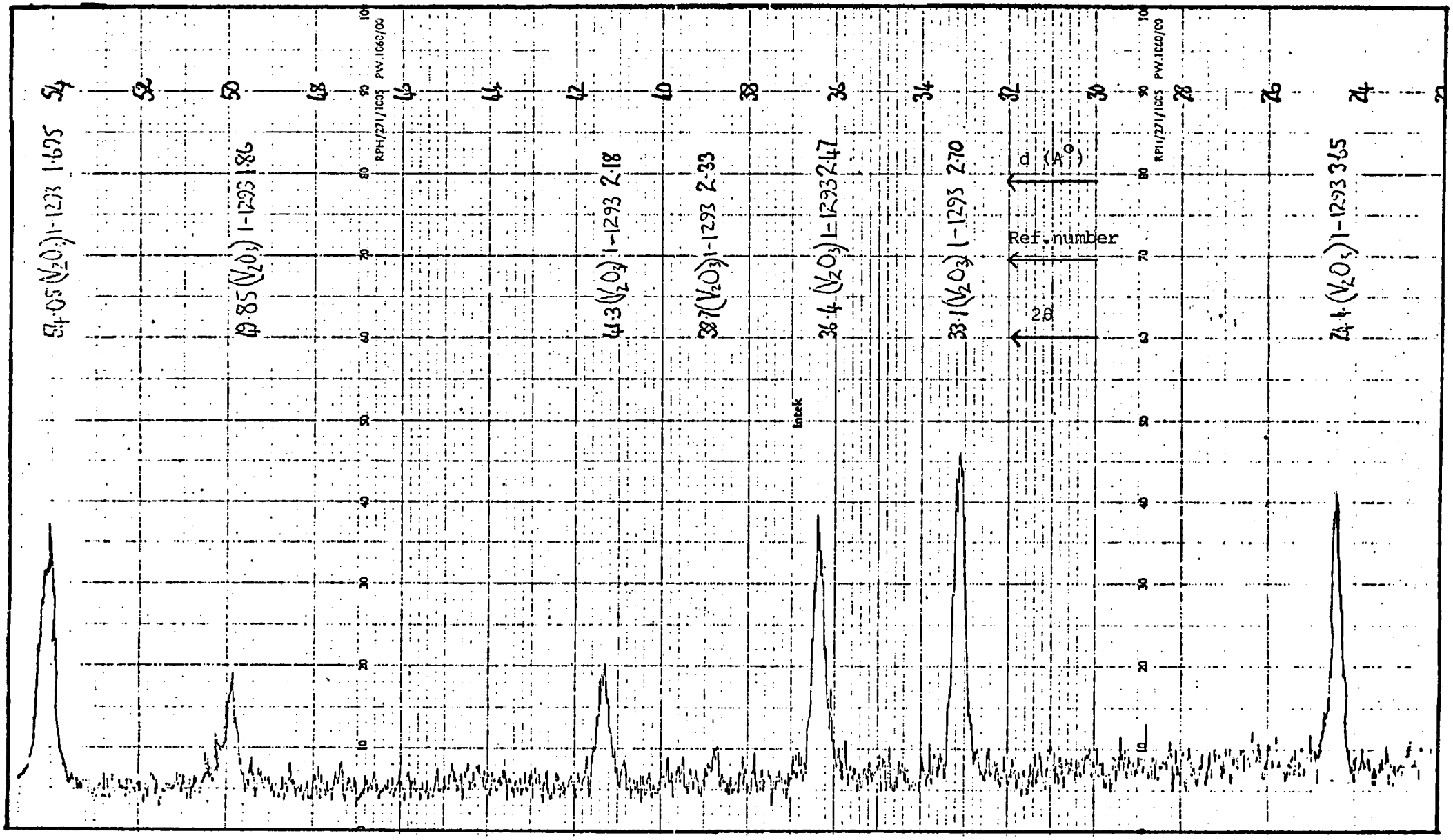

FIG. 4.7 X-RAY DIFFRACTION PATTERN FOR PURE V_2O_3. NICKEL FILTERED COPPER RADIATION

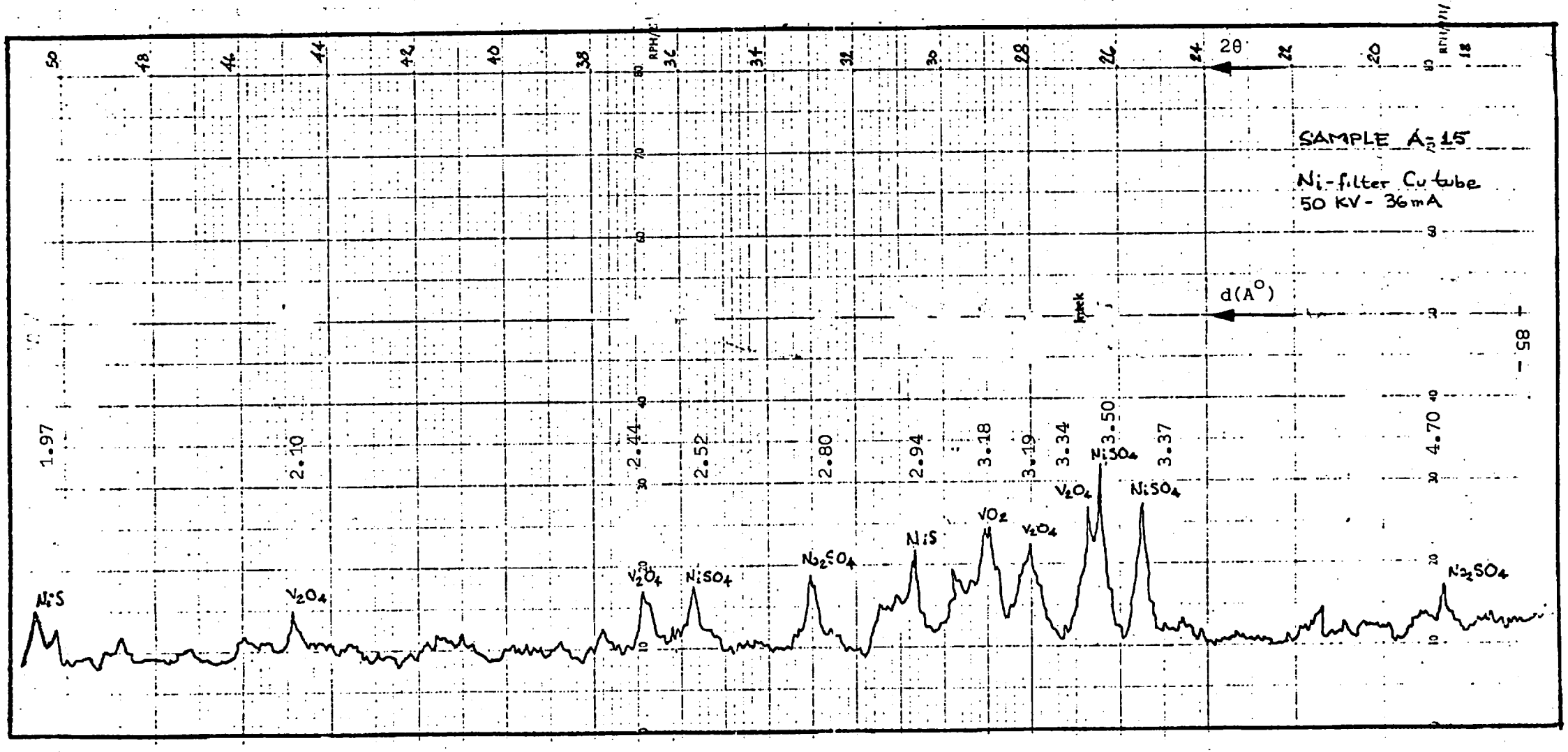

Fig. 4.8 X-ray Diffraction Pattern For Air Atomised Solid Product of Combustion.

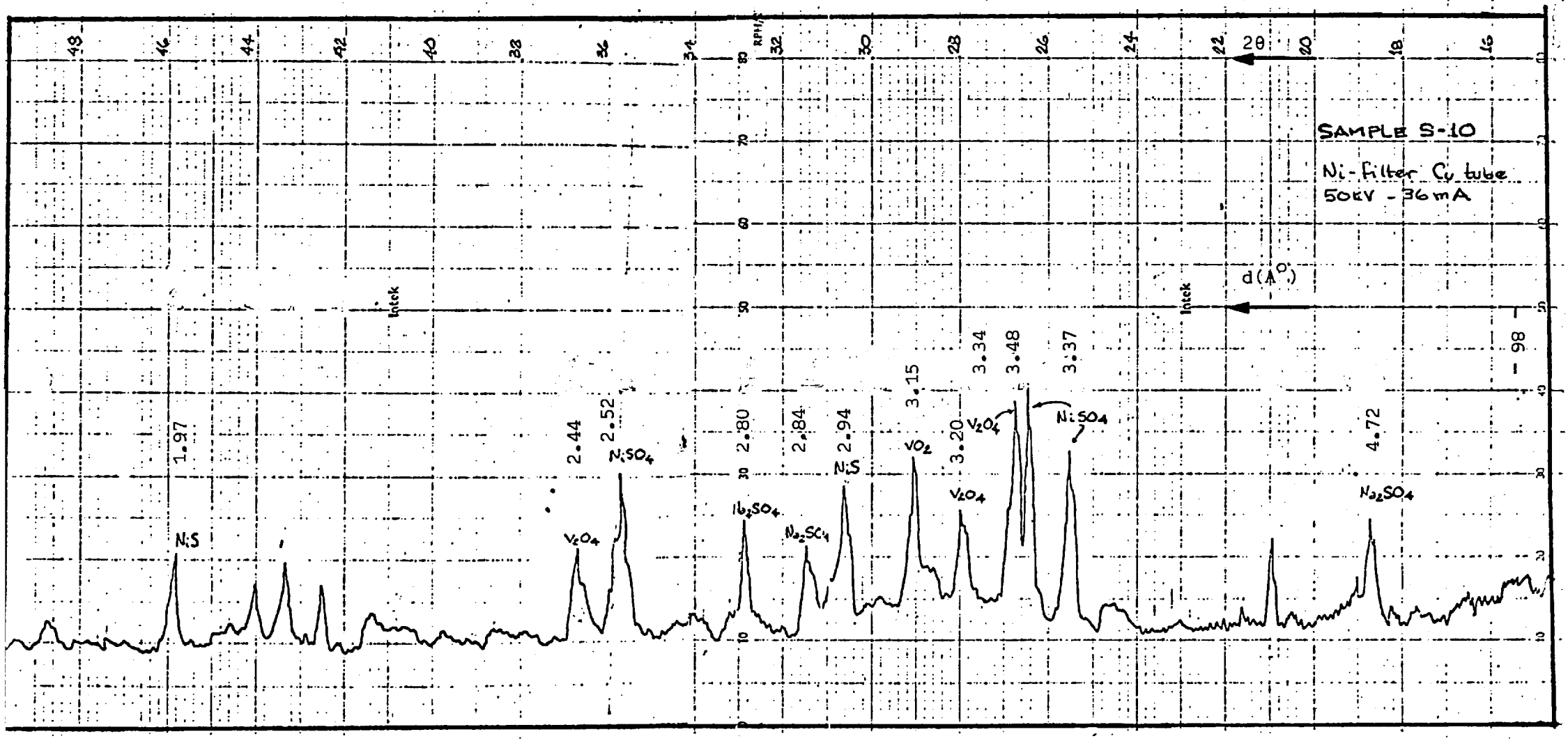

Fig. 4.9 X-ray Diffraction Pattern for Steam Atomised Solid Product of Combustion

CHAPTER 5

THEORETICAL RESULTS

In a chemical reacting mixture thermodynamic equilibrium considerations provide a way of determining maximum attainable values if reactions are allowed to proceed espontaneously. Equilibrium values are not dependant on the kinetics of the process but on the intensive thermodynamic properties that define the system. Thermodynamic predictions using equilibrium criterium are discussed in this chapter. The calculations are applied both to the gaseous products of combustion of fuel oil and to the metallic oxides formed in the solid products. In the former, calculations are done based on 6 gaseous reactions and in the latter predictions on vanadium oxides formation are obtained.

5.1 Equilibrium Models for Gaseous Products

A well established model for the investigation of combustion temperatures and compositions of products from "Vanilla" fuel-oil has been previously used by Johns(66) and Archer (2). It is based on the assumption that products of combustion are in equilibrium according to the so-called water-gas shift reaction:

$$CO\ (g) + H_2O\ (g) \rightleftharpoons CO_2\ (g) + H_2\ (g) \quad \ldots\ldots\ldots\ldots \quad (5.1)$$

An initial approach was instrumented ignoring sulphur content in the residual fuel-oil and ignoring carbon formation as a solid product. A second approach included sulphur in the fuel and considered solid carbon formation. Major gaseous compounds compositions were predicted using both steam and air as atomising fluid.

Finally, in this work a multireaction model was developed involving 11 gaseous compounds so as to obtain thermodynamic equilibrium values for the important pollutants species such as NO_x and SO_x.

5.1.1 Water-gas Shift Reaction Controlling Equilibrium

I. Simple Model (2):

Most important features of this model are:

a) "Vanilla" fuel-oil was represented by the formula $CnH_{1.532n}$ thus ignoring sulphur.

b) No carbon was formed.

c) The gasification model was thus represented:

$$\frac{1}{n} CnH_{1.532n} + aO_2 + hN_2 + mH_2O \longrightarrow$$

$$bCO_2 + cCO + dH_2O + fH_2 + hN_2 \quad \ldots\ldots\ldots \quad (5.2)$$

d) Provisions were taken for steam injection.

e) Water shift reaction was assumed to be controlling the equilibrium of the products

$$CO + H_2O \rightleftharpoons CO_2 + H_2 \quad \ldots\ldots\ldots\ldots\ldots\ldots \quad (5.1)$$

$$K = \exp\left[2.303 \left(36.72508 - \frac{3994.704}{T} + 0.00446241\ T - 6.71\ T^2 \times 10^{-7} - 5.305\ \mathrm{Ln}\ T\right)\right] \quad \ldots\ldots\ldots\ldots \quad (5.3)$$

$$K = \frac{(CO_2)\ (H_2)}{(CO)\ (H_2O)} = \frac{b \times f}{c \times d} \quad \ldots\ldots\ldots\ldots \quad (5.4)$$

where K : Equilibrium Constant

T : Gas Stream Temperature (^{o}K)

The solution of this model is presented in Fig. 5.1, and was obtained combining carbon, hydrogen, nitrogen and oxygen mass balances with enthalpy balance. As it can be seen gas compositions were expressed as CO_2, CO, H_2O, H_2 and N_2 as a function of equivalence ratio for two different atomising steam to fuel mass ratio.

II. Extended Model (2).

The additional improvements of this model to the previous gasification model can be summarized as follows:

a) A more accurate representation of the formula of "Vanilla" fuel-oil is given by $C_n H_{1.532n} S_{0.0104n}$ with a molecular weight of (13.87)n, thus taking sulphur into account.

b) Model is extended to account for sulphur, carbon and methane in the gasification products.

c) The gasification with steam injection of "Vanilla" fuel-oil now may be represented by:

$$\frac{1}{n} CnH_{1.532n}S_{0.0104n} + aO_2 + hN_2 + mH_2O \longrightarrow$$

$$bCO_2 + cCO + dH_2O + fH_2 + hN_2 + wCH_4 + rSO_2 + sC + tS$$

and equilibrium controlled by water-shift gas reaction (eq. 5.1)

The experimental data for carbon, sulphur and methane in the products were used to solve the mass balance equations. The effect of steam injection on combustion gas temperature was obtained by this model and is presented in Fig. 5.2.

Although the author describes in detail the extended model fundamental equations, a graphical solution involving gas composition and temperatures failed to be presented.

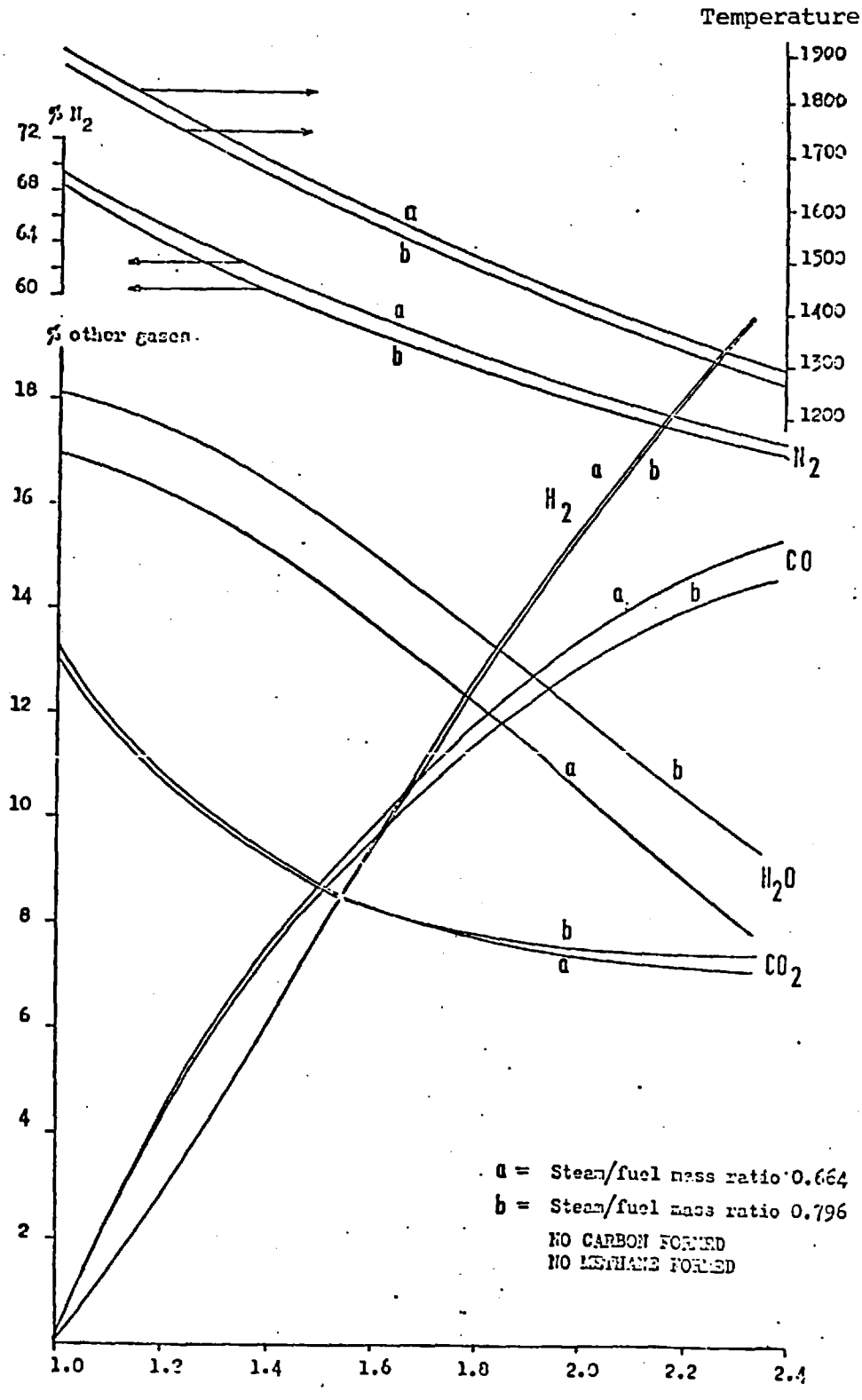

FIG.5.1 WET GAS COMPOSITIONS AND TEMPERATURES FOR SIMPLE EQUILIBRIUM MODEL. Ref. (2)

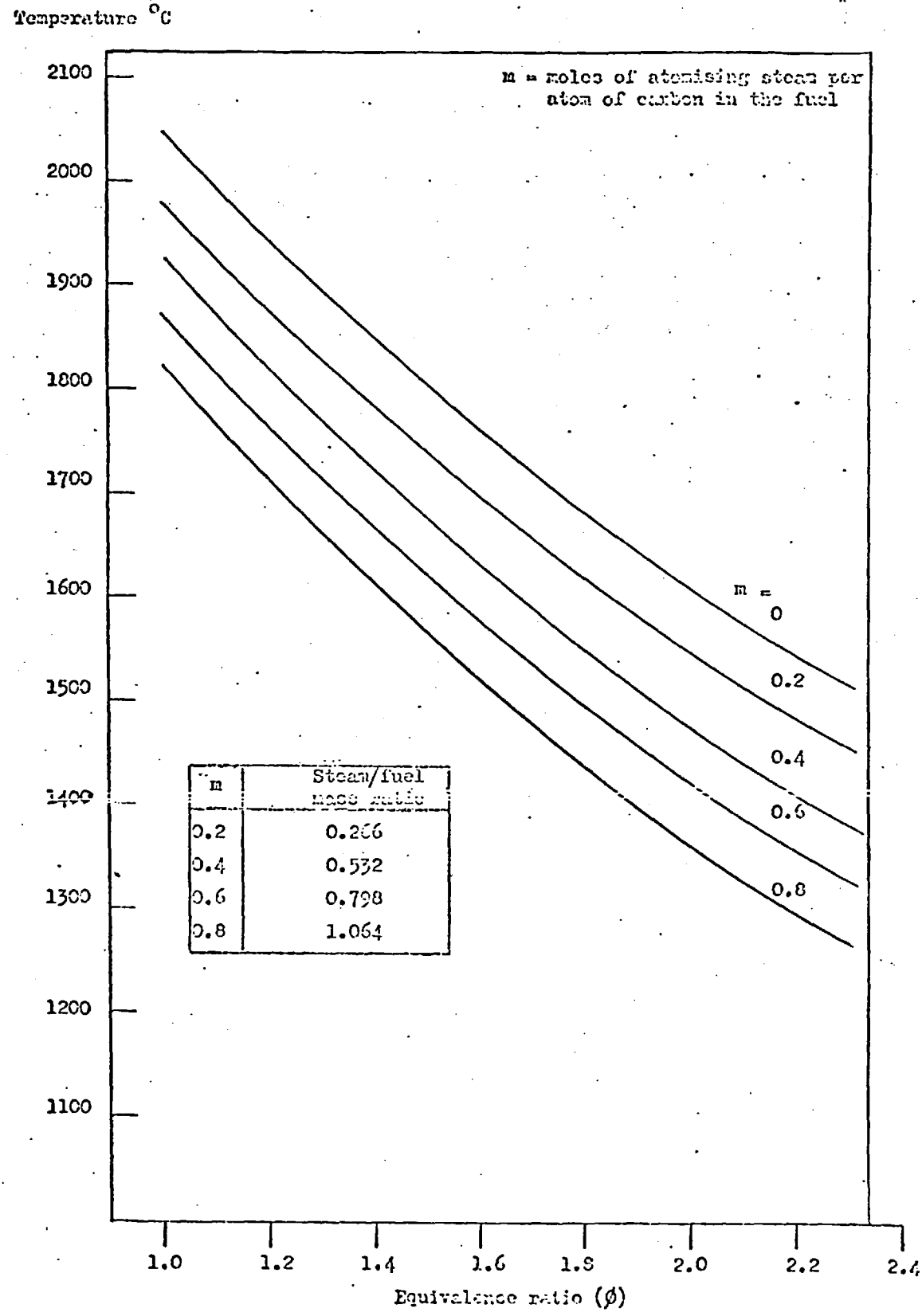

Fig. 5.2 Effect of Steam Injection on combustion gas Temperature as Predicted by the Extended Model Ref.(2)

5.1.2 Multi-reaction Equilibrium Model. In the investigation of compositions of gaseous combustion products resulting from "Vanilla" fuel oil, simple model based on water-shift gas reaction was found (54) to be satisfactory in predicting gas compositions of CO_2, CO, H_2, H_2O and N_2. Nevertheless, there was a need to devise a model which included composition of important gaseous pollutants such as NO, NO_2, SO_2 and SO_3.

The multi-reaction equilibrium model is based on the thermodynamic equilibrium of the following compounds: CO, CO_2, N_2, NO, NO_2, O_2, H_2O, SO_2, SO_3, CH_4 and H_2. The "Vanilla" fuel oil formula was taken as $CnH_{1.532n}S_{0.0104n}$ with a molecular weight of (13.87)n. Complete specification of "Vanilla" fuel is presented in Appendix 8.2.

The minimum set of equations which describe the mentioned eleven compound system is given by the following primary equations:

$$CO + H_2O \rightleftharpoons CO_2 + H_2 \quad \ldots\ldots\ldots\ldots\ldots\ldots \quad (5.6)$$

$$2H_2O \rightleftharpoons 2H_2 + O_2 \quad \ldots\ldots\ldots\ldots\ldots\ldots \quad (5.7)$$

$$CH_4 + 2O_2 \rightleftharpoons CO_2 + 2H_2O \quad \ldots\ldots\ldots\ldots\ldots\ldots \quad (5.8)$$

$$N_2 + O_2 \rightleftharpoons 2NO \quad \ldots\ldots\ldots\ldots\ldots\ldots \quad (5.9)$$

$$NO + \tfrac{1}{2}O_2 \rightleftharpoons NO_2 \quad \ldots\ldots\ldots\ldots\ldots\ldots \quad (5.10)$$

$$SO_2 + \tfrac{1}{2}O_2 \rightleftharpoons SO_3 \quad \ldots\ldots\ldots\ldots\ldots\ldots \quad (5.11)$$

The stoichiometric equation for a single reaction, where components A_1, A_2, A_3, ... react to form the products ..., A_{c-1}, A_c according to the reaction

$$-\alpha_1 A_1 - \alpha_2 A_2 - \cdots \longrightarrow \cdots \alpha_{c-1} A_{c-1} + \alpha_c A_c$$

can be written as:

$$\sum_{i=1}^{c} \alpha_i A_i = 0 \qquad \ldots\ldots\ldots\ldots\ldots\ldots\ldots\ldots\ldots\ldots \quad (5.12)$$

Where α_i is the stoichiometric coefficient of the i th species. α_i is negative if it is a reactant and is positive if it is a product.

A_i is the species i .

In the case when there are several equations occurring simultaneously, a separate equation for each reaction should be written. For N reactions:

$$\sum_{i=1}^{c} \alpha_{ji} A_i = 0 \qquad j = 1,2, \ldots N \quad \ldots\ldots\ldots\ldots \quad (5.13)$$

Where:

j : reaction index.

α_{ji} : stoichiometric coefficient of the i th species in the j th reaction.

N : number of reaction under consideration

The minimum number of primary reactions is equal to the rank of the matrix α_{ij} . Primary reactions are those which are linearly independent. Linearly dependent reactions can be ruled out by means of the Gauss Elimination Algorithm (67) or simply by inspection.

The Criterium for equilibrium when the six primary reactions are competing can be established by saying that the composition at equilibrium is that composition corresponding the minimum total Gibbs Free Energy of the reacting mixture.

The total Gibbs free energy of the system of C components containing N_i moles of component i is written as:

$$G = \sum_{i=1}^{C} N_i \bar{G}_i = \sum_{i=1}^{C} N_i \left[(\bar{G}_i - \underline{G}_i^o) + \underline{G}_i^o \right] \quad \ldots\ldots\ldots\ldots \quad (5.14)$$

where $\bar{G}_i$: free energy of component i

$\underline{G}_i^o$: free energy of component i at standard state.

introducing the concept of fugacity, gives

$$\bar{G}_i - \underline{G}_i^o = RT \ \text{Ln} \ \frac{\bar{f}i}{fi^o} \quad \ldots\ldots\ldots\ldots\ldots\ldots\ldots\ldots \quad (5.15)$$

and assuming the gaseous phase to be an ideal mixture

$$\frac{\bar{f}i}{fi^o} = \frac{N_i}{N}$$

$\bar{f}i$: fugacity of component i in the mixture.

fi^o: fugacity of component i at standard state.

N_i : Number of moles of component i in reacting mixture

N : total number of moles in reacting mixture (including non-reacting species)

equation (5.15) can be written:

$$G = \sum_{i=1}^{C} N_i \left\{ \underline{G}_i^o + RT \ \text{Ln}\left[\frac{N_i}{N}\right] \right\} \quad \ldots\ldots\ldots\ldots\ldots\ldots \quad (5.16)$$

Since equilibrium calculations are done at constant absolute temperature, the above equation may be conveniently written:

$$F = \frac{G}{RT} = \sum_{i=1}^{c} Ni \left\{ \frac{G_i^o}{RT} + Ln\left[\frac{Ni}{N}\right] \right\} \quad \ldots\ldots\ldots\ldots (5.17)$$

The problem is reduced to finding the component amounts N_i which corresponds to the minimum $\frac{G}{RT}$.

The solution is constrained by an additional equation : the conservation of atomic species, thus N_i must satisfy:

$$\sum_{i=1}^{c} a_{ji} N_i = bj \qquad 1 \leq j \leq M \quad \ldots\ldots\ldots\ldots\ldots\ldots (5.18)$$

where:

a_{ji} : Number of atoms of element (atomic) j in a molecule i

M : Number of elements present.

bj : total number of gr-atomes of element j in the reacting mixture.

Minimization of G/RT was performed by the iterative steepest descent method, which assumes an approximate solution for the equilibrium mole numbers,

$N_1^k, N_2^k, \ldots\ldots N_c^k$

which satisfies the conservation of atoms equation (e q.5.18)

A particular application of this method can be found in Balzhiser (68).

In order to determine flame adiabatic temperature and gas stream temperature at different levels of heat removals it became necessary to link the equilibrium equations with those resulting from an enthalpy balance. Thermodynamic data for all components involved is found in the Janaf Tables (69).

Since thermodynamic properties are no path functions any convenient reaction mechanism can be postulated to calculate property changes. Thus in calculating enthalpy changes in the combustion of "Vanilla" residual fuel oil, the following scheme has been utilized.

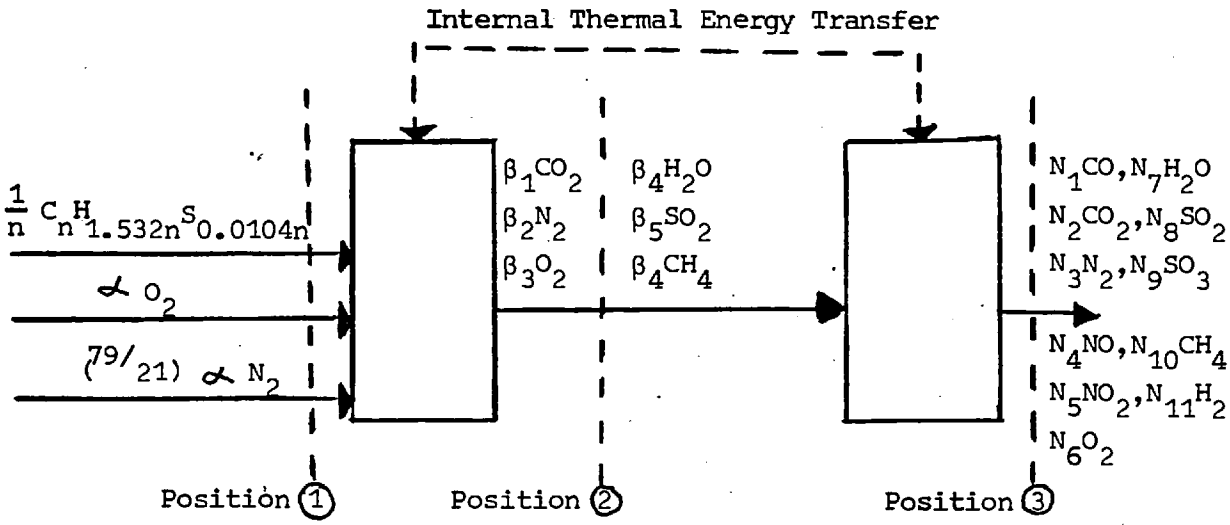

representing the overall process,

$$\frac{1}{n} C_nH_{1.532n}S_{0.0104n} + \alpha O_2 + (79/21)\ N_2 \longrightarrow$$

$$N_1CO + N_2CO_2 + N_3N_2 + N_4NO + N_5NO_2 + N_6O_2 + N_7H_2O + N_8SO_2 + N_9SO_3 + N_{10}CH_4 + N_{11}H_2$$

where α is the number of moles of oxygen injected.

The reactants enter in the first section where "Vanilla" fuel oil is decomposed into CO_2, N_2, O_2, H_2O, SO_2 and CH_4 and cooled down to $T_2 = 25^oC$. It should be noted that only internal energy transfer is taking place. The number of moles at point 2 is given by βi, i = 1,6 respectively. These values are calculated in terms of equivalence ratio. In the second section these compounds absorbing thermal energy from the first section react to reach thermodynamic equilibrium (given by minimum $G/_{RT}$ for the system), at the adiabatic flame temperature.

The relationship between equivalence ratio and number of moles of oxygen injected to the system is given by:

$$\phi = \frac{1.391}{\alpha} \qquad \ldots\ldots\ldots\ldots\ldots\ldots\ldots\ldots\ldots\ldots\ldots\ldots\ldots\ldots (5.19)$$

The enthalpy change between points 1 and 2 is given by:

$$\Delta H_{12} = \Delta H_D + \sum_{i=1}^{6} \beta i^{(*)} \Delta H^{o}_{fi} \quad \ldots\ldots\ldots\ldots\ldots\ldots (5.20)$$

where,

ΔH_D : Heat released by the fuel when transforming into its elements.

ΔH^{o}_{fi} : Standard enthalpy of formation of species i at condition 2

i = 1, 6; CO_2, N_2, O_2, H_2O, SO_2, CH_4

βi : number of moles of species i at level 2.

the enthalpy change between points 2 and 3 is given by:

$$\Delta H_{23} = \sum_{i=1}^{6} \beta i \int_{T_2}^{T_3} Cpi \, dT + \sum_{i=1}^{6} Xi \, \Delta H_{Ri}, T_3 \ldots\ldots (5.21)$$

where Cpi : Constant pressure Heat capacity of compound i

(*) For vanilla fuel oil the following values of βi were conveniently chosen. They can be calculated from mass balance equations and do not represent a unique solution.

(i) For $\phi \geq 1$

$\beta_1 = \frac{a}{2} + 0.3033$

$\beta_2 = \frac{(79)}{21} a$

$\beta_3 = 0$

$\beta_4 = a - 0.6274$

$\beta_5 = 0.0104$

$\beta_6 = 0.6967 - \frac{a}{2}$

(ii) For $\phi < 1$

$\beta_1 = 0.3033$

$\beta_2 = (\frac{79}{21}) a$

$\beta_3 = a - 0.3830$

$\beta_4 = 0.1386$

$\beta_5 = 0.0104$

$\beta_6 = 0.6967$

X_i : yield of the i th reaction . . . . . (5.22)

$$X_i = \frac{\beta i - Ni}{\beta_i}$$

$\Delta H_{Ri}, T_3$: Enthalpy of reaction at T_3 for reaction i th.

Equation 5.21 may also be written in terms of enthalpies, as they are tabulated in reference (69) Thus:

$$\Delta H_{23} = \sum_{i=1}^{6} \beta i \int_{T_2}^{T_3} CpidT + \sum_{j=1}^{11} Njhj,T_3 - \sum_{i=1}^{6} \beta i\ hi,T_3 \quad . . \quad (5.23)$$

The iterative process can be summarized as follows:

a. At the chosen equivalence ratio ϕ calculate βi, i=1,6

b. Assume final temperature T_3^k

c. Calculate $Fi = \frac{Gi}{RT}_k$ for each component, i=1,11

d. Calculate by an iterative minimization of the function

$G/RT = \sum_{i=1}^{11} NiFi$, the number of moles of each compound at equilibrium

at temperature T_3^k.

Equations 5.17 and 5.18.

e. Calculate ΔH_{12} (equation 5.20) and ΔH_{23} (equation 5.23)

f. Calculate total enthalpy change $\Delta H_{13} = \Delta H_{12} + \Delta H_{23}$

e. If ΔH_{23} is less than zero ($\Delta H_{13}<0$), then the assumed temperature T_3^k was below adiabatic flame temperature. Go back to section b and increase assumed temperature T_3^k (k = k+1). Iteration stops when $\Delta H_{13} = 0$, then T_3^k is equal to adiabatic flame temperature.

It should be noted that ΔH_{13} represents the total enthalpy change which is in turn the amount of heat exchanged with the surroundings when

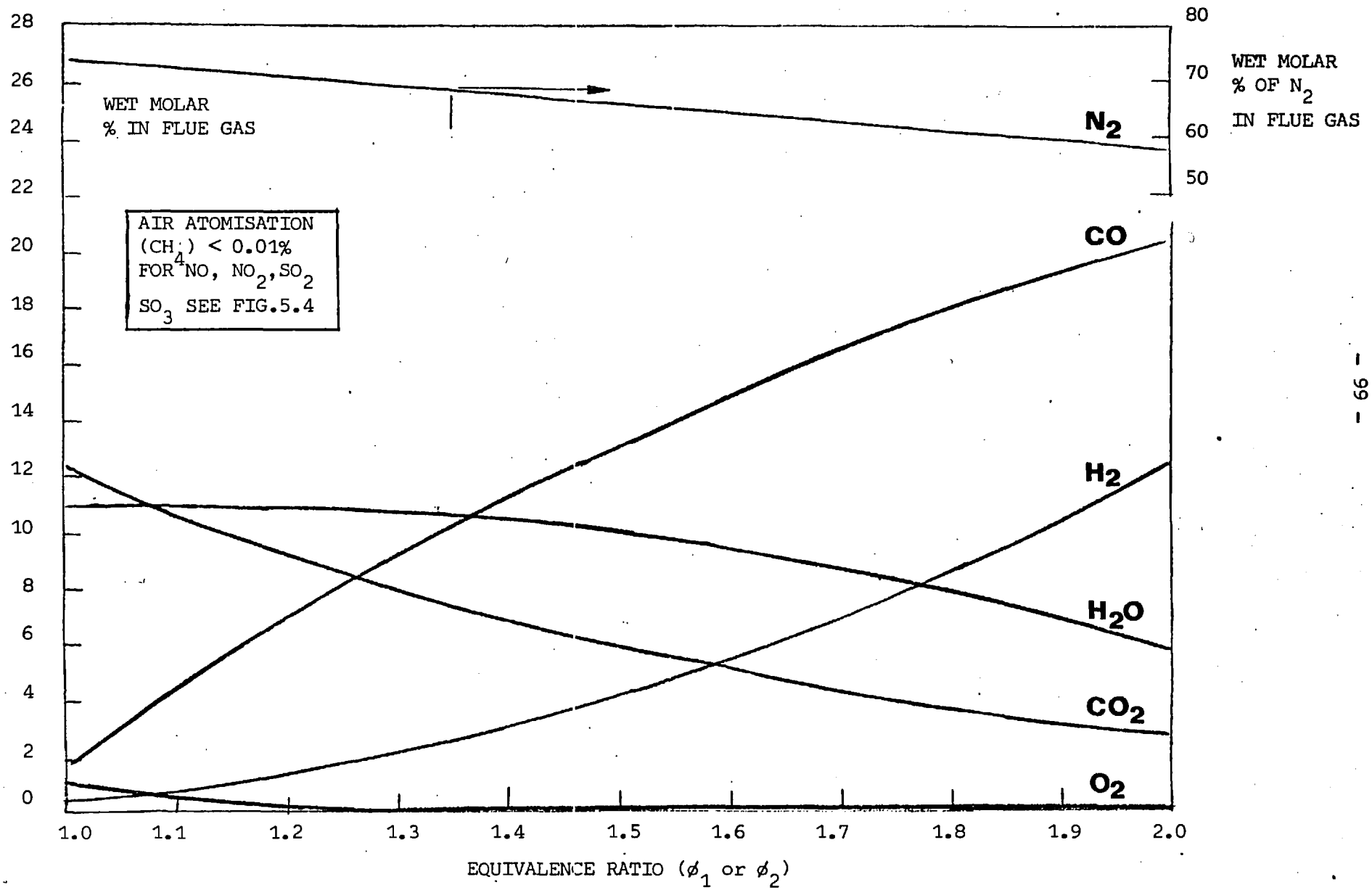

FIG.5.3. WET GAS COMPOSITION FOR MULTIREACTION EQUILIBRIUM MODEL WITH NO HEAT REMOVAL

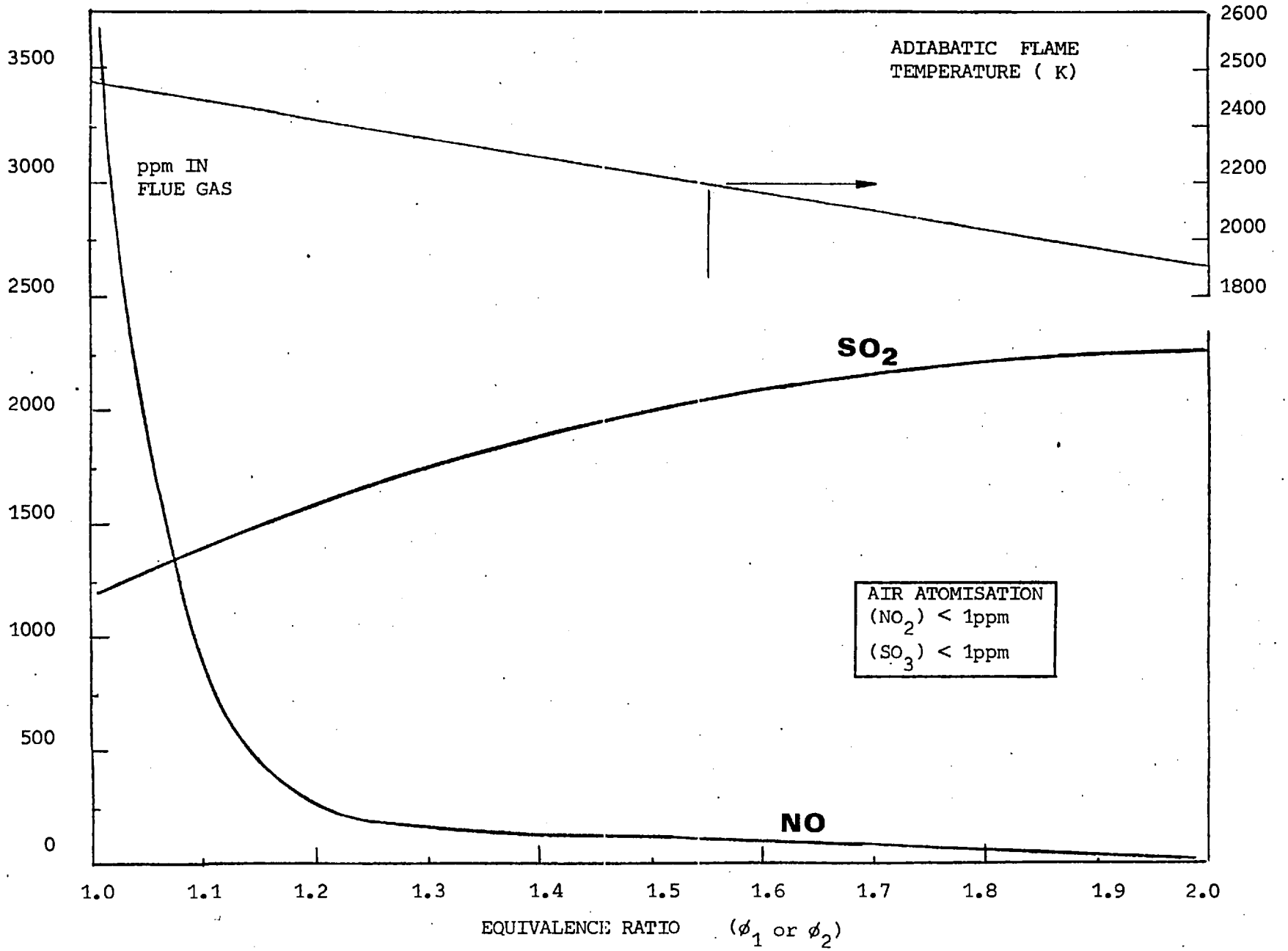

FIG. 5.4 MULTIREACTION EQUILIBRIUM MODEL NO_x AND SO_x LEVELS. NO HEAT REMOVAL.

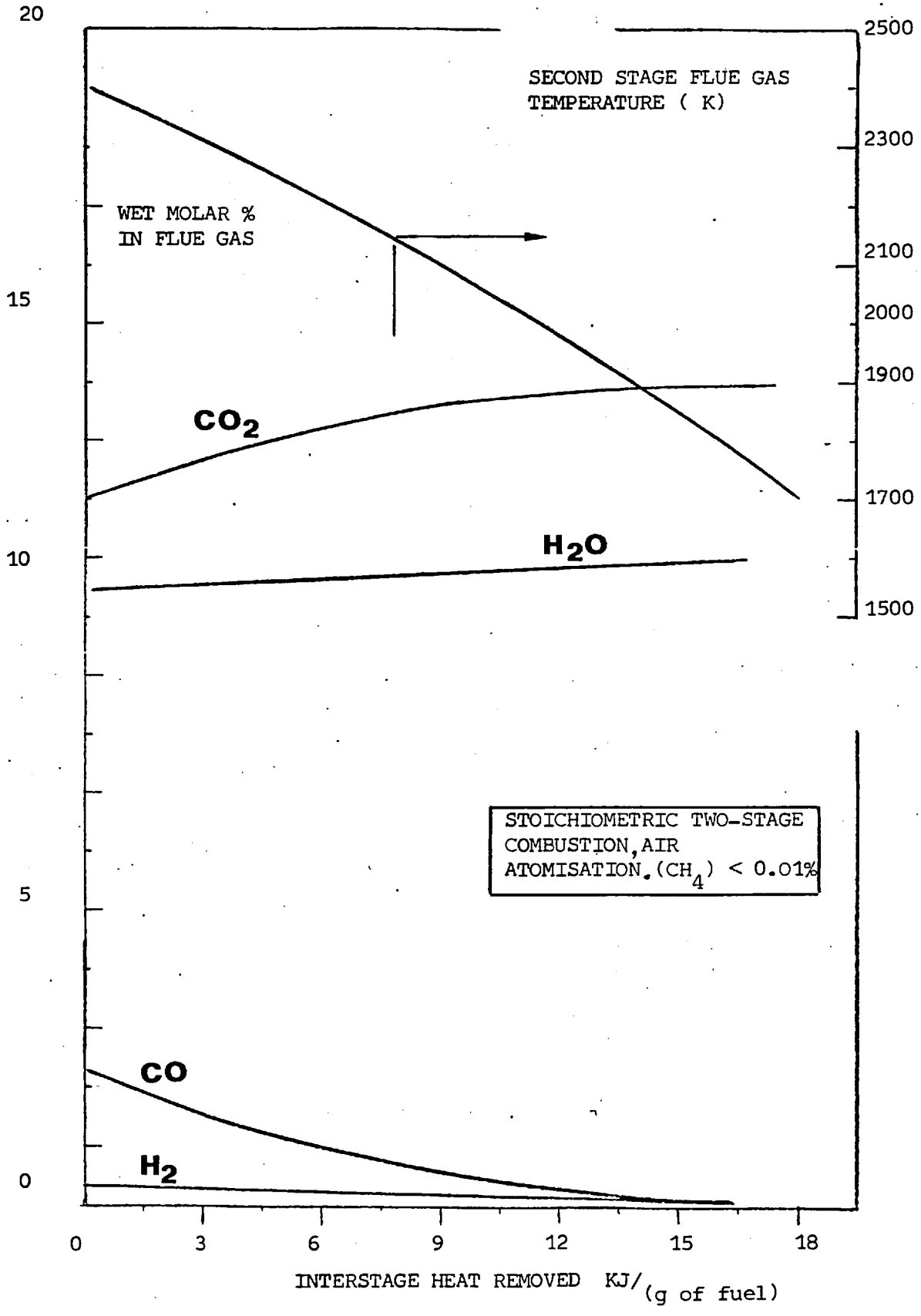

FIG. 5.5 WET GAS COMPOSITION FOR MULTIREACTION EQUILIBRIUM MODEL AFTER SECOND STAGE

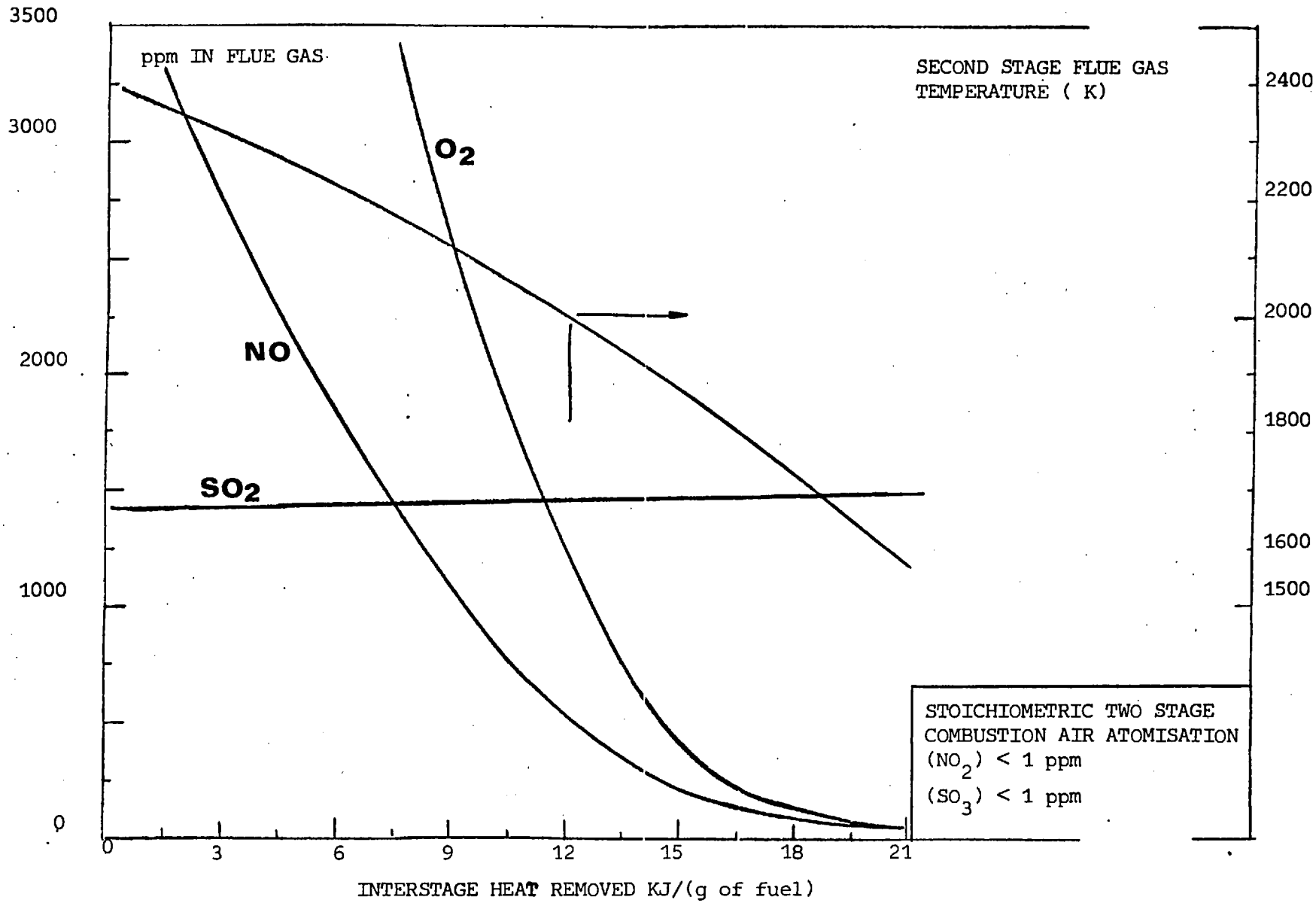

FIG. 5.6 MULTIREACTION EQUILIBRIUM MODEL NO_x AND SO_x LEVELS FROM SECOND STAGE

final products of combustion reached final temperature T_3^k.

The above procedure was performed by means of a computer program which contained the equilibrium equations and the enthalpy balance as subprograms. The results are presented in Figs. 5.3, 5.4, 5.5 and 5.6. Net molar composition of major gaseous compnents CO, N_2, H_2, H_2O, CO_2, and O_2 are presented in Fig. 5.3 as a funtion of equivalence ratio, whereas gaseous pollutants concentrations in flue gas are presented in Fig. 5.4. Wet molar fractions of H_2, CO, H_2O, CO_2 in flue gas as a function of interstage heat removed is plotted in Fig. 5.5. Gas stream termperatures are also given. A similar graph for minor components NO, NO_2, SO_2, SO_3 and O_2 is plotted in Fig 5.6. It is to be noted that Figs. 5.5 and 5.6 are only valid for an overall equivalence ratio $\phi = 1.0$.

5.2 Thermodynamic Equilibrium Model for Vanadium Oxides. Thermodynamic data for vanadium oxides are well documented. see Appendix 8.6; thermodynamic consideration and calculations on vanadium oxides have previously been applied (23). In this section, general predictions and particularaly calculations on vanadium oxidesformation following thermodynamic consideration in the two-stage combustion of "Vanilla" fuel oil are implemented.

5.2.1 General Predictions. A two stage combustion system consists primarily of a gasifier, heat exchanger and converter. Fuel oil is injected into the gasifier (First stage) which operates at substoichiometric conditions (fuel rich conditions), the remaining air is withheld and injected to the converter (2nd stage). Thus carrying out the operation at overall stoichiometric conditions. Nowhere in the system there is excess of oxygen available to form high vanadium oxide V_2O_5.

On the grounds of thermodynamics, it can be shown in Fig. 5.7, at temperatures existing in combustion chambers, vanadium will oxidise first to its lower oxides VO, V_2O_3 or V_2O_4 and if reactions come to equilibrium and there is no excess oxygen present, as long as there is any carbon or hydrogen from the organic compounds, these lower oxides will not yield V_2O_5.

At particular conditions given by temperature and oxygen level it is possible to predict whether a particular vanadium oxide may be spontaneously brought to higher level of oxidation. It should be noted (see chapter 2)that V_2O_5 is largely responsible for formation of highly corrosive complexes in combustion systems. The reactions investigated are:

$$(i)\quad V_2O_3 + \tfrac{1}{2}O_2 \rightleftharpoons V_2O_4 \qquad \ldots\ldots\ldots\ldots\ldots\ldots\ldots\ldots (5.24)$$

$$Ka = \exp\left[\left(\frac{43065 - 14.6T}{1.987T}\right)\right] \qquad \ldots\ldots\ldots\ldots\ldots\ldots (5.25)$$

$$(ii)\quad V_2O_4 + \tfrac{1}{2}O_2 \rightleftharpoons V_2O_5 \qquad \ldots\ldots\ldots\ldots\ldots\ldots\ldots\ldots (5.26)$$

$$Ka = \exp\left[\left(\frac{16450 - 6.8T}{1.987\ T}\right)\right] \qquad \ldots\ldots\ldots\ldots\ldots\ldots\ldots (5.27)$$

$$(iii)\quad V_2O_3 + O_2 \rightleftharpoons V_2O_5 \qquad \ldots\ldots\ldots\ldots\ldots\ldots\ldots\ldots (5.28)$$

$$Ka = \exp\left[\left(\frac{59670 - 21.5\ T}{1.987T}\right)\right] \qquad \ldots\ldots\ldots\ldots\ldots\ldots (5.29)$$

where Ka : Thermodynamic equilibrium constant

T : Absolute temperature (^oK)

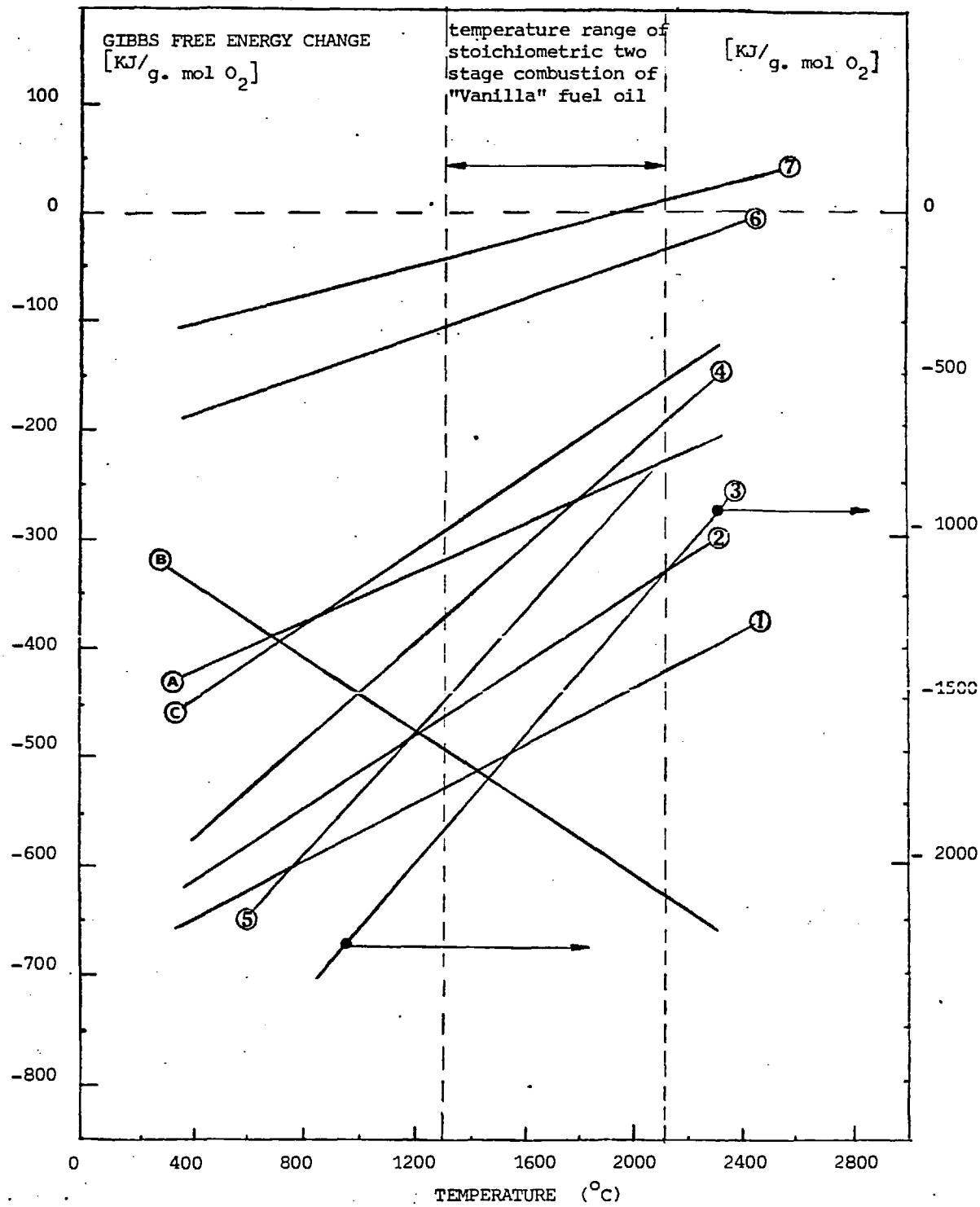

FIG. 5.7 OXIDATION POTENTIAL DIAGRAM (Key on next page)

KEY FOR THE OXIDATION POTENTIAL DIAGRAM

1.- $2V + O_2 \rightleftharpoons 2VO$

2.- $2VO + O_2 \rightleftharpoons 2VO_2$

3.- $4VO + O_2 \rightleftharpoons 2V_2O_3$

4.- $2VO_2 \rightleftharpoons V_2O_3 + \frac{1}{2} O_2$

5.- $2VO_2 \rightleftharpoons V_2O_4$

6.- $V_2O_3 + O_2 \rightleftharpoons V_2O_5$

7.- $2V_2O_4 + O_2 \rightleftharpoons 2V_2O_5$

A.- $2H_2 + O_2 \rightleftharpoons 2H_2O$

B.- $2C + O_2 \rightleftharpoons 2CO$

C.- $2CO + O_2 \rightleftharpoons 2CO_2$

The values of Ka can be calculated from the thermodynamic data given in Appendix 8.6.

The temperature and oxygen level related to a specific value of first stage equivalence ratio using "Vanilla" fuel oil were obtained as previously shown in section 5.1.

The general principles of thermodynamic predictions on higher vanadium oxides formation in the two-stage system under discussion can be summarized as follows:

a. The equilibrium constant applies only to activites in a reacting mixture that is at chemical equilibrium, and it is related to temperature and Gibbs free energy change by:

$$\Delta G^{o} = - RT \text{ Ln } Ka \quad \ldots\ldots\ldots\ldots\ldots\ldots\ldots\ldots \quad (5.30)$$

b. Activity ratio based on inlet conditions for a reaction $\sum_{i=1}^{c} \alpha_i A_i = 0$

is defined by:

$$(Ja)_{in} = \frac{\prod_{Prod} \left[A_i\right]_{in}^{\alpha_i}}{\prod_{react} \left[A_i\right]_{in}^{-\alpha_i}} = \prod_{i=1}^{c} (A_i)_{in}^{\alpha_i} \quad \ldots\ldots(5.31)$$

where A_i : activity of specie i th, defined as ratio of fugacity of species i th in the mixture at temperature T and total pressure of the mixture to fugacity of specie i th at standard reference state conditions.

$$A_i = \frac{\bar{f}_i}{f_i^{o}}$$

α_i : stoichiometric coefficient of specie i th in the reaction.

c. In a chemically reacting mixture at thermodynamic equilibrium the basic relation:

$$-\Delta \underline{G}^{o} = RT \text{ Ln } Ka = RT \text{ Ln } \prod_{i=1}^{c} (A_i)^{\alpha_i} \quad \ldots\ldots\ldots\ldots (5.32)$$

also holds for heterogeneous systems.

d. By examining the activity ratio Ja calculated from its present composition, it is possible to determine much about the state of a chemically reacting mixture, considering a stream entering a chemical reactor.

(i) If $(Ja)_{in} = Ka$, Mixture is at equilibrium and no reaction will occurr.

(ii) If $(Ja)_{in} < Ka$, reaction will proceed in direction written.

(iii) If $(Ja)_{in} > Ka$, reaction will proceed in reverse direction from that written.

The main equations ans steps in order to determine activity ratio Ja for the reactions under consideration are presented as follows:

(i) $V_2O_3\ (s) + \frac{1}{2}\ O_2\ (g) \rightleftharpoons V_2O_4\ (s)$

inlet activity ratio is:

$$(Ja)_{in} = \prod_{i=1}^{c} (A_1)_{in}^{\alpha_i} = (A_{V_2O_4})\ (A_{V_2O_3})^{-1}\ (A_{VO_2})^{-\frac{1}{2}} \quad \ldots\ldots (5.33)$$

activity for solid phase compounds:

$$A_{V_2O_4} = A_{V_2O_3} \approx 1$$

activity for gaseous compounds:

$$A_{VO_2} = \frac{\bar{f}_{O_2}}{\underline{f}^{o}_{O_2}}$$

where,

$\bar{f}_{O_2}$: fugacity of oxygen evaluated at its partial pressure and temperature T.

$f^{o}_{O_2}$: fugacity of oxygen evaluated at standard reference state conditions

$f^{o}_{O_2} = 1$

following Lewis and Randall rule:

$$\bar{f}_{O_2} = Y_{O_2} \bar{f}_{O_2, P} \quad \ldots\ldots\ldots\ldots\ldots\ldots\ldots\ldots (5.34)$$

where Y_{O_2} : molar fraction of oxygen in flue gas.

$f_{O_2,P}$: fugacity of oxygen evaluated at total pressure of the system P and temperature T.

and operating at low pressures so as ideal gaseous phase can be assumed, then equation 5.33 becomes:

$$(Ja)_{in} = \left(\frac{1}{Y_{O_2} P}\right)^{\frac{1}{2}} \quad \ldots\ldots\ldots\ldots\ldots\ldots\ldots\ldots\ldots\ldots (5.35)$$

following similar procedure,

(ii) $V_2O_4(s) + \frac{1}{2}O_2(g) \rightleftharpoons V_2O_5(l)$

$$(Ja)_{in} = \left(\frac{1}{Y_{O_2} P}\right)^{\frac{1}{2}} \quad \ldots\ldots\ldots\ldots\ldots\ldots\ldots\ldots\ldots\ldots (5.36)$$

(iii) $V_2O_3\ (s) + O_2\ (g) \rightleftharpoons V_2O_5\ (l)$

$$(Ja)_{in} = \frac{1}{Y_{O_2} P} \quad \ldots\ldots\ldots\ldots\ldots\ldots\ldots\ldots\ldots\ldots\ldots\ldots (5.37)$$

The results obtained for the mentioned reactions are plotted in Figs. 5.8, 5.9 and 5.10. Equations 5.25, 5.27 and 5.29 were plotted against absolute temperature. The activity ratio for equilibrium conditions given by equations 5.35, 5.36 and 5.37 were also graphed against temperature. Oxygen levels and temperatures corresponding to differents equivalence ratios were obtained by means of the multireaction equilibrium model and the vanadium inlet level is that of "Vanilla" fuel oil (365 ppm as V). From the figures 5.8, 5.9 and 5.10 the following main conclusions can be drawn.

(i) System $V_2O_3/O_2/V_2O_4$.

a. For a two-stage combustion of "Vanilla" fuel oil (overall equivalence ratio = 1.0) oxidation to V_2O_4 will proceed at combustion temperatures below 2000°K. Under this temperature $(Ja)_{in} < Ka$.

b. At oxidation conditions, say overall equivalence ratio of 0.7, oxidation to V_2O_4 will proceed at combustion temperatures below 2200°K. $(Ja)_{in} < Ka$

c. At reducing conditions (fuel rich) of equivalence ratio = 1.2 or above, exidation to V_2O_4 will not spontaneously proceed $(Ja)_{in} > Ka$.

(ii) System $V_2O_4/O_2/V_2O_5$

a. V_2O_5 is expected to be formed as a result of V_2O_4 oxidation at air rich conditions (Equivalence ratio =0.7 or less) below temperatures of 1750°K.

$(Ja)_{in} < Ka$.

b. For a two stage combustion of "Vanilla" fuel oil (overall equivalence ratio = 1.0) oxidation of V_2O_4 to V_2O_5 will not spontaneously proceed $(Ja)_{in} > Ka$.

(iii) System $V_2O_3/O_2/V_2O_5$

a. V_2O_5 is expected to be formed at air rich conditions (Equivalence ratio = 0.7) below temperatures of 2075°K. $(Ja)_{in} < K_a$

b. For a two stage combustion of "Vanilla" fuel oil (overall equivalence ratio = 1.0) oxidation of V_2O_3 to V_2O_5 will not spontaneously proceed. $(Ja)_{in} > Ka$.

5.2.2 Vanadium Oxides Ratio in Solid Products. It was concluded in the previous section that during two-stage combustion of "Vanilla" fuel oil operating at overall equivalence ratio of one (ϕ = 1.0) if reaction come to equilibrium so that nowhere in the system there is excess of oxygen the vanadium oxides to be found in the solids product of combustion are expected to be V_2O_3 and V_2O_4.

Thus based on the assumption that all vanadium brought into the system by the fuel will be present in the solid products on the solely form of V_2O_3 and V_2O_4 an equilibrium model can be put forward. Equilibrium ratio of V_2O_3 to V_2O_4 in the solid formed can be calculated from equations 5.25 and 5.30. The results in terms of temperature of the system and overall equivalence ratio are plotted in Fig. 5.11.

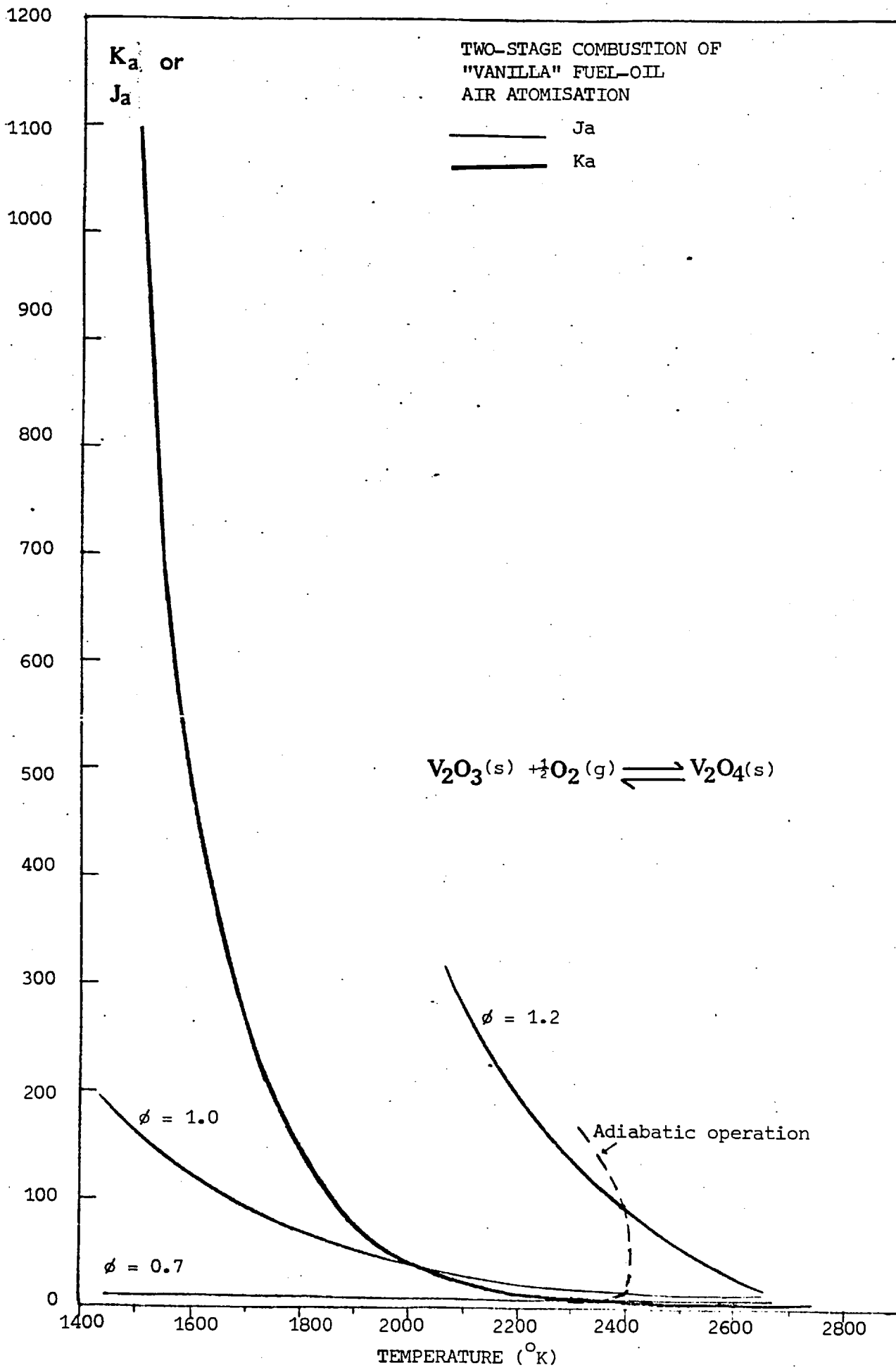

FIG. 5.8 OPERATING REGIONS FOR V_2O_4 FORMATION FROM V_2O_3.

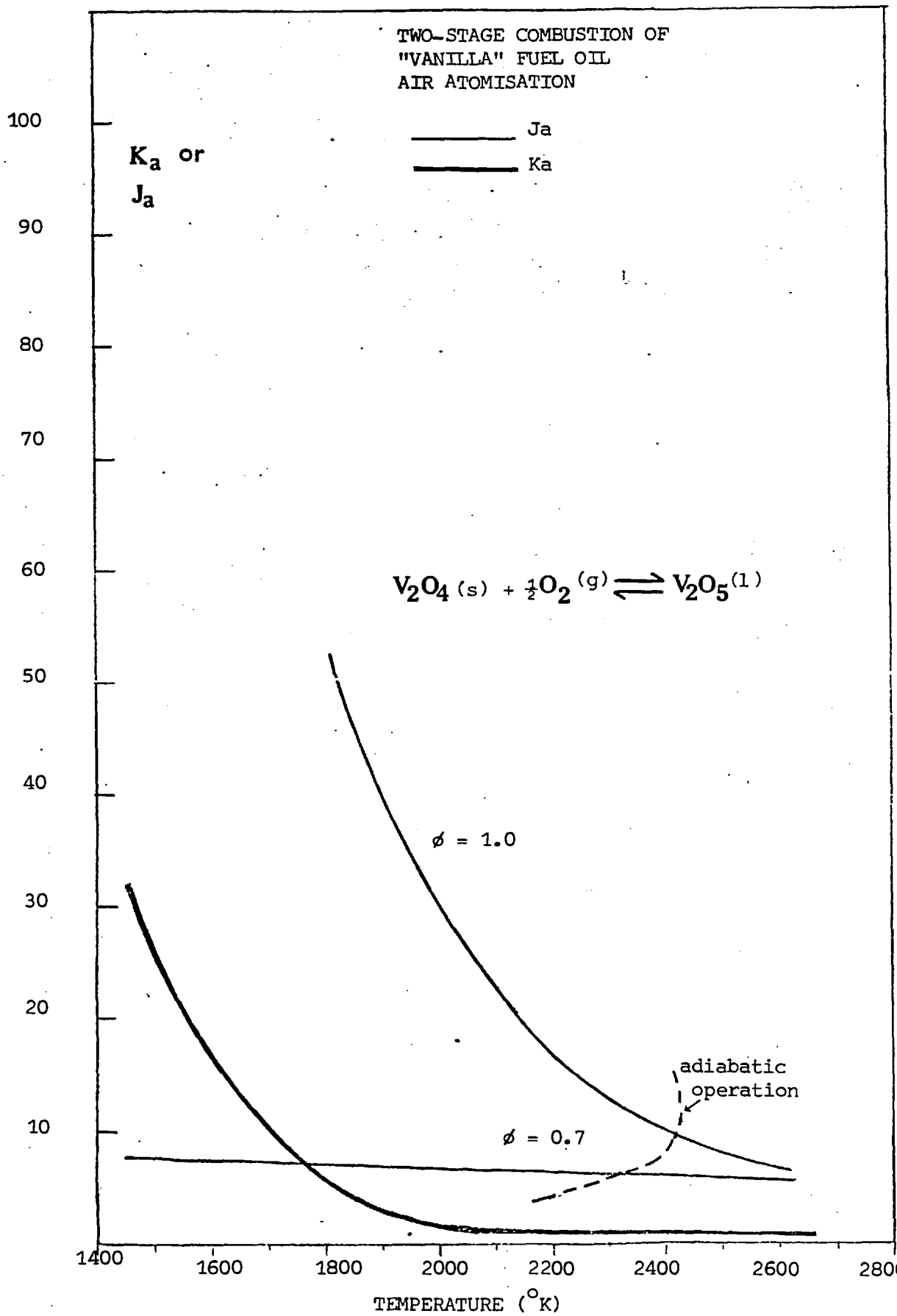

FIG. 5.9 OPERATING REGIONS FOR V_2O_5 FORMATION FROM V_2O_4.

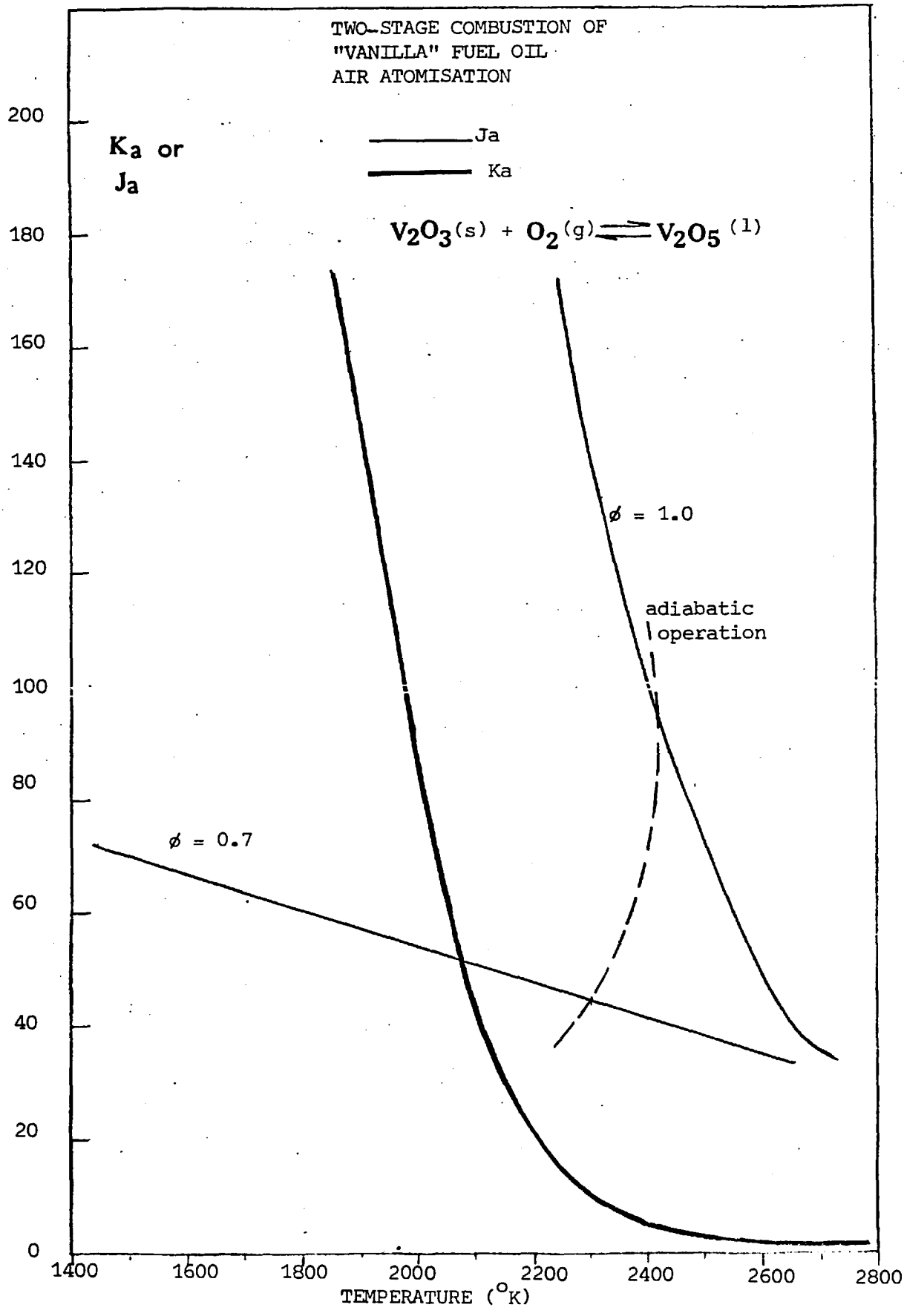

FIG. 5.10 OPERATING REGIONS FOR V_2O_5 FORMATION FROM V_2O_3.

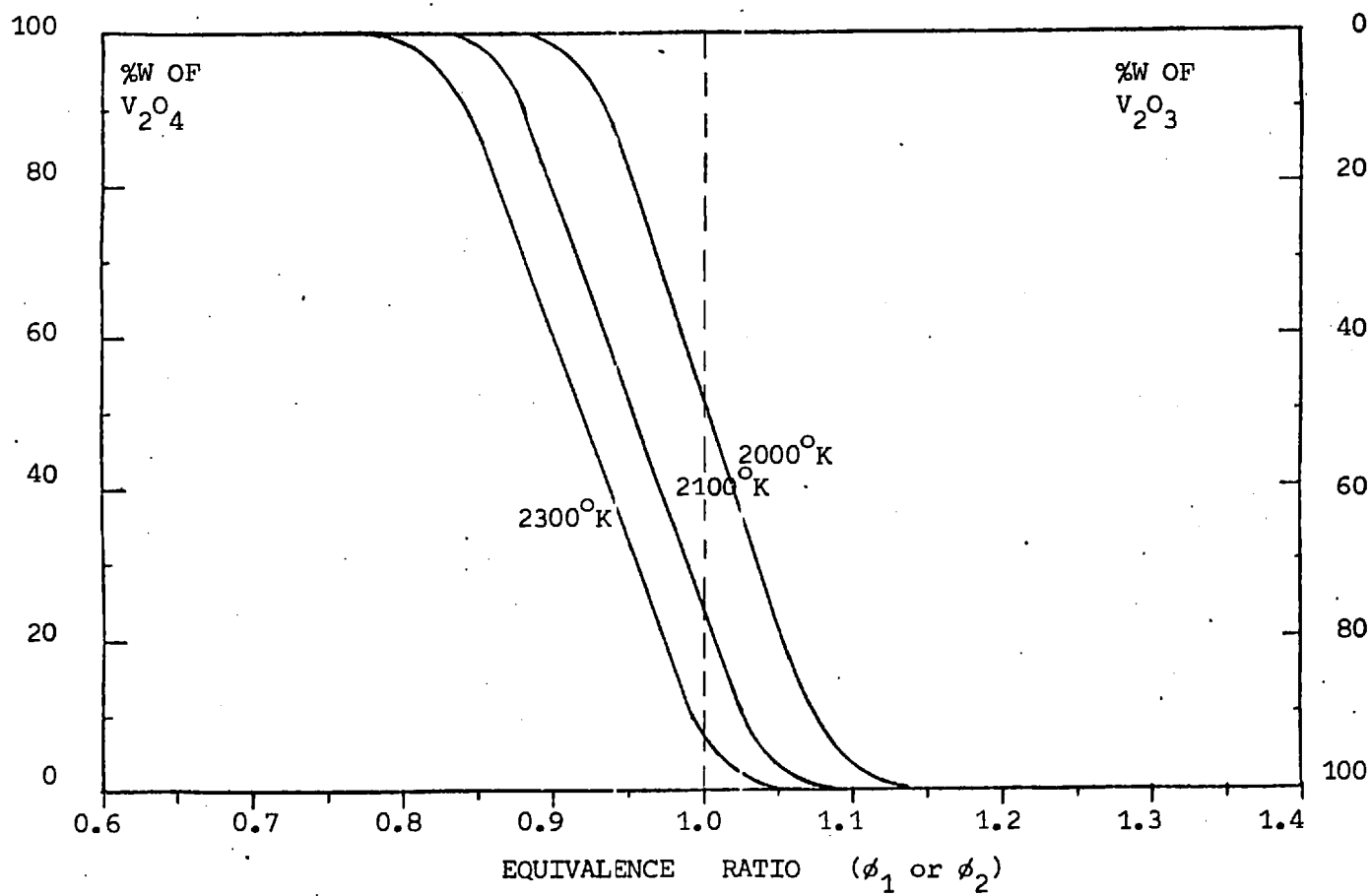

FIG. 5.11. $\underline{V_2O_3}/\underline{V_2O_4}$ PREDICTED RATIO IN SOLID PRODUCT OF "VANILLA" FUEL OIL COMBUSTION

CHAPTER 6

EXPERIMENTAL RESULTS AND DISCUSSION

Following the experimental program described in Chapter 3 and the instrumental techniques presented in Chapter 4 the following experimental data were obtained. The experimental settings and relevant data for the runs discusses in this chapter are tabulated in Appendix 8.1.

6.1 Gaseous Phase Composition.

Using gas chromatograpy, mass spectrometry and chemiluminescence, the experimental determination of major gaseous components CO_2, CO, N_2, H_2O, H_2, O_2 and the gaseous pollutants concentrations of NO_x and SO_2 yielded the following results.

6.1.1 Major Gaseous Components. Samples of combustion gaseous products were withdrawn from the second stage sampling port (T-piece) using a stainless steel, steam cooled sampling probe. The results using air as atomising fluid are listed in Table A-1 in Appendix 8.1. The analysis of CO_2, CO, H_2O, H_2, N_2 and O_2 were obtained by gas chromatography (see section 4.1.1). Using steam as atomising fluid in similar equipment Archer (2) obtained gas composition by gas chromatography from x-piece (first stage) and T-piece (second stage). His results are presented in Fig. 6.1, which include dry gas composition of the gas stream in terms of CO_2, CO, H_2 and CH_4. The graph is valid for both first and second stage. He found that the water-gas shift reaction equilibrium was not attained in the first stage gas phase whereas it was established in the second stage chamber.

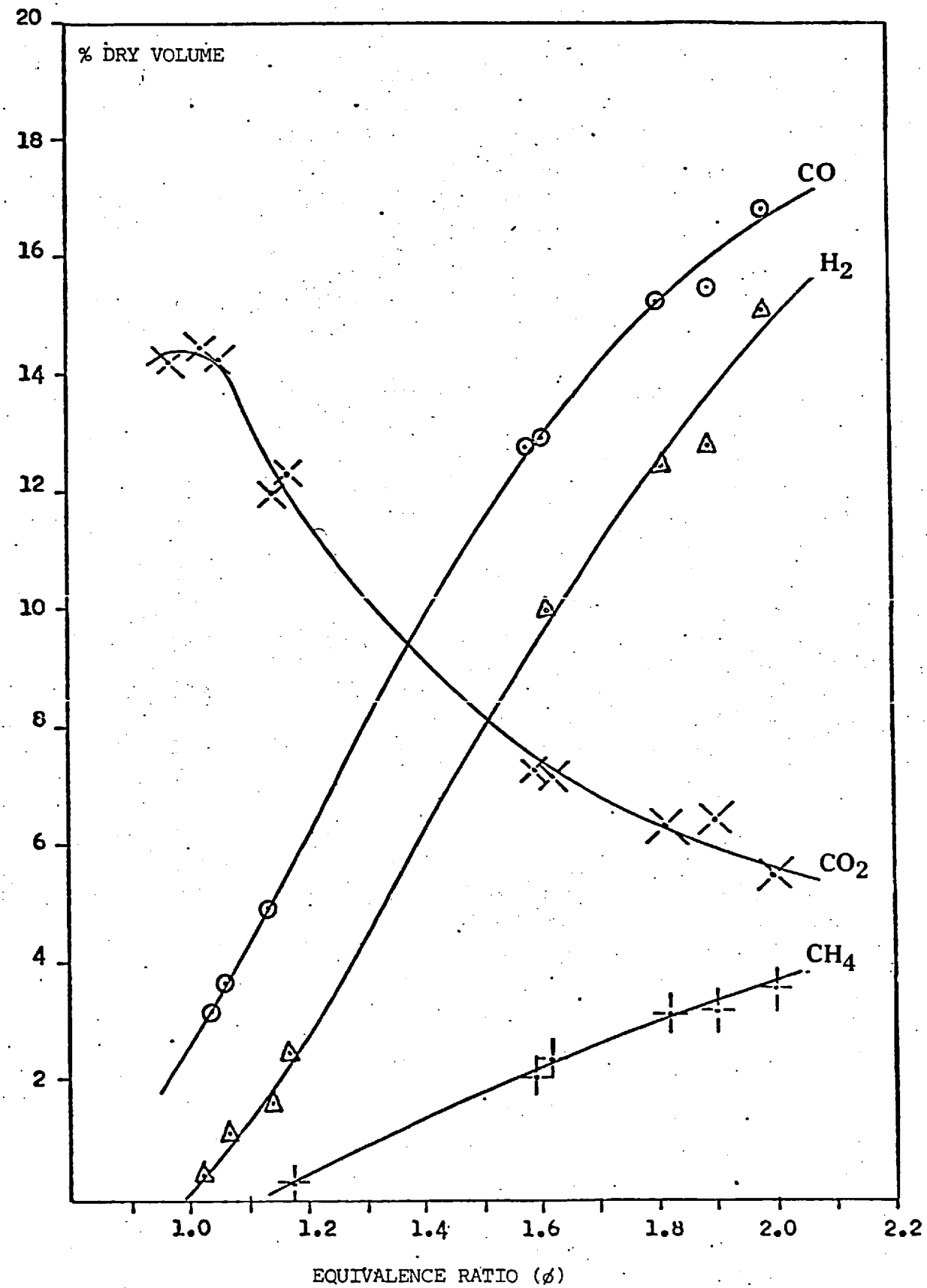

FIG. 6.1 MEASURED DRY GAS ANALYSIS FOR STEAM ATOMISATION Ref(2)

The experimental results for air atomised tests tabulated in Table A-1 are plotted in Fig. 6.2. The wet percent molar composition corresponds to samples with-drawn from the sampling section of the second stage at the first stage equivalence ratio stated. During most of the runs the overall equivalence ratio of the system and hence the second stage equivalence ratio was deliberately fixed to one.

In Fig. 5.5 it can be observed that second stage equilibrium compositions are a function of second stage temperature, which in turn is a function of interstage heat removal. Thus, comparation of the obtained experimental results with the values predicted from the multireaction equilibrium model should include either second stage gas stream temperature or interstage heat removal. From Figs. 5.5 and 6.2 it can be seen that for any first stage equivalence ratio ϕ_1 greater than 1.0 the experimental concentration of CO_2 is always below the theoretically expected values for any amount of heat removal. For $\phi_1 > 1.25$ the experimental concentrations of H_2 and CO are slightly higher than those from the equilibrium model and the deviations are seen to continously increase with increasing ϕ_1. This finding is an indication that the actual flue gas from the second stage during air atomised runs has not attained thermodynamic equilibrium values.

6.1.2 SO_2 Results. The chromatography preocedure was originally devised to give SO_2 by means of the Poropak column (see Section 4.1) at around 80°C. Although technically feasible, large amounts of water vapour produced a tailing effect that in some runs precluded an accurate estimation of SO_2. Sulphur dioxide measurements were however made possible by mass spectrometry. Samples were withdrawn from the second stage and bottled for posterior analysis. The experimental data thus obtained are

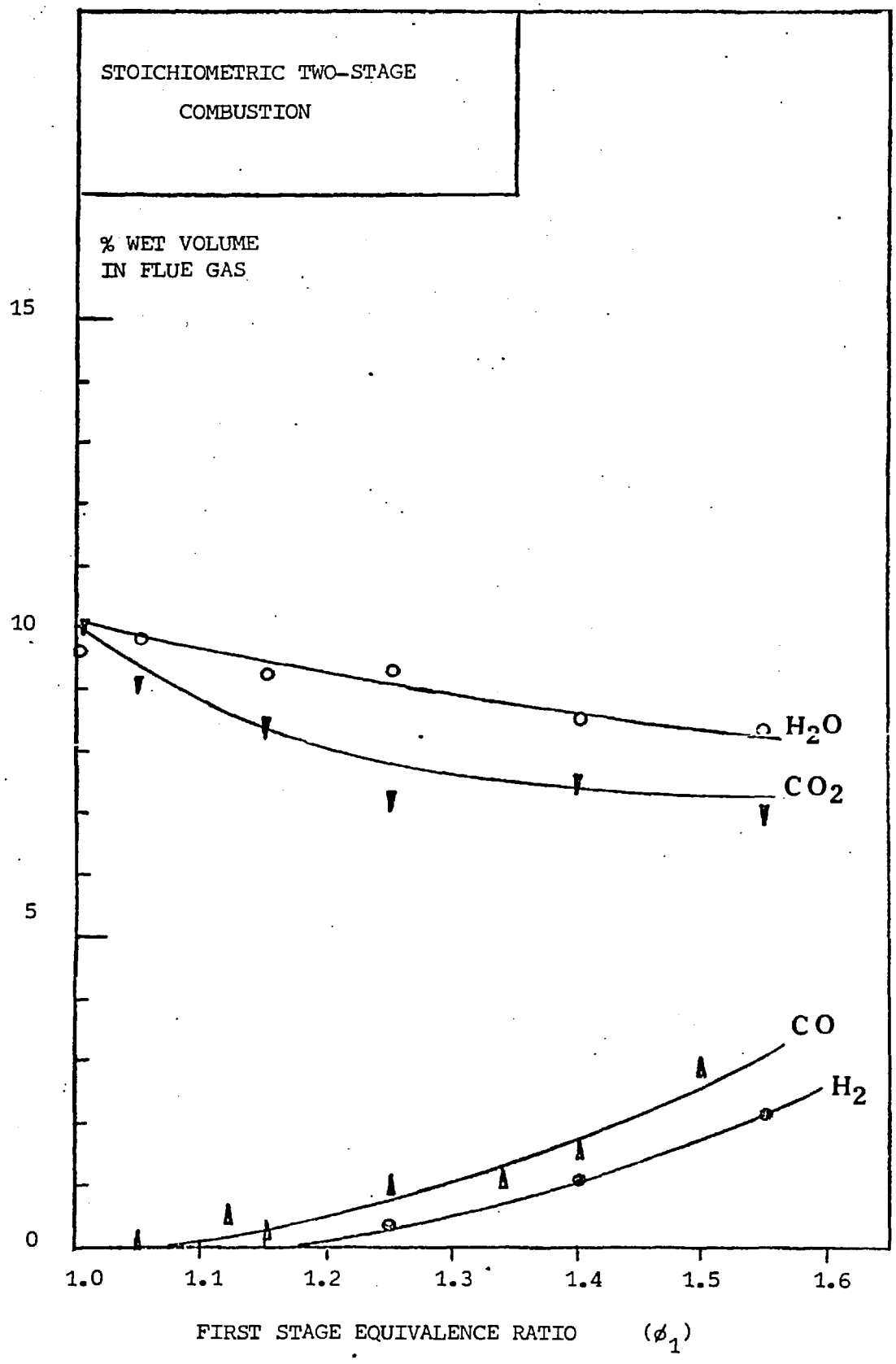

FIG. 6.2. EXPERIMENTAL GAS COMPOSITION IN FLUE GAS AFTER SECOND STAGE FOR AIR ATOMISATION

tabulated in Table A-2 and plotted in Fig. 6.3 as SO_2 emissions from the second stage as a function of first stage equivalence ratio for both air atomised and steam atomised tests.

Air atomised combustion emission were found slightly higher than those obtained by steam atomising, this would probably be due to higher temperatures in the system leading to a more efficient sulphur vaporization from the spray.

Both emissions are less than those expected by the multireaction equilibrium model which in turn assumed that all the sulphur contained in the residual fuel oil vaporized and oxidised in the gaseous phase. This assumption was established by phase equilibrium at temperatures of around $2000^{o}K$. Since some sulphur from the fuel remained associated with the solid it can reasonably be assumed that gaseous SO_2 compositions will actually be lower than those predicted values.

Johnson et al (13) working with propane-1%SO_2 mixture, found that for equivalence ratio greater than 0.80, SO_2 was the predominant sulphur containing specie, and for residence time greater than 8 milliseconds the SO_2 attained thermodynamic equilibrium. In the present work a first stage residence time varying from 44 to 62 milliseconds has been reported (2). If the gaseous sulphur dioxide is to be considered as at equilibrium conditions in the gaseous phase, the concentration predicted by such a system given in the previous chapter leads to values for SO_3 emission as low as 1 ppm.

6.1.3 <u>NO_x Results.</u> NO and NO_2 concentrations in the gas stream were measured using chemiluminescent methods from both the first and the second stage. The complete description of the sampling procedure and of the chemiluminescent unit has been discussed in section 4.1.3 and the

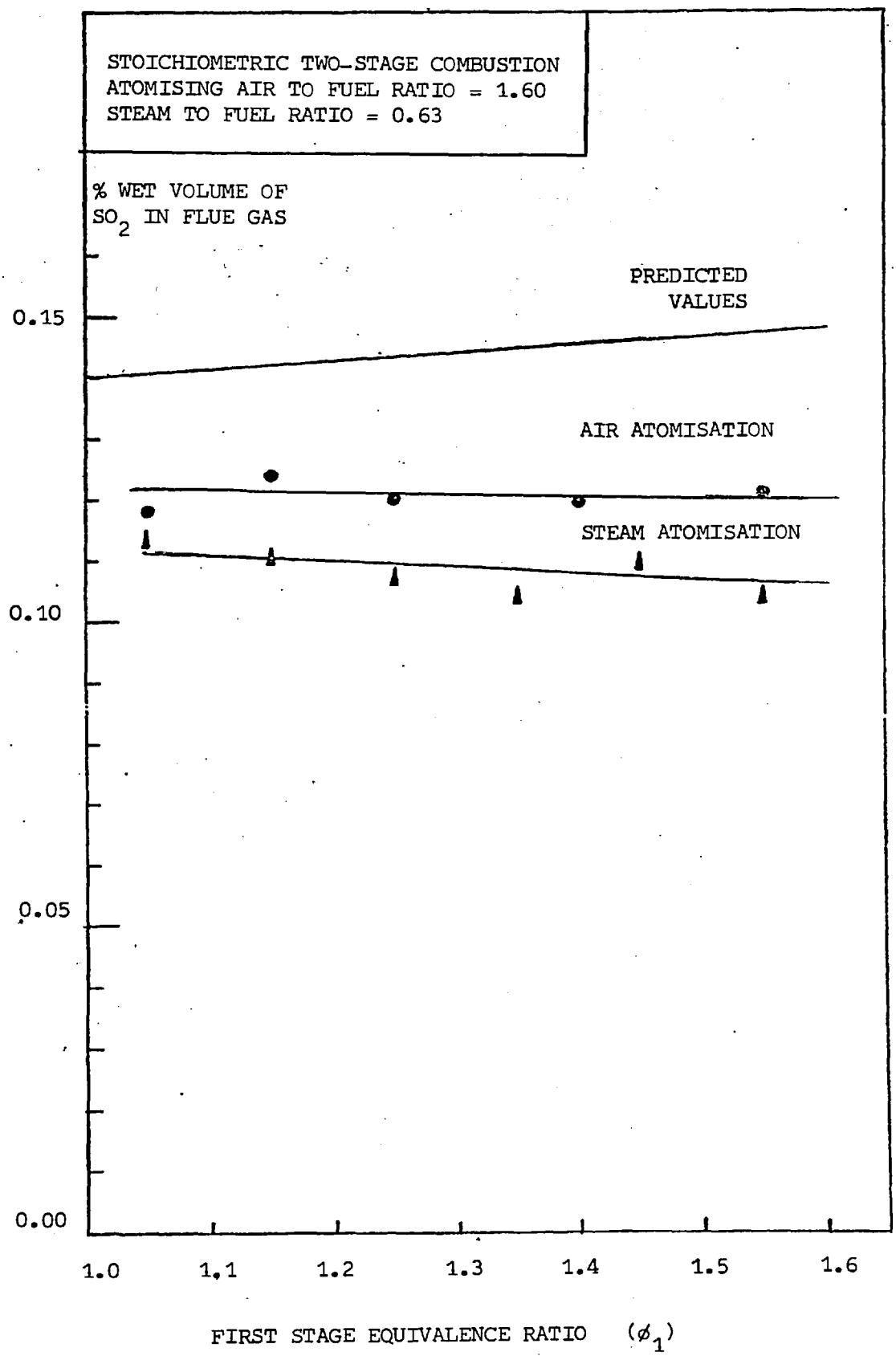

FIG. 6.3 EXPERIMENTAL SO_2 LEVEL FROM SECOND STAGE

experimental data are tabulated in Table A-3. Results for both air and steam atomised tests are plotted in Fig. 6.4, and Fig. 6.5. For all runs, either air or steam atomised, the NO_2 concentration in the gas stream from either the gasifier or the converter was found to be negligible, thus making NO_x = NO.

Chemiluminescence monitor proved to be a quick, reliable and accurate method for NO_x measurements. At a particular experimental setting NO_x level was found to be very stable and fluctuations were minimum.

As predicted by Bartok (33) from his kenetic model for NO_x formation two-stage combustion constitutes a means for reducing NO emission. As it was seen in section 2.2.2 this effect is due to kinetical limitation of thermal NO by lower temperatures. For air atomised tests NO reduction by two stage combustion reached 72%, and 92% reduction was obtained in steam atomised runs comparing with sinle stage operation. A considerable reduction in NO_x concentration in the flue gas was obtained when atomising with steam comparing with air atomised tests. For ϕ = 1.0, NO_x level in flue gas from second stage was brought down from 360 (air atomised value) to 105 ppm (steam atomised value) and for ϕ_1 = 1.5, ϕ_2 = 1.0 was reduced from 130 ppm (air atomised value) down to 5 ppm (steam atomised value).

Comparing in Fig. 6.4. the NO level from first stage with the equilibrium values obtained by the multireaction equilibrium model, it can be seen that working at values of ϕ_1 closed to 1.0 the NO formed during combustion does not reach the thermodynamic values, and for ϕ > 1.25 the NO emitted is above the equilibrium established for NO thermal. This latter result indicates that a fraction of the NO formed in the first stage is provenient from the nitrogen of fuel. NO_x formed that originates from the nitrogen of the fuel is known as Fuel-NO_x and is mainly formed in the flame region (see Section 2.2.2)

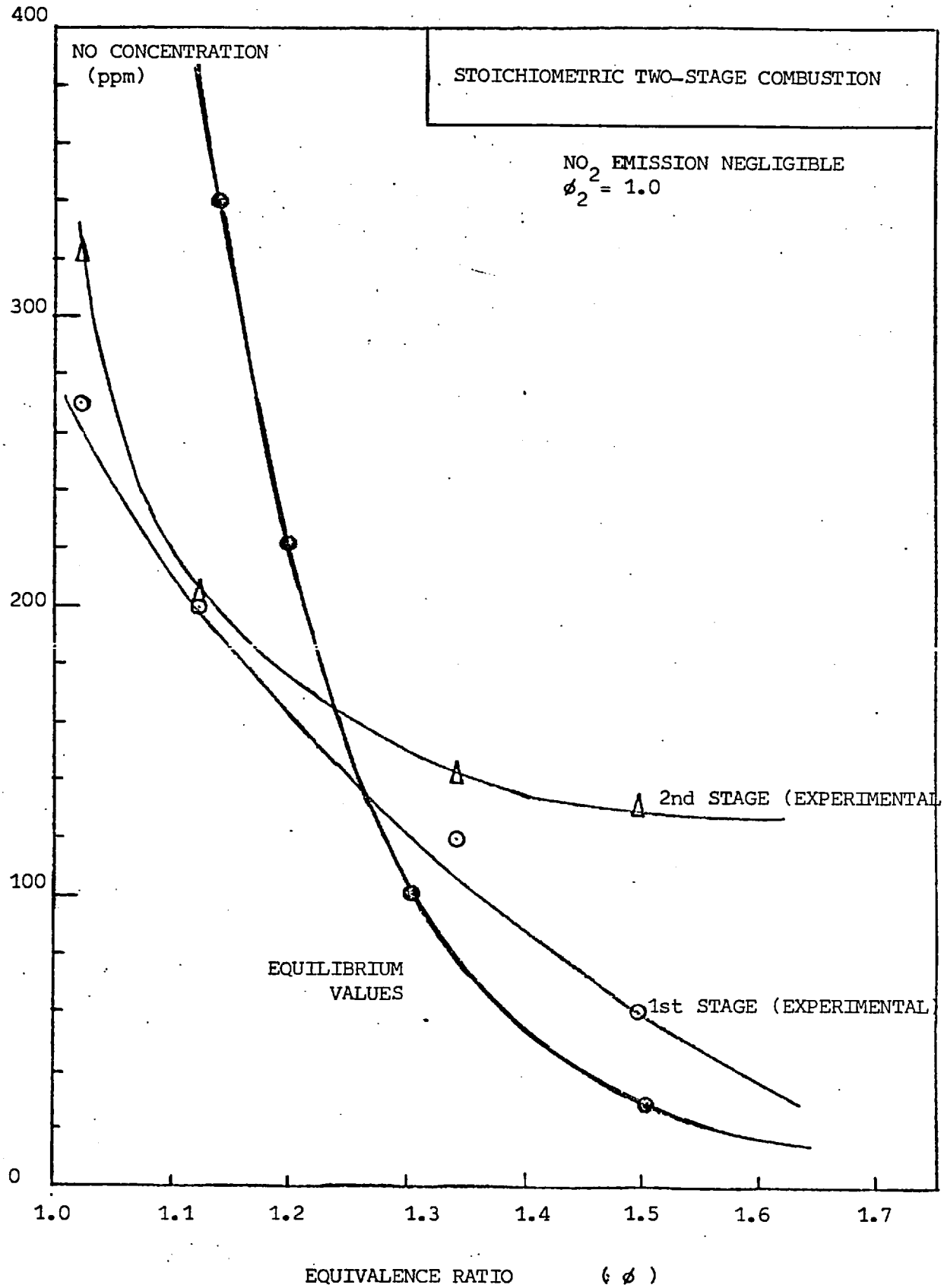

FIG. 6.4. NITRIC OXIDE VALUES FOR AIR ATOMISATION

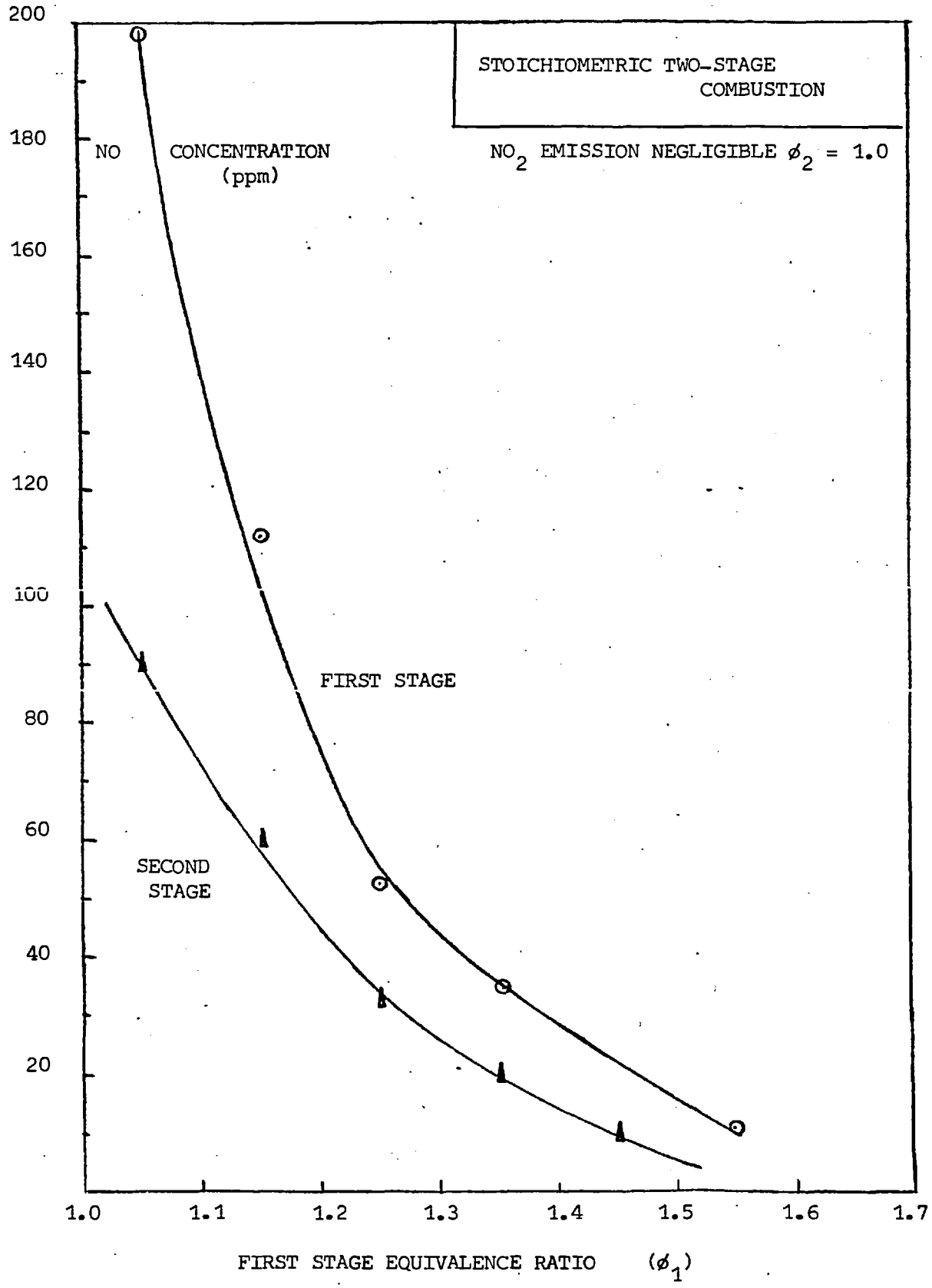

FIG. 6.5 NO_x EXPERIMENTAL VALUES FOR STEAM ATOMISATION

6.2 Solid Loading.

Solid loading measurements were obtained by filtering and drying the slurry collected in the collector tank and pumped out to a sampling point. During the actual runs 65 g/s of water was used through the scrubber section sprays.

The experimental solid loading measurements for both air and steam atomised tests are tabulated in tables A-4 and A-5 respectively. Solid loading is expressed as solid collected as percentage of fuel oil input. Results are plotted in Fig. 6.6 in terms of first stage equivalence ratio and of atomising fluid to fuel mass ratio.

Archer (2) obtained experimental data of solid loading of the second stage working on similar equipment and using steam atomised runs, his results are plotted in Fig. 2.16.

Comparing the results for solid loading of the second stage for steam atomised tests as given in Fig. 6.6 with those presented by Archer (2) show that a significant reduction in solid loading has been achieved. In the present work for steam to fuel mass ratio of r_{sf} = 0.84 for first stage equivalence ratio ranging from 1.05 to 1.6 the reduction in solids emitted varies from 70 to 67% compared with those obtained by Archer. For steam to fuel mass ratio r_{sf} = 0.63 and for same first stage equivalence ratio range, the reduction in solid loading was greater and reached values of between 72 and 74%. One of the reasons that would probably explain this significant reduction in solid loading is the spray characteristics. One fundamental factor in fuel spray characteristics of twin fluid atomiser is the atomiser shim, which affects the velocity of the atomising fluid. In the present work a shim size of 7.26 mm (0.2865 ins) was used. The air atomised solid loading results Fig. 6.6 show different trends than those for steam atomised runs. In the former solid loading

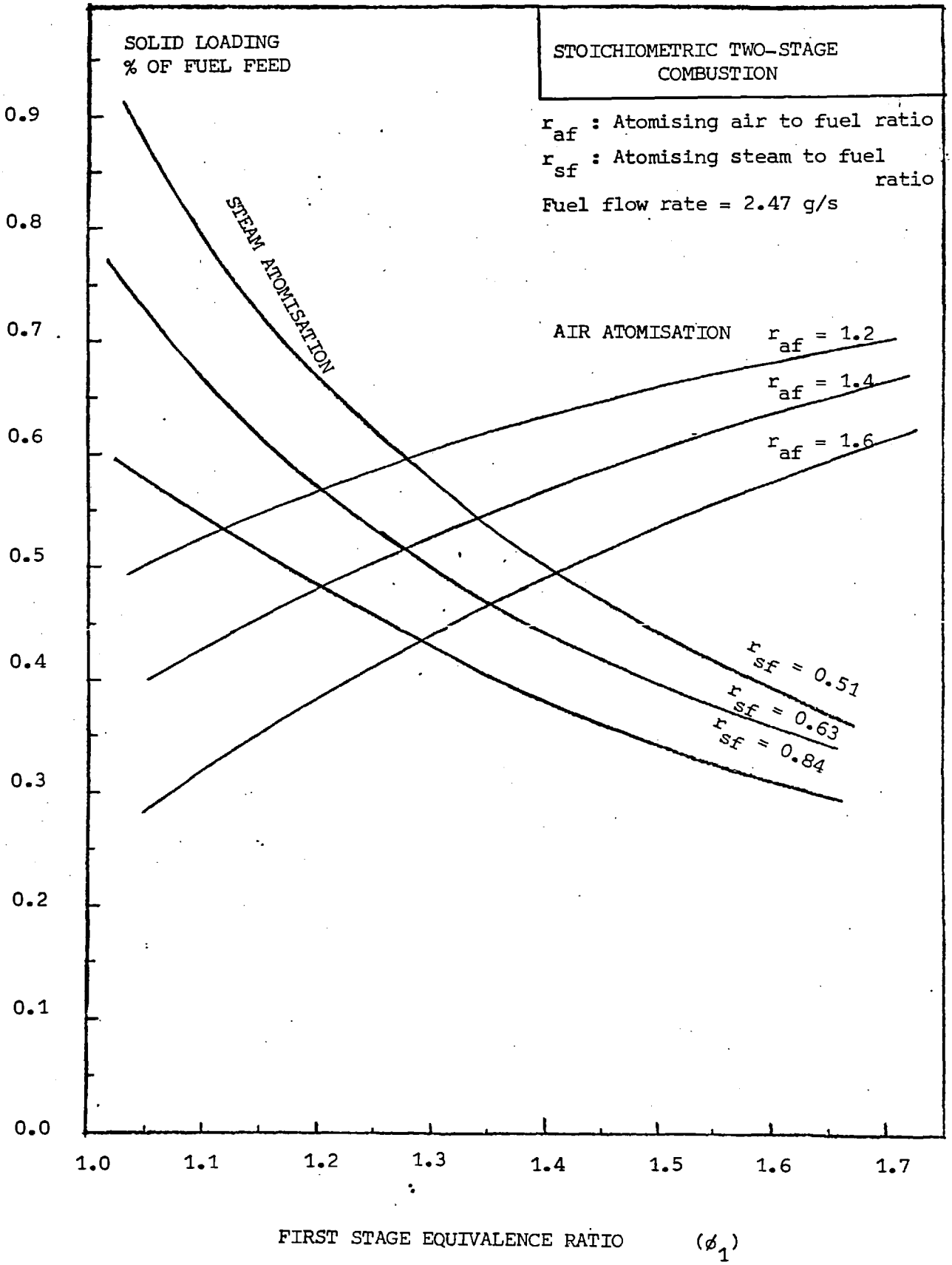

FIG. 6.6 SOLID LOADING FROM SECOND STAGE

increases in first stage equivalence ratio which follows that one stage stoichiometric operation ($\phi_1 = 1.0$) emitts less solids than two-stage stoichiometric operation ($\phi_1 > 1.0$, $\phi_2 = 1.0$).

It is understood that the use of air as atomising fluid with very small shims such as the one used in the present work, involves a high degree of by-passing in the first stage. This is produced when the cone angle of the spray is acuted at small shims therefore there is a strong possibility of forming soot immediately after the first stage chamber. This would mean a shorter residence time available for the soot to be burnt in the system.

In previous work (70) the mass of soot formed per mass of fuel was calculated by subtracting the estimated mass of char from the total mass of solid which is determined experimentally. Amount and size distribution of char can be modelled by techniques evolved from the spray evaporation model.

Following the above procedure an expiric equation for soot formation has been presented (70):

$$M_s \pm 0.0061 = F_1^2 (0.0184 - 0.161 \times 10^{-4} T) + 0.417 \times 10^{-4} F_1 T - 0.1132 \quad \ldots\ldots\ldots\ldots\ldots\ldots\ldots\ldots (6.1)$$

where M_s is the soot/fuel mass ratio, F_1 is the fuel flow rate (Kg/s) and T is the gasifier temperature (^{o}K). The above equartion shows a dependency on fuel flow rate and temperature. Temperature is understood to affect M_s through (OH) concentration.

The use of steam as atomising fluid produces a decrease in first stage temperature and would most probably increase (OH) concentration thus favouring CO_2 formation. Nevertheless, the precise effects of these

parameters on soot formation have not yet been assessed.

The particular effect of atomising fluid to fuel mass ratio on solid loading is explained through the initial spray drop size. An increase in atomising fluid to fuel mass ratio brings about a reduction in drop size with improved combustion characteristics. Due to difficulties encountered during the actual runs using air as atomising fluid in keeping constant the mass ratio of atomising air to fuel injected, attempts where made to correlate the relevants experimental data in terms of a variable that incorporates the atomising air to fuel ratio. It was found that within a deviation of $\pm 2\%$ the solid loading could be well represented by a function of (ϕ_1/r_{af}):

$$S = -0.852 + 2.329 \left(\frac{\phi_1}{r_{af}}\right) - 0.901 \left(\frac{\phi_1}{r_{af}}\right)^2 \quad \ldots\ldots\ldots\ldots \quad (6.2)$$

range $1.2 > \dfrac{\phi_1}{r_{af}} > 0.6$ and $1.55 > \phi_1 > 1.0$

where: S : Solid loading % of fuel input

ϕ_1: First stage equivalence ratio

r_{af}: Atomising air to fuel mass ratio

6.3. Solid Composition.

Solids collected were subjected to a qualitative and quantitative analysis, following techniques described in sections 4.3 and 4.4. Qualitative analysis was done by X-ray diffraction giving the major constituents of the ash. Quantitative analysis was carried out in order to obtain elemental compositions of carbon, hydrogen, vanadium, sodium, nickel and sulphur in the solid collected.

6.3.1., Qualitative Analysis. The major compounds in the solid are vanadium oxides, metallic oxides, sulphates and sodium-vanadium complexes. An X-ray diffraction pattern of the solid sample was obtained from the analytical services laboratory in every run for both air and steam atomised tests, and it was carefully analysed by comparation with standard patterns and patterns of pure prepared samples. It should be noted that emphasis on vanadium oxides was made due to its importance as deposit forming and corrosion agent.

. A list of the interplanar spacings of the three strongest lines of the diffraction pattern and its relative intensities of the relevant compounds is presented in Appendix 8.4.

The results obtained are listed in Tables A-6 and A-7 (Appendix 8.4) for both air and steam atomised tests.

I. Air Atomised Tests. Table A-6, Solid collected for runs using air as atomising fluid and for first stage equivalence ratio (maintaining overall stoichiometric onditions, $\phi_2 = 1.0$) from $\phi_1 = 1.0$ to $\phi = 1.55$, contained major amounts of V_2O_4, $NiSO_4$ and NiS. These compounds were fully identified by comparing the interplanar spacings of the three strongest radiations as tabulated in Appendix 8.4. Na_2SO_4 was fully indentified in certain runs. It should be noted that when identifying a compound by X-ray diffraction it is required to identify at least the interplanar spacings of the three strongest radiations. The solely strongest radiation corresponding to the interplanar spacing for VO_2 was also found but again its identification is left open to further investigation. The complex vanadyl-vanadete (1.1.5) $Na_2O.V_2O_4.5V_2O_5$ and the V_2O_5 oxide were not detected in any run. This is in close agreement with theoretical predictions that stoichiometric two-stage combustion of vanilla fuel oil would not lead to vanadium pentoxide (V_2O_5) formation.

Vanadium trioxide (V_2O_3) was not detected in the solid. Nevertheless this oxide is the major vanadium oxide expected to be present in the solids. V_2O_3 is very soluble in hot water (see Appendix 8.7). Vanadium containing solid particles are not larger than 15 μm (2), thus there is the strong possibility of vanadium trioxide being washed out the solid during the scrubbing, collecting and filtering process. The temperature of the slurry, from collector tank, was about 80°C. V_2O_3 or V_2O_4 cannot have been vaporized within the system since their boiling points are above 3000°C a temperature much higher than the maximum operating temperature of the system (2100°C).

Sodium metavanadates were not detected. They are expected to be formed from V_2O_5 reactions, following equations 2.29 and 2.31.

$$2NaOH + V_2O_5 \rightleftharpoons 2NaVO_3 + H_2O \quad \ldots\ldots\ldots\ldots (2.29)$$

$$Na_2SO_4 + 6V_2O_5 \rightleftharpoons Na_2O.6V_2O_5 + SO_3 \quad \ldots\ldots\ldots\ldots (2.31)$$

Since V_2O_5 and sodium metavanadates were not detected it follows that reactions 2.29 and 2.31 did not take place in the system.

II. Steam Atomised Tests. (Table A-7). Solids collected using steam as atomising fluid for first stage equivalence ratio ranging from $\phi_1 = 1.0$ to $\phi_1 = 1.55$ (maintaining overall stoichiometric conditions, $\phi_2 = 1.0$) contained major amounts of V_2O_4, $NiSO_4$, NiS, Na_2SO_4. These compounds were fully identified in the X-ray diffraction patterns. Sodium Sulphate was found throughout , but its presence is only in minor amounts. Vanadium pentoxide V_2O_5 was not detected in any run, neither the vanadyl-vanadate complex $Na_2O.V_2O_4.5V_2O_5$.

The results which are tabulated in Tables A-6 and A-7 show that vanadium bearing compounds in the solids do not differ much for air or steam atomised modes. The previous qualitative analysis for solid collected in the two atomising modes corroborates the theory elsewhere published (70) that two stage combustion constitutes a means of avoiding high temperature corrosion by precluding formation of V_2O_5. This finding is apparently unaffected by atomising modes (air or steam). The vanadium oxides formed during the process are limited to lower oxides V_2O_4 and possible V_2O_3.

6.3.2. Vanadium, Nickel, Sodium and Sulphur. Elemental analysis of the solid samples for vanadium, nickel, sodium and sulphur were done in the Analytical Services Laboratory. Vanadium, nickel and sulphur analysis was carried out by X-ray fluorescence. Sodium was determined by flame photometry. The results obtained with these techniques are presented in Table A-8 for air atomised and in Table A-9 for steam atomised tests.

Based on the Eq. 6.2 was made possible to establish the limits to vanadium , nickel and sodium content in the solids, this together with the experimental determination of the above metals in the solids collected would enable us to estimate the amount of those elements that were washed out. Maximum vanadium content in solid would be given assuming that all vandium input of the fuel would appear in the solids. This means that all vanadium bearing compounds in the solid have been taken as having solubility zero in hot water. This maximum limit to vanadium content thus calculated is plotted in Fig. 6.7 together with experimental data for vanadium content in solid. Similar results for nickel, sodium and sulphur involving concentrations of these elements both for maximum limits and experimental data correlated in terms of ϕ_1/r_{af} are presented in Figs. 6.8, 6.9 and 6.10.

Thus:

$$\text{Maximum limit to vanadium content in solid} = \frac{3.65}{S} \quad \ldots\ldots\ldots (6.3)$$

$$\text{Maximum limit to nickel content in solid} = \frac{0.476}{S} \quad \ldots\ldots (6.4)$$

$$\text{Maximum limit to sodium content in solid} = \frac{0.43}{S} \quad \ldots\ldots (6.5)$$

where, S is the solid loading from the second stage expressed as per cent of fuel input, and the metal content is given in weight per cent. Maximum limit for sulphur content in solid was not calculated since a large fraction is present in the gas phase. It can be seen that a large fraction of the vanadium, nickel and sodium intake to the system does not remain in the solid collected. The amount of vanadium, nickel and sodium that remain in the solid is plotted in Fig. 6.11, which shows that maximum nickel retained corresponds to 42% when $\phi_1/r_{af} = 1.2$. The maximum amounts of vanadium and sodium retained in the solids are 23% and 10% respectively. Fig. 6.12 shows that vanadium retained in the solid decreases as effect of increasing the atomising air to fuel ratio.

Similar results for steam atomised tests are plotted in Figs. 6.13, 6.14, 6.15, 6.16, 6.17, 6.18. The general trends for the fractions of vanadium, nickel and sodium can be seen in Fig. 6.17. It can be observed that these latter results present similar trends than those for air atomised test, Fig. 6.11. Actual results are somewhat slightly higher except for values of sodium.

As discussed in the previous section 6.3.1, the vanadium compound that presumibly was washed out of the solid was most probably V_2O_3. Theoretical predictions (see Section 5.3.2) on the quilibrium values of the system $V_2O_3/O_2/V_2O_4$ in stoichiometric combustion of "Vanilla" fuel oil, show that only V_2O_3 and V_2O_4 are expected in the solid. It follows

that vanadium oxides on the ash during two-stage combustion of "Vanilla" fuel oil are in close agreement with equilibrium values. Theorectical predictions that a decrease in temperature (Fig. 5.10) follows an increase in V_2O_4/V_2O_3 equilibrium ratio are fullfilled, since increasing the first stage equivalence ratio values above $\phi_1 = 1.0$ brings about a decrease in first stage combustion temperature. This suggests that $V_2O_3/O_2/V_2O_4$ equilibrium is reached in the first stage independently of the atomising mode (air or steam).

Sodium was barely detected in the outgoing solids, the maximum amount of sodium that remained in the solids was 10% of the input for air atomised runs at $\phi_1 = 1.5$. Sodium usually occurs in fuel oil mostly in form of NaCl that during spray combustion vaporises with consequent hydrolisis as follows

$$NaCl\ (g) + H_2O\ (g) \rightleftharpoons NaOH\ (g) + HCl\ (g)$$

NaOH having a high vapour pressure (bp = 1387°C) will initiate a reaction in vapour phase (see Section 2.4.5), a proposed reaction is:

$$2NaOH\ (g) + SO_2 + \tfrac{1}{2}O_2 \rightleftharpoons Na_2SO_4\ (cond.) + H_2O\ (g)$$

Sodium sulphate is very soluble in hot water so that it may well have been washed out during wet collection of the solids.

The fraction of sulphur intake to the system by the fuel that was retained in the solid for both atomising modes is plotted in Fig. 6.19 as a function of first stage equivalence ratio. Trends are seen to be different in the same fashion as solid emission for both atomising modes. While fraction of input sulphur that remained in the solid decreases with increasing first stage equivalence ratio for steam atomisation it increases

for air atomisation. These observations together with the fact that for air atomised tests the second stage gaseous phase was continuously deviating from thermodynamic equilibrium for increasing first stage equivalence ratio, $\phi_1 > 1.0$, suggests that for air atomisation solids are being formed in the second stage therfore increasing solid loading with equivalence ratio, and limiting sulphur vaporization. Steam atomisation improves spray combustion characteristics leading to a higher vaporization efficiencies.

6.3.3 Carbon and Hydrogen. The resuts of the carbon and hydrogen analyisis of the solids collected from the second stage are plotted in Fig. 6.20. It shows that two-stage steam atomised combustion brings abdout a strong reduction in amount of carbon and hydrogen compared with a stoichiometric one-stage operation. For steam atomised runs carbon content of the solid was brought down from values of 90% to 66%, first stage equivalence ratio ranging from $\phi_1 = 1.0$ to $\phi_1 = 1.55$. This represents a reduction of about 25.6%. Hydrogen content in solid was reduced from around 1.0% down to 0.15% in the same range of first stage equivalence ratio mentioned above. This represents a reduction of around 85% compared with single stage operation.

A decreasing carbon and hydrogen content of the solids with an increasing first stage equivalence ratio using steam as atomising fluid is also another indication that drop combustion is improved thus diminishing carbon and hydrogen residues.

The effect of steam on the combustion process of the residual carbon that follows the thermal cracking of heavy hydrocarbons in the fuel drops may be visualized through some important gasification reactions (78, 80) :

$$C + H_2O + 131 \times 10^3 \text{ KJ/Kg mol} \longrightarrow CO + H_2 \quad \ldots\ldots\ldots (6.7)$$

$$CO + H_2O \longrightarrow CO_2 + H_2 + 41 \times 10^3 \text{ KJ/Kg mol} \quad \ldots\ldots\ldots \quad (6.8)$$

$$CO + CO_2 + 173 \times 10^3 \text{ KJ/Kg mol} \longrightarrow 2\,CO \quad \ldots\ldots\ldots \quad (6.9)$$

$$C + 2H_2 \longrightarrow CH_4 + 75 \times 10^3 \text{ KJ/Kg mol} \quad \ldots\ldots\ldots \quad (6.10)$$

The carbon-steam reaction may become important in the second stage, whereas combustion is given by:

$$C + \tfrac{1}{2}O_2 \longrightarrow CO + 111 \times 10^3 \text{ KJ/Kg mol} \quad \ldots\ldots\ldots \quad (6.11)$$

$$C + O_2 \longrightarrow CO_2 + 394 \times 10^3 \text{ KJ/Kg mol} \quad \ldots\ldots\ldots \quad (6.12)$$

Injection of steam may well increase CO production via eq. 6.7 thus affecting water-gas shift reaction equilibrium (eq. 6.8) towards favouring CO_2 concentrations.

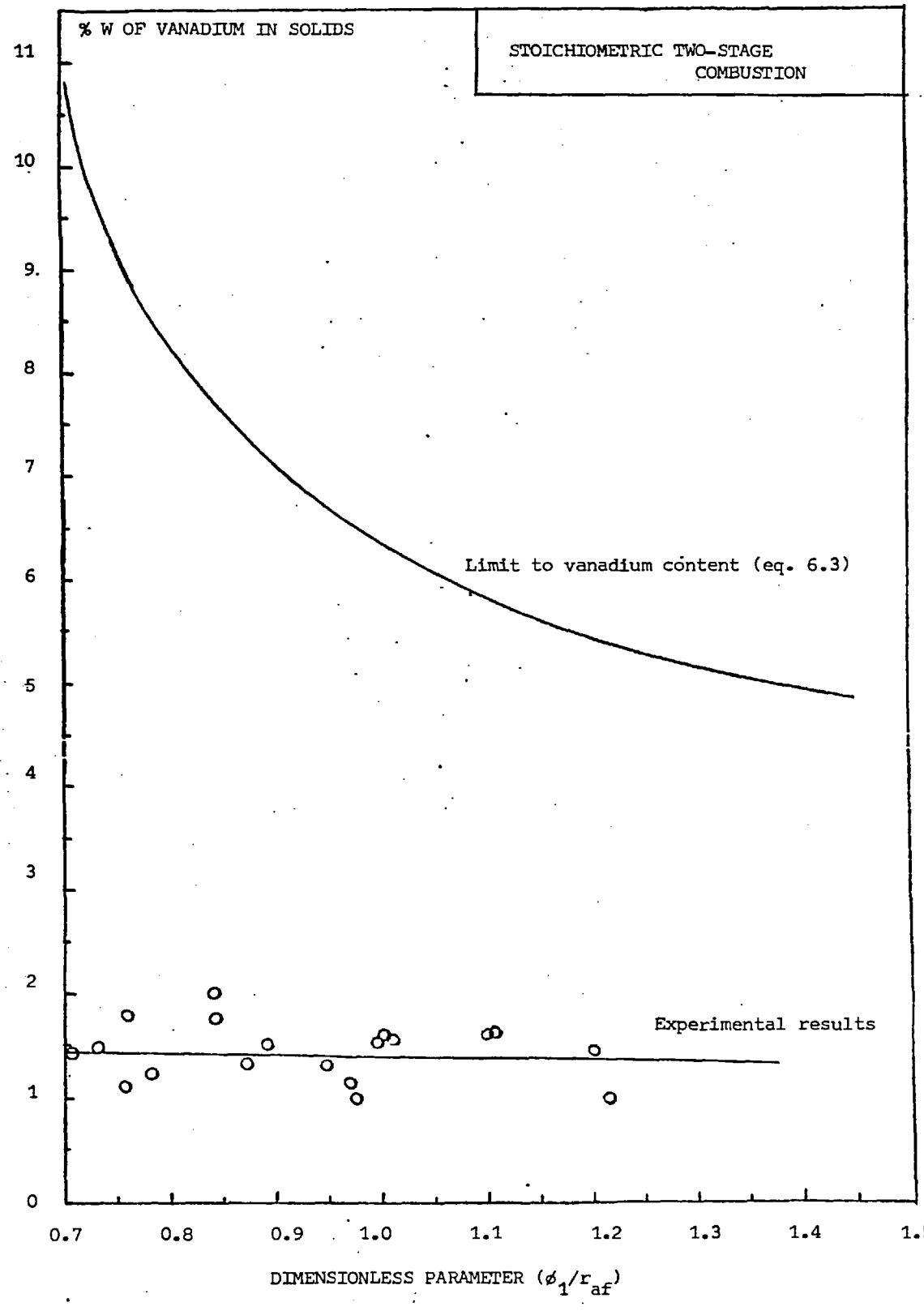

FIG. 6.7 VANADIUM CONTENT IN SOLIDS FOR AIR ATOMISATION

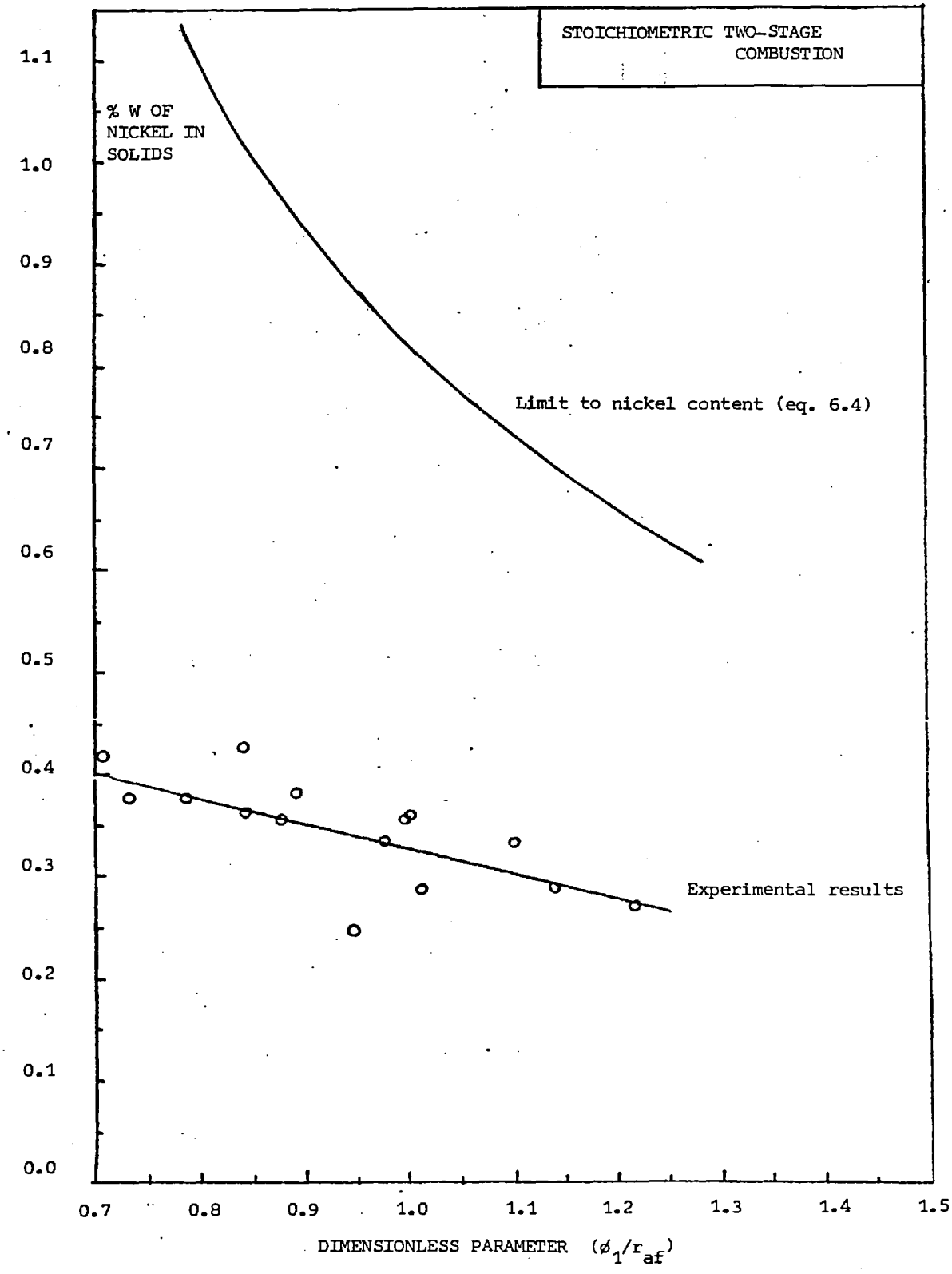

FIG. 6.8. NICKEL CONTENT IN SOLIDS FOR AIR ATOMISATION

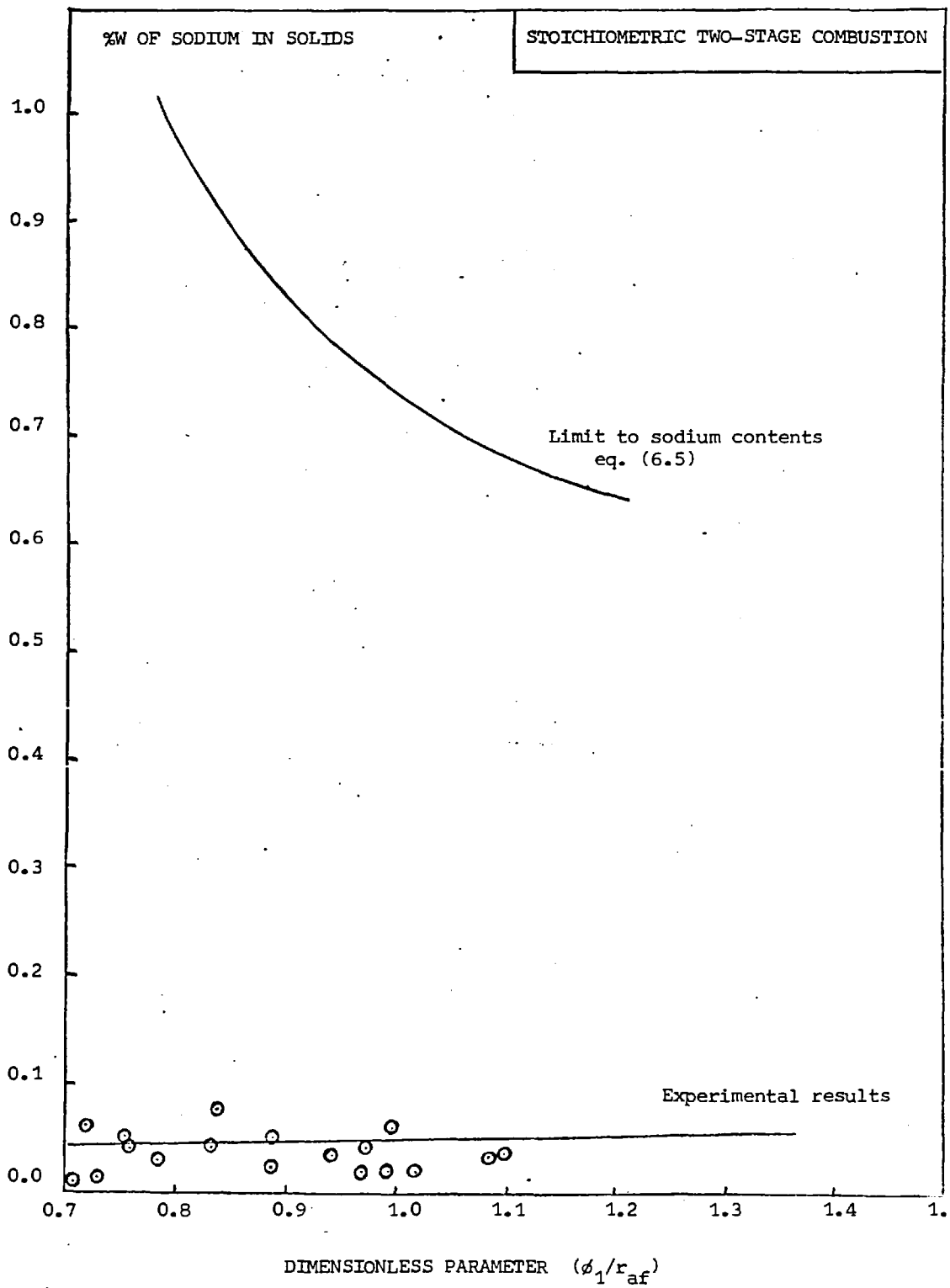

FIG. 6.9 SODIUM CONTENT IN SOLIDS FOR AIR ATOMISATION

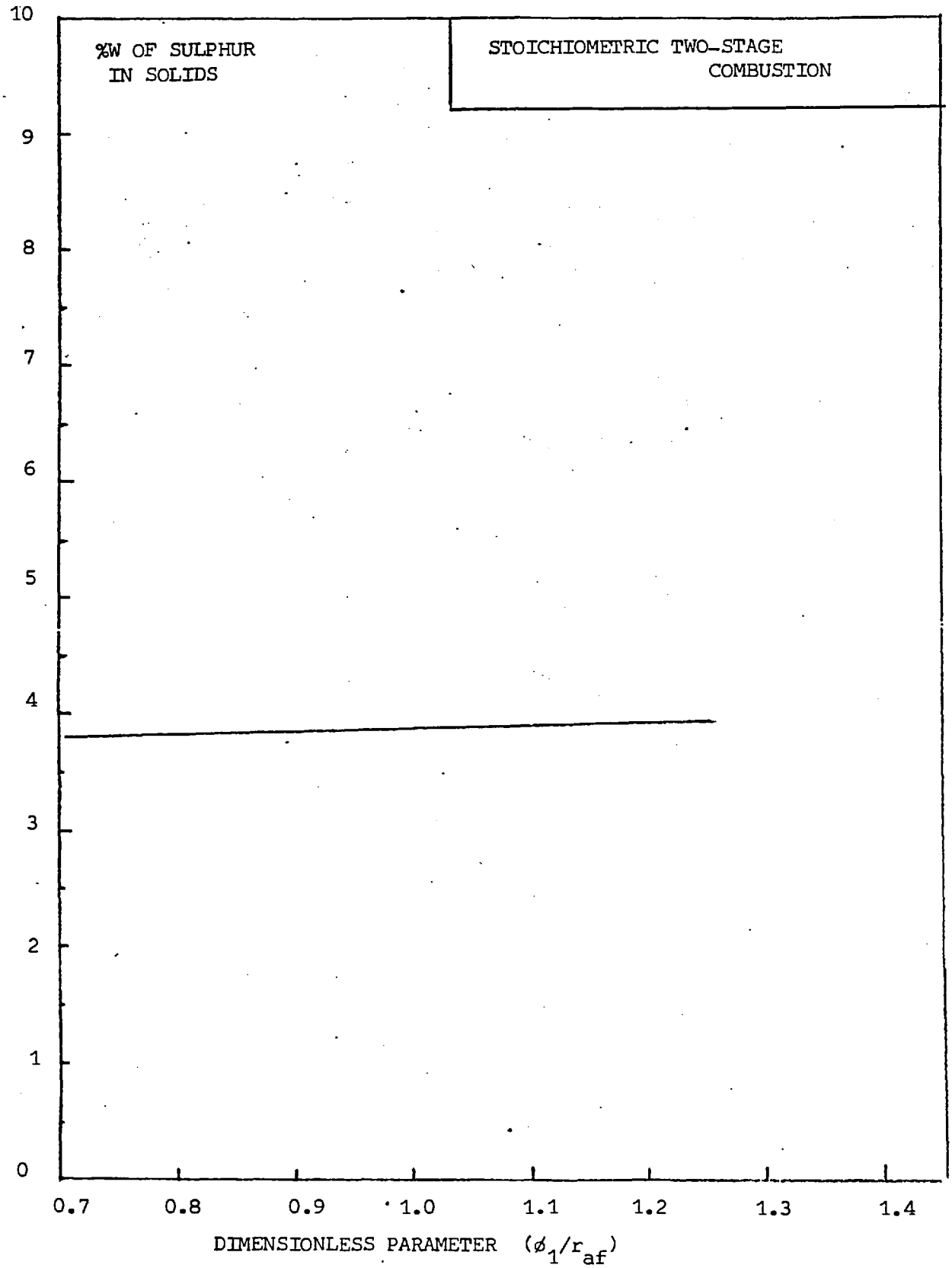

FIG. 6.10. EXPERIMENTAL SULPHUR CONTENT IN SOLIDS FOR AIR ATOMISATION

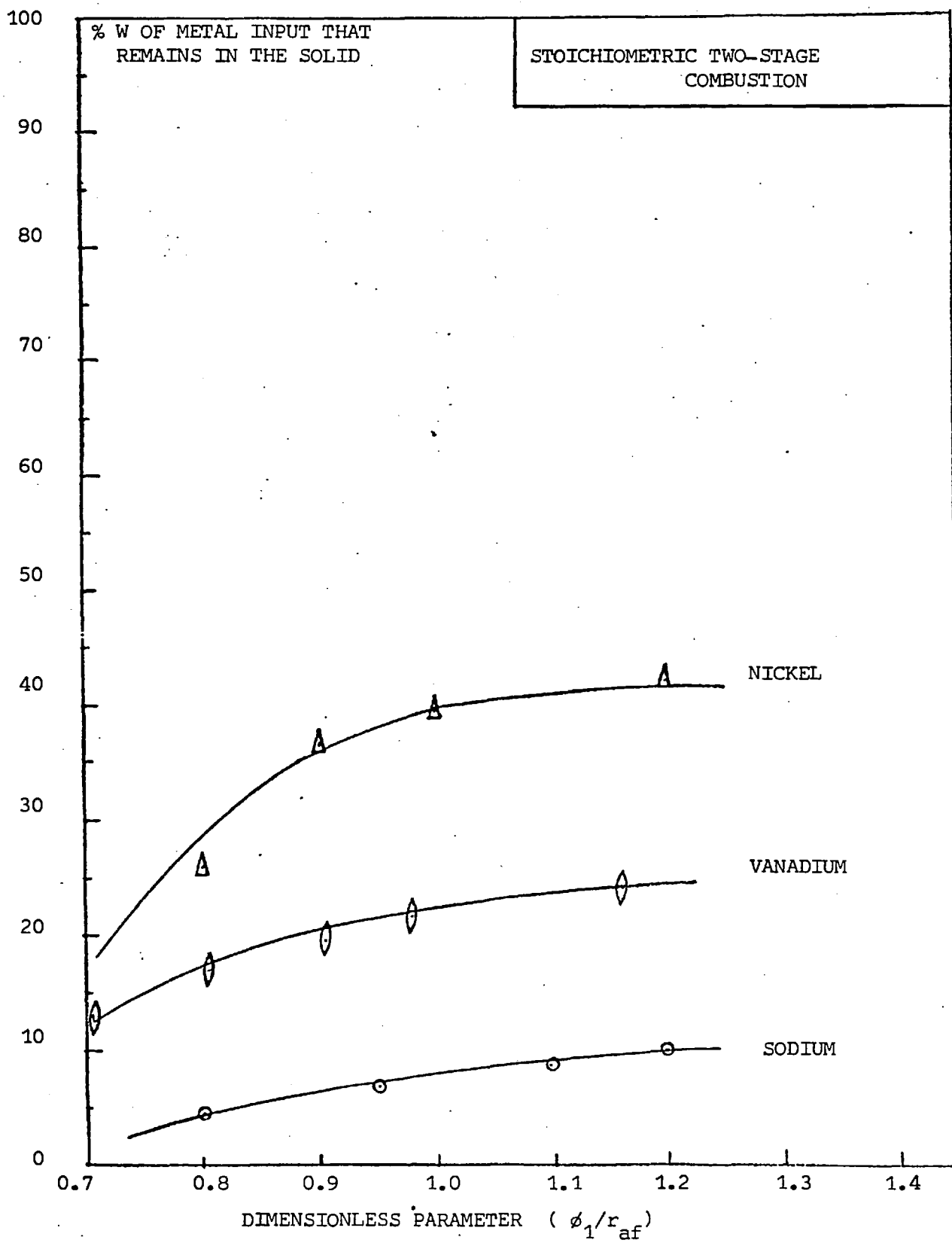

FIG. 6.11. METAL INPUT REMAINING IN THE SOLID COLLECTED FROM THE SECOND STAGE FOR AIR ATOMISATION

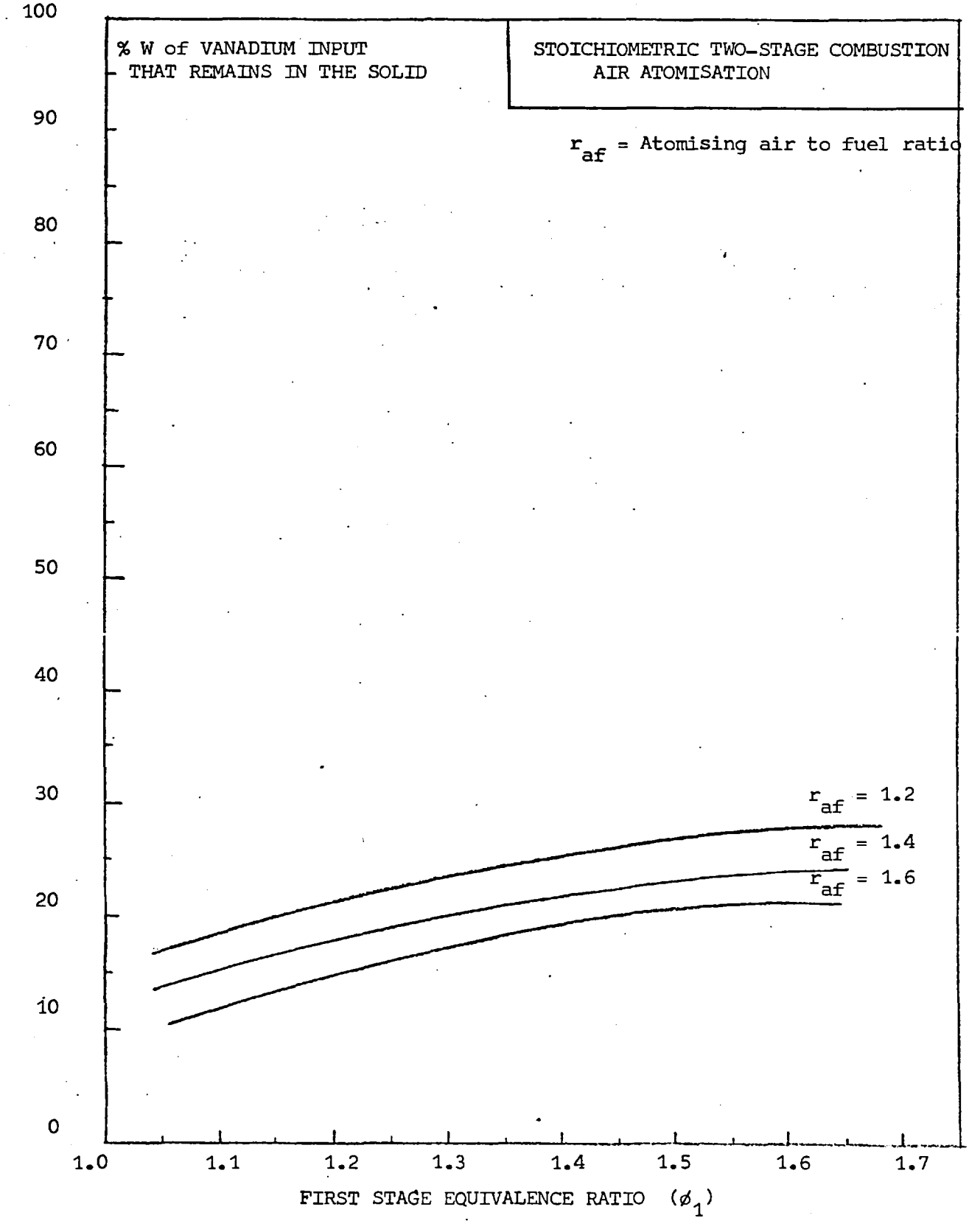

FIG. 6.12. EFFECT OF ATOMISING AIR TO FUEL RATIO ON THE FRACTION OF ORIGINAL VANADIUM THAT REMAINED IN THE SECOND STAGE SOLIDS.

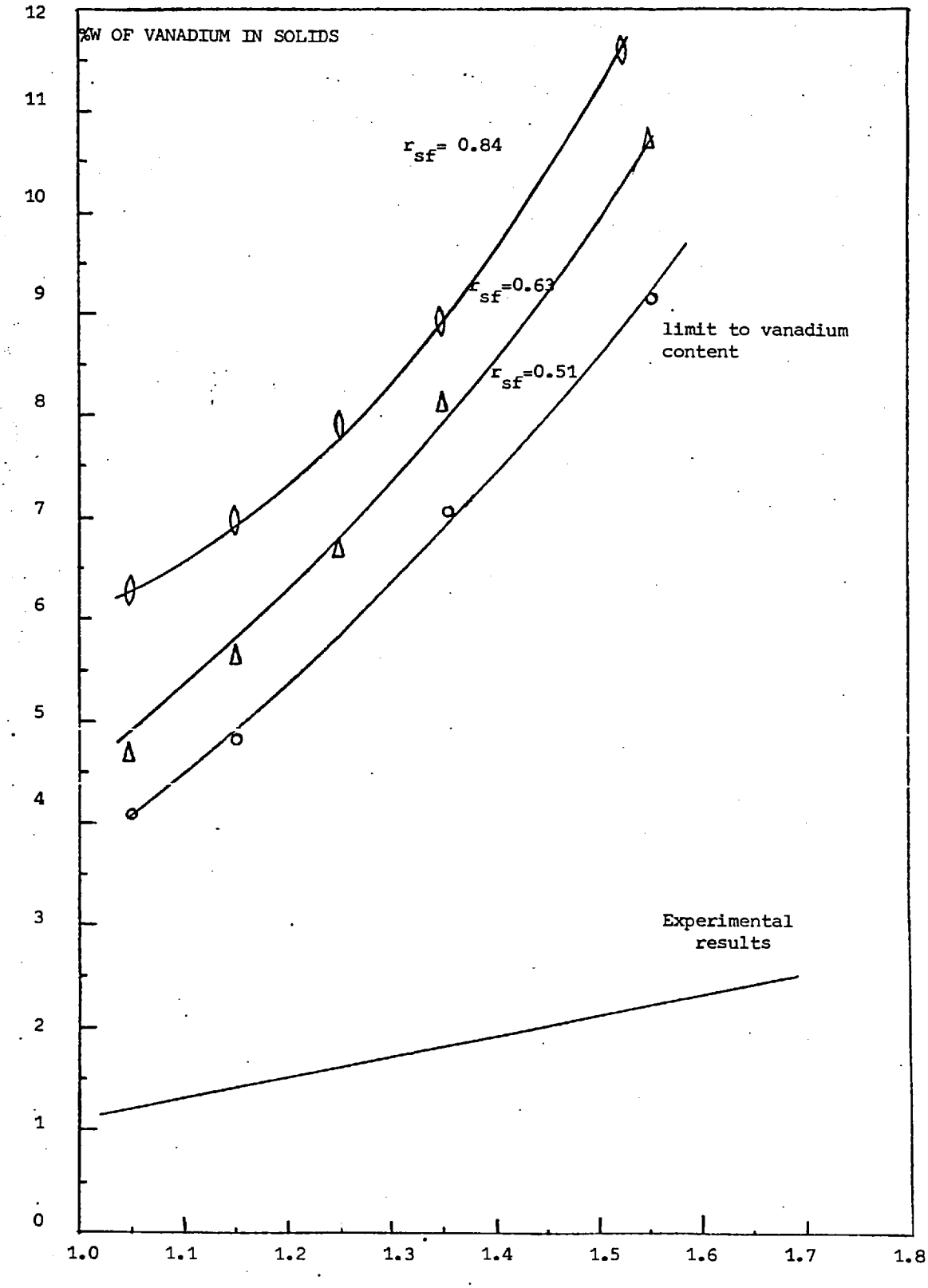

FIG. 6.13. VANADIUM CONTENT IN SOLIDS FOR STEAM ATOMISATION

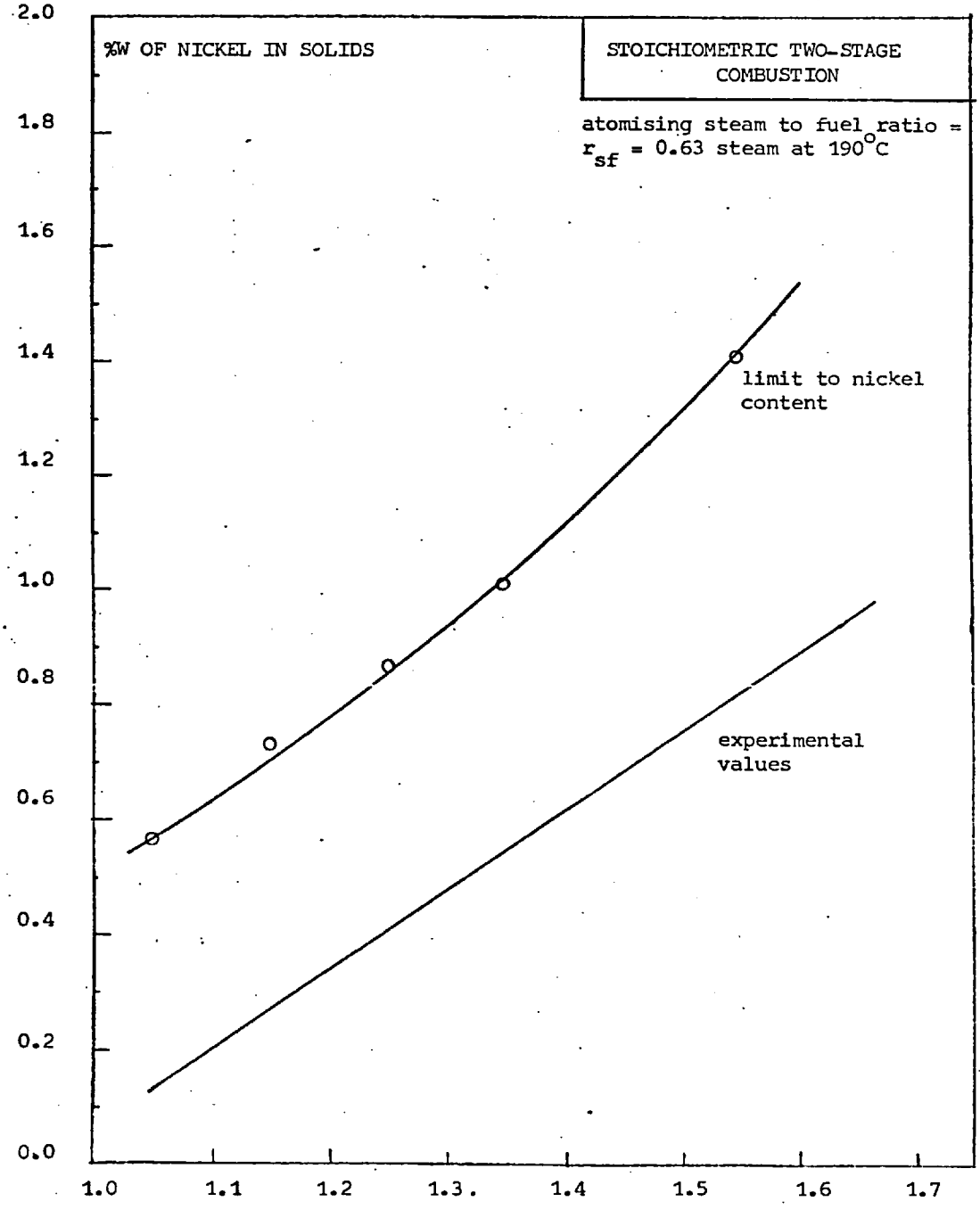

FIG. 6.14 NICKEL CONTENT IN SOLIDS FOR STEAM ATOMISATION

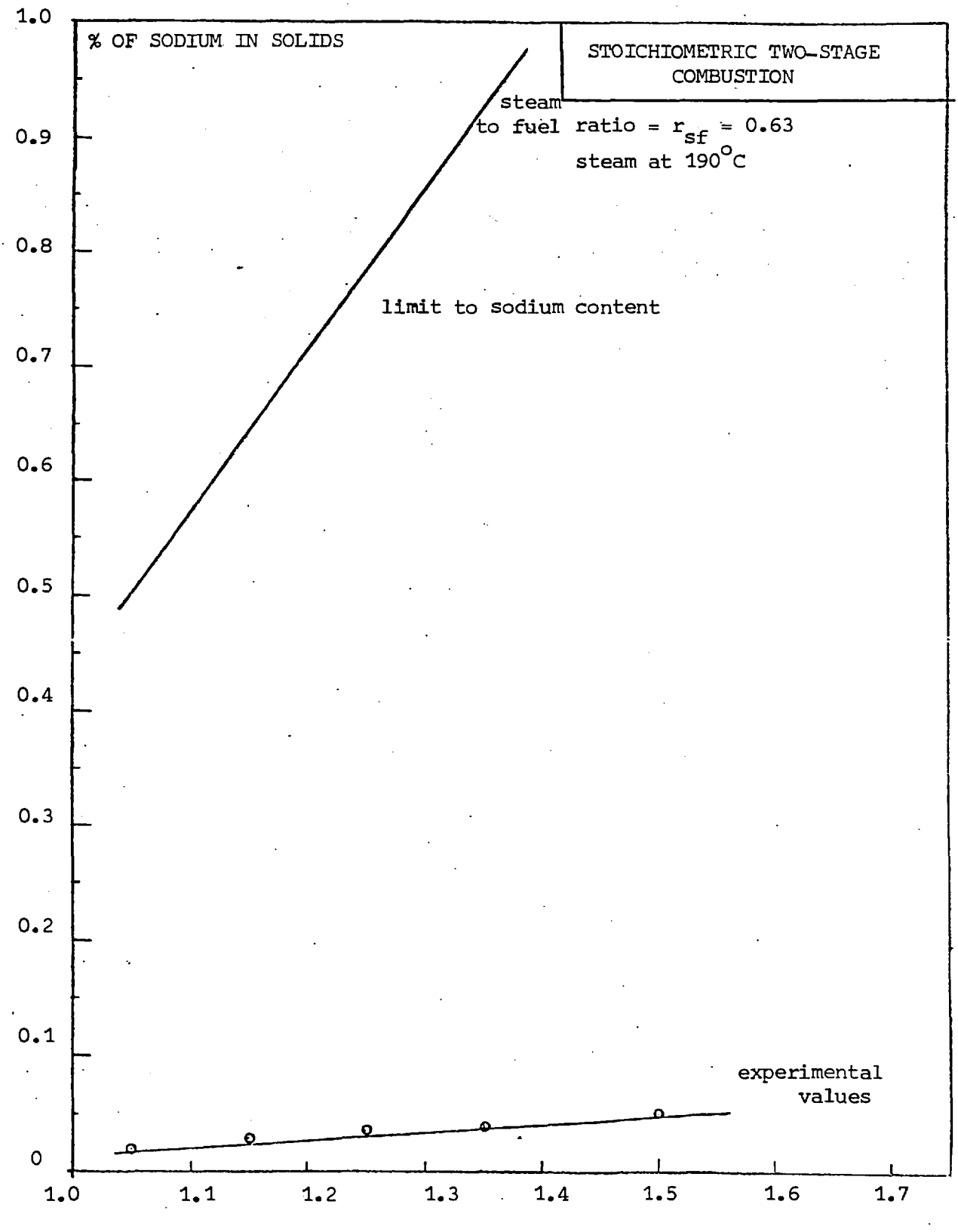

FIG. 6.15 SODIUM CONTENT IN SOLIDS FOR STEAM ATOMISATION

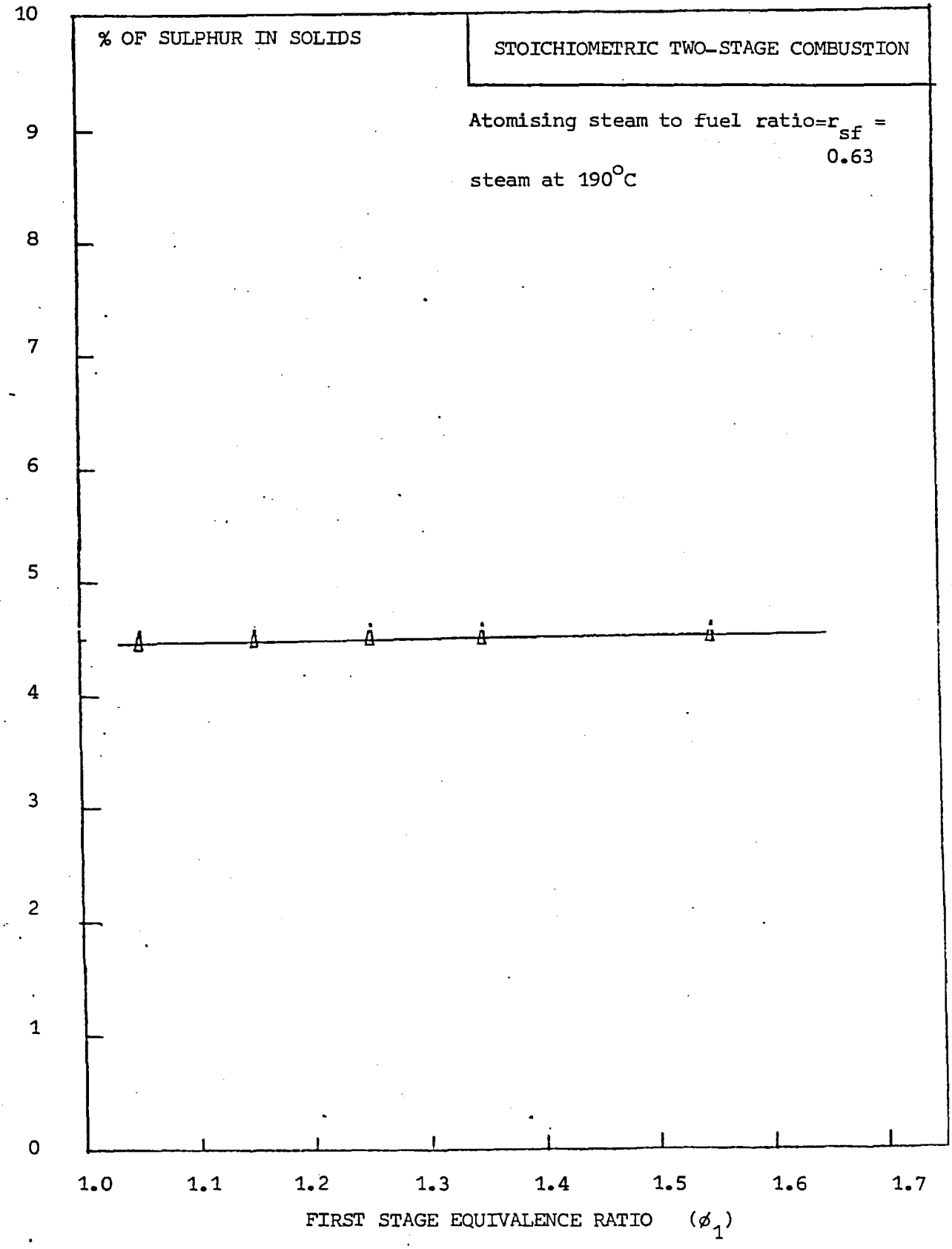

FIG. 6.16. SULPHUR CONTENT IN SOLIDS FOR STEAM ATOMISATION

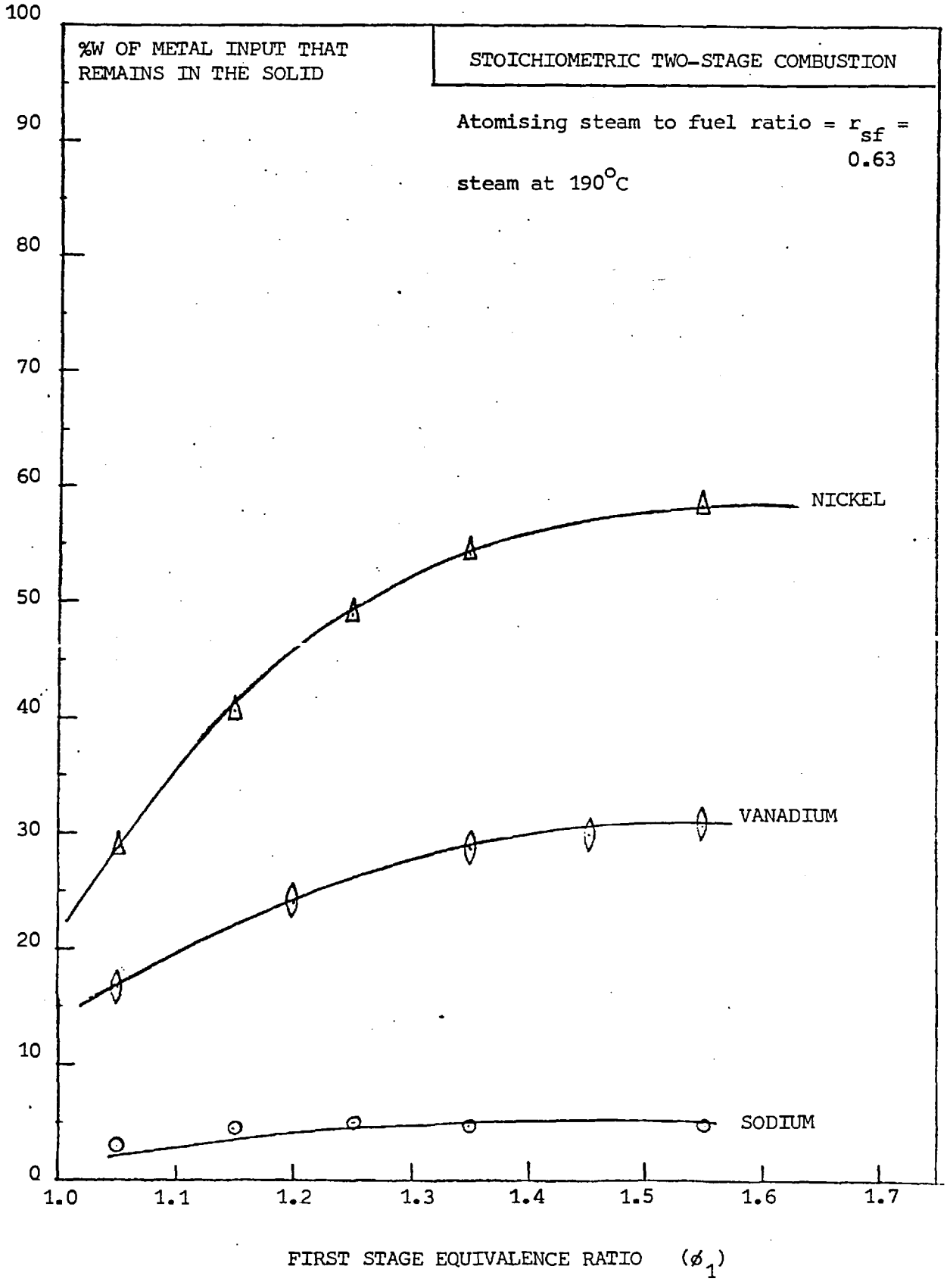

FIG. 6.17. METAL INPUT REMAINING IN THE SOLID COLLECTED FROM THE SECOND STAGE FOR STEAM ATOMISATION

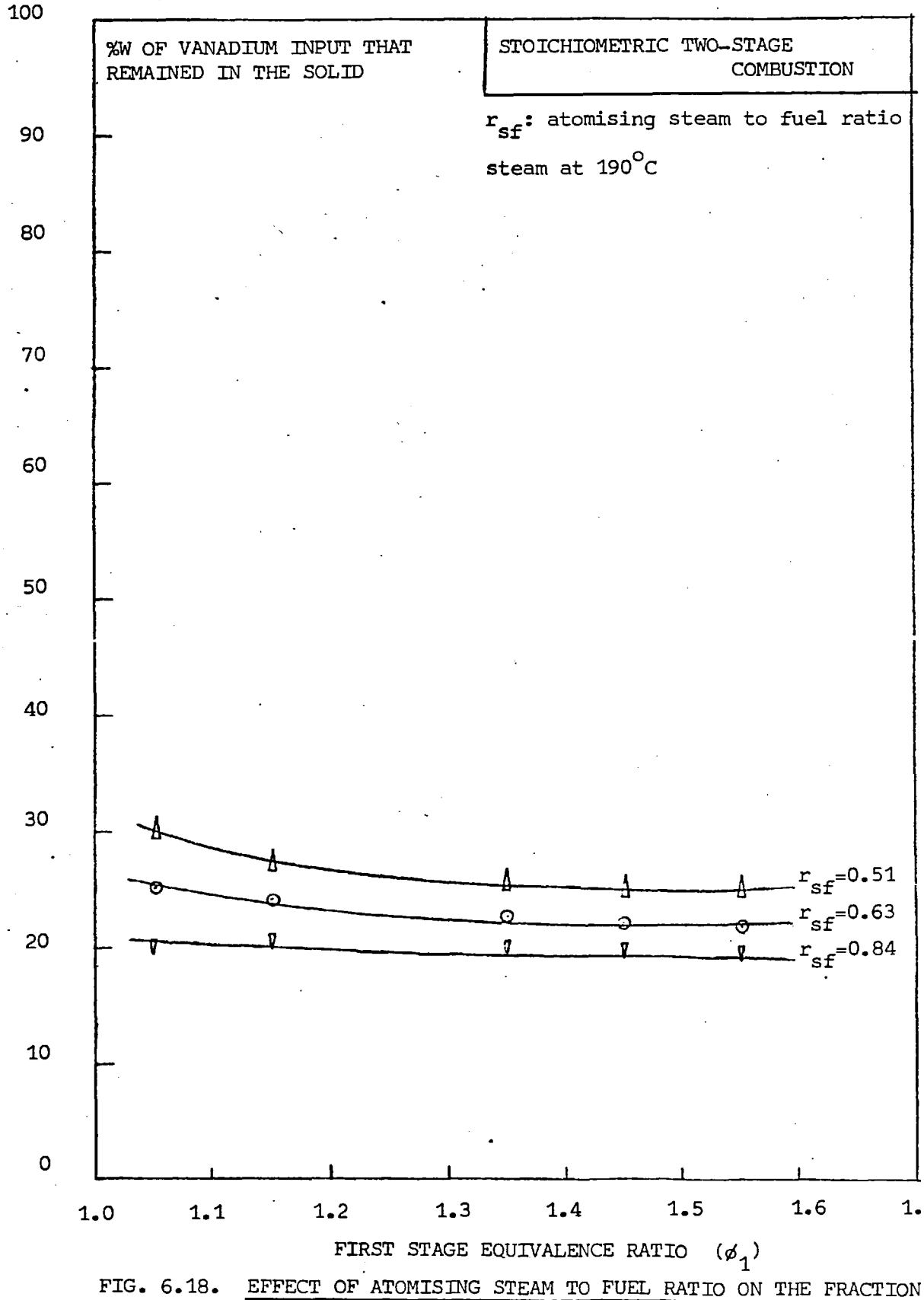

FIG. 6.18. EFFECT OF ATOMISING STEAM TO FUEL RATIO ON THE FRACTION OF ORINGINAL VANADIUM THAT REMAINED IN THE SECOND STAGE SOLIDS

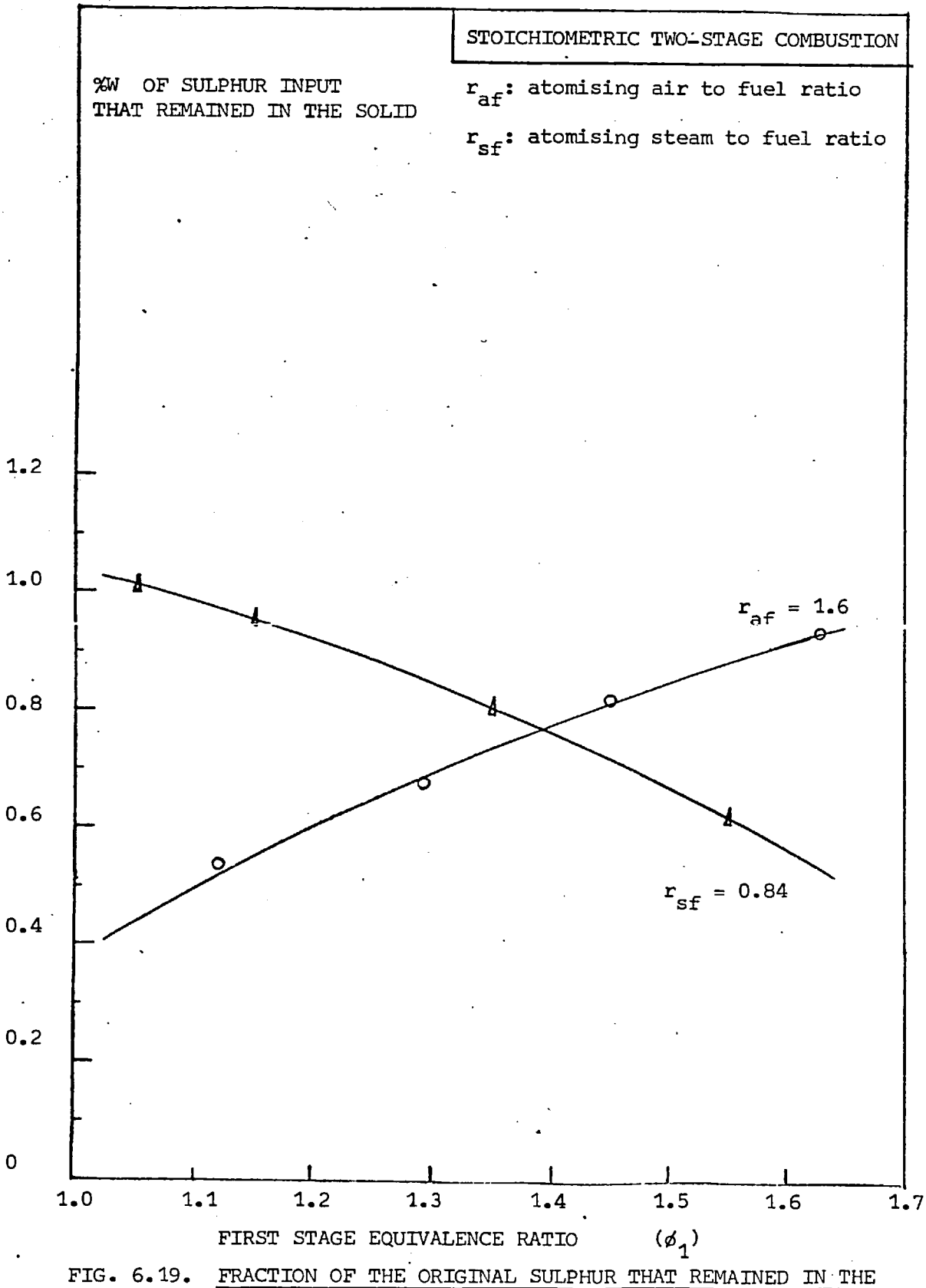

FIG. 6.19. FRACTION OF THE ORIGINAL SULPHUR THAT REMAINED IN THE SECOND STAGE SOLIDS

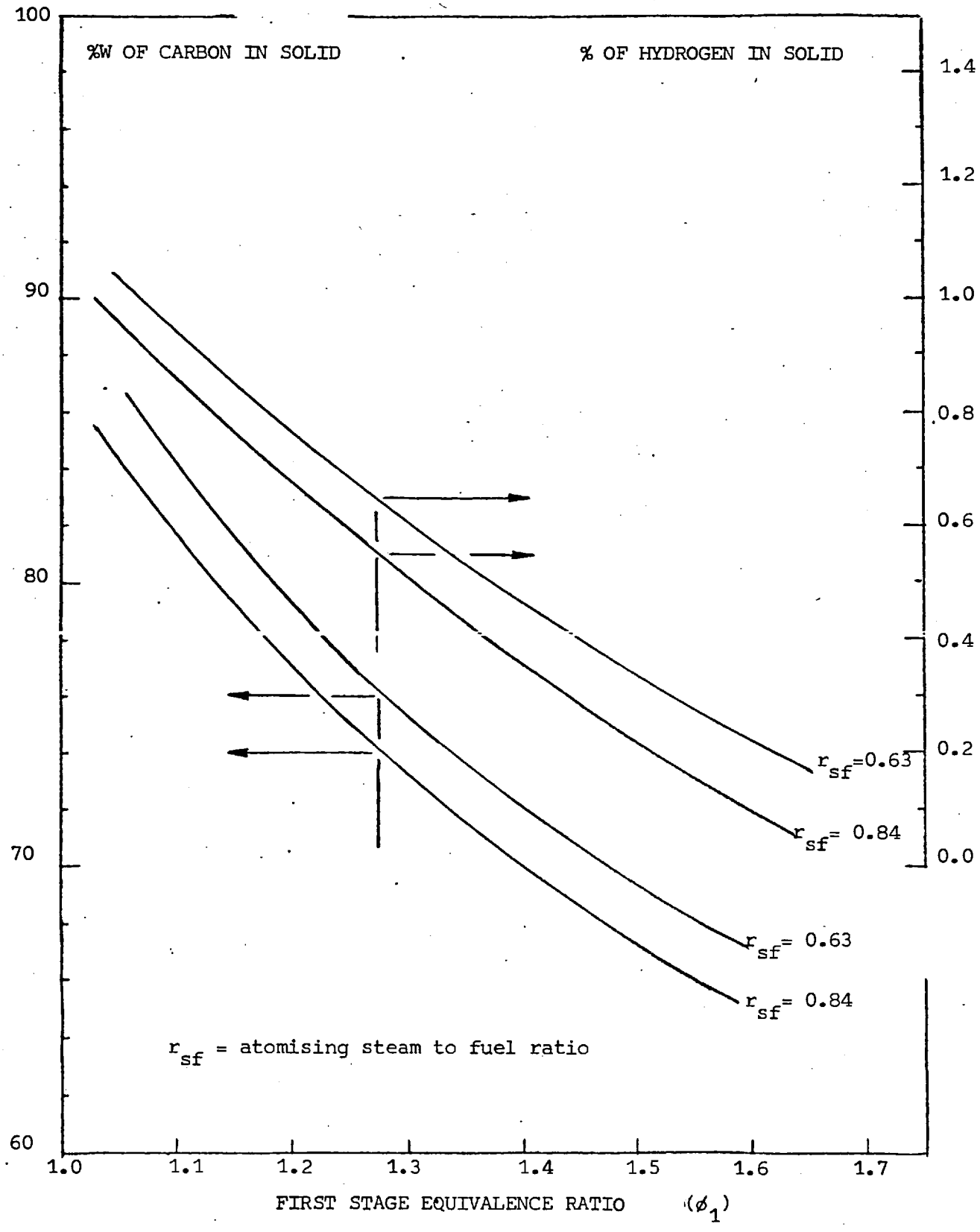

FIG. 6.20 CARBON AND HYDROGEN CONTENT IN SOLIDS FROM SECOND STAGE

CHAPTER 7

CONCLUSIONS

The spray combustion of "Vanilla"residual fuel-oil in a two stage system has been studied with particular emphasis on gaseous and particulate emission. For a wide range of conditions the following main conclusions can be drawn:

1. A multi-reaction equilibrium model for the gaseous products of Vanilla fuel oil was developed. Such model includes the components: CO, CO_2, N_2, NO, NO_2, O_2, H_2O, SO_2, SO_3 and CH_4. The reactions considered were:

$$CO + H_2O \rightleftharpoons CO_2 + H_2 \quad \ldots\ldots\ldots\ldots\ldots\ldots \quad (5.6)$$

$$2H_2O \rightleftharpoons 2H_2 + O_2 \quad \ldots\ldots\ldots\ldots\ldots\ldots \quad (5.7)$$

$$CH_4 + 2O_2 \rightleftharpoons CO_2 + 2H_2O \quad \ldots\ldots\ldots\ldots\ldots\ldots \quad (5.8)$$

$$N_2 + O_2 \rightleftharpoons 2NO \quad \ldots\ldots\ldots\ldots\ldots\ldots \quad (5.9)$$

$$NO + \tfrac{1}{2}O_2 \rightleftharpoons NO_2 \quad \ldots\ldots\ldots\ldots\ldots\ldots \quad (5.10)$$

$$SO_2 + \tfrac{1}{2}O_2 \rightleftharpoons SO_3 \quad \ldots\ldots\ldots\ldots\ldots\ldots \quad (5.11)$$

2. For air atomised runs and first stage equivalence ratio close to 1.0 ($1.0 < \phi_1 < 1.2$) the gaseous products of combustion sampled after the second stage could be considered at equilibrium for reactions

1, 2 and 3. Nevertheless for first stage equivalence ratio values greater than 1.25 ($\phi_1 > 1.25$, $\phi_2 = 1.0$) a continuously increasing deviation from the equilibrium values was noted. This suggests a decreasing gas phase combustion efficienty. Previous work (2) using steam as atomising fluid concluded that the second stage gas phase attained equilibrium according to water gas shift reaction (eq. 5.6).

3. Sulphur dioxide emission was found to be practically unaffected by first stage equivalence ratio. Air atomised tests showed values of around 0.12% molar. Steam atomised tests values showed a very slight decrease with first stage equivalence ratio; from SO_2 = 0.11% molar at ϕ_1 = 1.05 to SO_2 = 0.106% at ϕ_1 = 1.55.
If these values are to be considered in thermodynamic equilibrium with oxygen and sulphur trioxide, the theoretical predictions give SO_3 emissions of less than 1 ppm.

4. NO_x formed in the system, both from first and second stage, is mostly nitric oxide. NO_2 was found to be negligible.

5. It has been proved that two stage combustion can provide an effective method of limiting NO_x emission, due to low temperature profiles both for air and steam atomised runs. Reductions in NO_x were found to be of 72% for air atomised mode and of 92% for steam atomised mode compared with single stoichiometric stage operation.

6. The NO level emitted from the second stage in the range of ϕ_1= 1.0 to ϕ_1= 1.55 did never reach the predicted equilibrium values. At equivalence ratio ϕ_1 greater than 1.25 the NO level in the first stage exceeds the NO equilibrium values and it is presumably due to Fuel-NO formation. At ϕ_1 = 1.5, NO formed from the fuel nitrogen in the first stage reached 50% of all the total produced, if thermal NO attained equilibrium.

7. The use of steam as atomising fluid in two stage combustion of residual fuel oil brings about a significant reduction on particulate emission compared with single stage operation. Under this condition the use of small shims (7.26 mm) in the atomiser produced a reduction of 60% in solids emitted from second stage compared with previous work (2) in a similar plant.

   The use of air as atomising fluid in two stage combustion does not reduce particulate emission compared to those from single stage operation. A high degree of by-passing in the first stage chamber may have led to solid formation in the second stage thus limiting particles residence time. This observation is supported by the increasing gas phase deviation from the thermodynamic equilibrium values at increasing first stage equivalence ratio.

8. Stoichiometric two stage combustion of Vanilla fuel oil using air or steam as atomising fluid, does not lead to vanadium pentoxide (V_2O_5) formation. Since there is nowhere excess oxygen present, vanadium will oxidise to VO_2, V_2O_3 or V_2O_4 and as long as there is any carbon or hydrogen from the organic compounds these lower oxides will not yield V_2O_5. Thus the corrosive and deposit forming agent complex 1:1:5 sodium vanadyl-vanadate ($Na_2O.V_2O_4.5V_2O_5$) is not formed.

9. Elemental analysis of solid product of combustion show that a significant fraction of vanadium, nickel and sodium intaken to the system by the fuel was washed out of the solid during wet scrubbing and collection.

   For air atomised runs, maximum amount of vanadium, nickel, and sodium that remained in the solid are 23, 42 and 10% respectively.

For steam atomised runs maximum amount of vanadium nickel and sodium that remained in the solid are 30, 58 and 5% resprectively.

10. The above conclusion indicates that for vanadium beneficiation of the solids, wet-scrubbing is not a recommended technique since a maximum of only 30% of vanadium input remained in the wet collected solids.

11. The sulphur content in the solids collected is approximately independent of first stage equivalence ratio and its value is around 4% for air atomised and 4.5% for steam atomised runs.

12. Major non carbonaceous components of solid wet-collected formed during two stage combustion of "Vanilla" fuel-oil are:

VO_2, V_2O_4, Na_2SO_4, $NiSO_4$ and NiS.

CHAPTER 8

APPENDICES

APPENDIX 8 - 1

TABULATED RESULTS

TABLE A. EXPERIMENTAL SETTINGS

Run	First stage Equivalence ratio ϕ_1	Second Stage Equivalence ratio ϕ_2	Fuel Mass flow rate F (g/s)	Atomising fluid to fuel ratio. r_{af} or r_{sf}
Air Runs				
A-1	1.50	1.03	3.10	1.232
A-2	1.34	0.96	2.90	1.381
A-3	1.02	0.96	2.70	1.343
A-4	1.11	1.01	2.90	1.140
A-5	1.10	1.00	2.46	1.448
A-6	1.18	1.00	2.46	1.646
A-7	1.30	1.00	2.17	1.903
A-8	1.48	1.01	2.46	1.648
A-9	1.05	1.00	2.46	1.441
A-10	1.25	1.00	2.46	1.597
A-11	1.15	1.00	2.46	1.629
A-12	1.40	1.00	2.46	1.604
A-13	1.55	1.00	2.46	1.641
A-14	1.05	1.00	2.46	1.178
A-15	1.05	1.00	2.46	1.252
A-16	1.15	1.00	2.46	1.372
A-17	1.25	1.00	2.46	1.257
A-18	1.35	1.00	2.46	1.352
A-19	1.35	1.00	2.46	1.227
A-20	1.35	1.00	2.90	1.229
A-21	1.45	1.00	2.90	1.437
Steam Runs				
S-1	1.05	1.00	2.46	0.51
S-2	1.15	1.00	2.46	0.51
S-3	1.35	1.00	2.46	0.51
S-4	1.55	1.00	2.46	0.51
S-5	1.05	1.00	2.46	0.63
S-6	1.15	1.00	2.46	0.63
S-7	1.25	1.00	2.46	0.63
S-8	1.35	1.00	2.46	0.63
S-9	1.45	1.00	2.46	0.63
S-10	1.55	1.00	2.46	0.84
S-11	1.05	1.00	2.46	0.84
S-12	1.15	1.00	2.46	0.84
S-13	1.25	2.00	2.46	0.84
S-14	1.35	1.00	2.46	0.84
S-15	1.55	1.00	2.46	0.84

r_{af} = atomising air to fuel ratio.

r_{sf} = atomising steam to fuel ratio.

TABLE A-1. MAJOR GASEOUS COMPONENTS FROM SECOND STAGE AIR ATOMISED RUNS.

RUN	FIRST STAGE EQUIVALENCE RATIO ϕ_1	SECOND STAGE EQUIVALENCE RATIO ϕ_2	% Molar CO_2	% Molar CO	% Molar H_2O	% Molar H_2	% Molar N_2	% Molar O_2
A-1	1.50	1.03	9.50	2.9	10.5	N.D	72.0	<1.0
A-2	1.34	0.96	6.00	1.0	8.7	1.4	72.8	N.D.
A-3	1.02	0.96	10.00	N.D.	9.6	N.D.	72.5	N.D.
A-4	1.11	1.01	7.20	0.5	9.5	N.D.	72.9	<1.0
A-9	1.05	1.00	9.05	<0.2	9.8	N.D.	72.9	N.D.
A-10	1.25	1.00	6.90	1.0	9.3	0.4	73.5	N.D.
A-11	1.15	1.00	8.40	0.2	9.2	N.D.	72.8	N.D.
A-12	1.40	1.00	7.40	0.8	8.5	1.2	72.0	N.D.
A-13	1.55	1.00	6.95	2.0	8.3	2.2	72.0	N.D.

N.D. : NOT DETECTED

TABLE A-2.

SO_2 EMISSION FROM SECOND STAGE - AIR AND STEAM ATOMISED RUNS

RUN*	FIRST STAGE EQUIVALENCE RATIO ϕ_1	SECOND STAGE EQUIVALENCE RATIO ϕ_2	% MOLAR SO_2
A-9	1.05	1.00	0.118
A-10	1.25	1.00	0.120
A-11	1.15	1.00	0.124
A-12	1.40	1.00	0.119
A-13	1.55	1.00	0.121
S-5	1.05	1.00	0.115
S-6	1.15	1.00	0.110
S-7	1.25	1.00	0.107
S-8	1.35	1.00	0.103
S-9	1.45	1.00	0.110
S-10	1.55	1.00	0.104

* A : Air atomised run.

S : Steam atomised run.

TABLE A-3

NO_x EMISSION IN TWO-STAGE COMBUSTION SYSTEM

RUN	ATOMISING FLUID	FIRST STAGE EQUIVALENCE RATIO ϕ_1	SECOND STAGE EQUIVALENCE RATIO ϕ_2	NO_x LEVEL (ppm)	NO_x LEVEL (ppm)
				FIRST STAGE	SECOND STAGE
A-1	AIR	1.50	1.03	60	130
A-2	AIR	1.34	0.96	120	140
A-3	AIR	1.02	0.96	270	320
A-4	AIR	1.11	1.01	200	210
S-5	STEAM	1.05	1.00	198	90
S-6	STEAM	1.15	1.00	112	60
S-7	STEAM	1.25	1.00	52	32
S-8	STEAM	1.35	1.00	35	20
S-9	STEAM	1.45	1.00	-	10
S-10	STEAM	1.55	1.00	11	-

NO_x = NO , NO_2 = Negligible for all runs.

TABLE A-4

SOLID LOADING FROM SECOND STAGE. - AIR ATOMISED RUNS

RUN	FIRST STAGE EQUIVALENCE RATIO ϕ_1	SECOND STAGE EQUIVALENCE RATIO ϕ_2	FUEL MASS FLOW RATE F(G/s)	ATOMISING AIR TO FUEL RATIO r_{af}	SOLID LOADING % FUEL FEED s
A-1	1.50	1.03	3.10	1.232	0.80
A-2	1.34	0.96	2.90	1.381	0.50
A-3	1.02	0.96	2.70	1.343	0.45
A-4	1.11	1.01	2.90	1.140	0.84
A-5	1.10	1.00	2.46	1.448	0.52
A-6	1.18	1.00	2.46	1.646	0.33
A-7	1.30	1.00	2.17	1.903	0.31
A-8	1.48	1.01	2.46	1.648	0.54
A-9	1.05	1.00	2.46	1.441	0.50
A-10	1.25	1.00	2.46	1.597	0.45
A-11	1.15	1.00	2.46	1.629	0.38
A-12	1.40	1.00	2.46	1.604	0.40
A-13	1.55	1.00	2.46	1.641	0.51
A-14	1.05	1.00	2.46	1.178	0.44
A-15	1.05	1.00	2.46	1.252	0.41
A-16	1.15	1.00	2.46	1.372	0.34
A-17	1.25	1.00	2.46	1.257	0.53
A-18	1.35	1.00	2.46	1.352	0.35
A-19	1.35	1.00	2.46	1.227	0.57
A-20	1.35	1.00	2.90	1.229	0.60
A-21	1.45	1.00	2.90	1.437	0.64

TABLE A-5.

SOLID LOADING FROM SECOND STAGE - STEAM ATOMISED RUNS

RUN	FIRST STAGE EQUIVALENCE RATIO ϕ_1	SECOND STAGE EQUIVALENCE RATIO ϕ_2	FUEL MASS FLOW RATE F(g/s)	ATOMISING STEAM TO FUEL RATIO r_{sf}	SOLID LOADING % FUEL FEED s
S-1	1.05	1.00	2.46	0.51	1.04
S-2	1.15	1.00	2.46	0.51	0.61
S-3	1.35	1.00	2.46	0.51	0.59
S-4	1.55	1.00	2.46	0.51	0.42
S-5	1.05	1.00	2.46	0.63	0.85
S-6	1.15	1.00	2.46	0.63	0.65
S-7	1.25	1.00	2.46	0.63	0.48
S-8	1.35	1.00	2.46	0.63	0.41
S-9	1.45	1.00	2.46	0.63	-
S-10	1.55	1.00	2.46	0.84	0.38
S-11	1.05	1.00	2.46	0.84	0.72
S-12	1.15	1.00	2.46	0.84	0.47
S-13	1.25	1.00	2.46	0.84	0.36
S-14	1.35	1.00	2.46	0.84	0.45
S-15	1.55	1.00	2.46	0.84	0.36

TABLE A-6

MAJOR CONSTITUENTS OF SOLID PRODUCT OF COMBUSTION FOR AIR.

ATOMISED RUNS. (NO CARBON AND HYDROGEN CONSIDERED)

RUN	$Na_2O.V_2O_4.5V_2O_5$	$V_2O_4.6V_2O_5$	V_2O_5	V_2O_4	V_2O_3	VO_2	$NaVO_3$	α-$NaVO_3$	$V_2O_5.H_2O$	Na_2SO_4	NiO	$NiSO_4$	NiS
A-1	-	-	-	***	-	*	-	-	-	***	-	***	***
A-2	-	-	-	***	-	*	-	-	-	***	-	***	***
A-3	-	-	-	***	*	*	-	-	-	***	-	***	***
A-4	-	-	-	***	-	*	-	-	-	*	-	***	***
A-5	-	-	-	***	-	*	-	-	-	*	-	***	***
A-6	-	-	-	***	-	*	-	-	-	*	-	***	***
A-7	-	-	-	***	*	*	-	-	-	*	-	***	***
A-8	-	-	-	***	*	*	-	-	-	***	-	***	***
A-9	-	-	-	***	-	*	-	-	-	***	-	***	***
A-10	-	-	-	***	-	*	-	-	-	***	-	***	***
A-11	-	-	-	***	-	*	-	-	-	*	-	***	***
A-12	-	-	-	***	-	*	-	-	-	***	-	***	***
A-13	-	-	-	***	*	*	-	-	-	***	-	***	***
A-14	-	-	-	***	*	*	-	-	-	*	-	***	***
A-15	-	-	-	***	-	*	-	-	-	*	-	***	***
A-16	-	-	-	***	-	*	-	-	-	***	-	***	***
A-17	-	-	-	***	-	*	-	-	-	***	-	***	***
A-18	-	-	-	***	-	*	-	-	-	***	-	***	***
A-19	-	-	-	***	-	*	-	-	-	*	-	***	***
A-20	-	-	-	***	-	*	-	-	-	*	-	***	***
A-21	-	-	-	***	-	*	-	-	-	*	-	***	***

- : Not detected

* : Not fully detected

*** : Fully identified

TABLE A-7

MAJOR CONSTITUENTS OF SOLID PRODUCTS OF COMBUSTION FOR STEAM ATOMISED RUNS. NO CARBON AND HYDROGEN CONSIDERED.

RUN	$Na_2O.V_2O_4.5V_2O_5$	$V_2O_4.6V_2O_5$	V_2O_5	V_2O_4	V_2O_3	VO_2	$NaVO_3$	α-$NaVO_3$	$V_2O_5.H_2O$	Na_2SO_4	NiO	$NiSO_4$	NiS
S-1	-	-	-	***	-	*	-	*	-	***	-	***	***
S-2	-	-	-	***	-	***	-	-	-	***	-	***	***
S-3	-	-	-	***	-	*	-	-	-	***	-	***	***
S-4	-	-	-	***	-	****	-	-	-	***	-	***	***
S-5	-	-	-	***	-	*	-	-	-	***	-	***	***
S-6	-	-	-	***	-	*	-	-	-	***	-	***	***
S-7	-	-	-	***	-	*	-	-	-	***	-	***	***
S-8	-	-	-	***	-	***	-	-	-	***	-	***	***
S-9	-	-	-	***	-	*	-	-	-	***	-	***	***
S-10	-	-	-	***	-	*	-	-	-	***	-	***	***
S-11	-	-	-	***	-	*	-	-	-	***	-	***	***
S-12	-	-	-	***	-	*	-	-	-	***	-	***	***
S-13	-	-	-	***	-	***	-	-	-	***	-	***	***
S-14	-	-	-	***	-	***	-	-	-	***	-	***	***
S-15	-	-	-	***	-	*	-	-	-	***	-	***	***

\- : Not detected

* : Not fully identified

*** : Fully identified

TABLE A-8

ELEMENTAL ANALYSIS OF SOLID PRODUCTS OF COMBUSTION FROM SECOND STAGE (AIR ATOMISED RUNS).

RUN	DIMENSION LESS PARAMETER ϕ_1/r_{af}	% W OF VANADIUM ± 1%	% W OF NICKEL ± 2%	% W OF SODIUM ± .005	% W OF SULPHUR ± 2.8%	% W OF CARBON ± 0.5%	% W OF HYDROGEN ± 0.5%
A-1	1.215	.94	.181	.020	3.06	-	-
A-2	.972	1.14	.183	.020	3.15	-	-
A-3	.759	1.68	.309	.040	2.92	-	-
A-4	.975	1.00	.336	.040	3.04	-	-
A-5	.756	1.11	.257	.050	2.35	80.7	Nil
A-6	.719	1.00	.288	.060	2.49	80.4	Nil
A-7	.685	.85	.250	.040	2.50	83.9	0.63
A-8	.898	.81	.208	.010	2.66	85.1	Nil
A-9	.729	1.47	.375	.015	3.90	76.8	Nil
A-10	.783	1.22	.376	.030	3.33	81.7	Nil
A-11	.706	1.40	.413	.010	4.49	79.5	0.35
A-12	.873	1.30	.357	.115	5.43	83.4	0.39
A-13	.945	1.27	.245	.035	3.66	86.2	0.39
A-14	.891	1.52	.382	.050	4.31	-	-
A-15	.839	1.75	.359	.075	4.63	-	-
A-16	.838	2.01	.423	.040	4.92	-	-
A-17	.994	1.49	.354	.020	4.57	-	-
A-18	.999	1.58	.358	.060	4.72	-	-
A-19	1.100	1.60	.330	.035	4.63	-	-
A-20	1.098	1.58	.284	.020	4.22	-	-
A-21	1.009	1.55	.294	.065	2.88	-	-

ϕ_1 : First stage equivalence ratio

r_{af} : Atomising air to fuel mass ratio

TABLE A-9.

ELEMENTAL ANALYSIS OF SOLID PRODUCTS OF COMBUSTION FROM SECOND STAGE

(STEAM ATOMISED RUNS)

RUN	ATOMISING PRESSURE (BARS)	% W OF VANADIUM ± 1.2%	% W OF NICKEL ± 1.5%	% W OF SODIUM ± 0.05	% W OF SULPHUR ± 3.0%	% W OF CARBON ± 0.5%	% W OF HYDROGEN ± 0.5%
S-1	1.0	1.70	.288	0.010	3.89	70.31	1.246
S-2	1.0	1.12	.277	.110	4.25	77.10	1.022
S-3	1.0	1.54	.347	ND	4.37	72.67	.740
S-4	1.0	2.05	.404	.010	4.63	73.64	.790
S-5	1.4	1.52	.321	.045	5.24	86.20	1.050
S-6	1.4	1.29	.307	.025	4.31	80.67	.810
S-7	1.4	1.19	.303	.010	4.46	77.27	.600
S-8	1.4	1.11	.325	.020	4.31	71.82	.580
S-9	1.4	-	-	-	-	70.23	.420
S-10	1.4	4.09	.996	.075	4.27	68.93	.280
S-11	2.0	1.46	.306	.015	4.09	86.19	0.980
S-12	2.0	2.09	.503	.010	4.52	78.53	.880
S-13	2.0	1.51	.425	.030	5.00	75.74	.510
S-14	2.0	1.80	.457	.010	5.33	69.05	.370
S-15	2.0	1.45	.385	0.010	4.30	68.62	.160

APPENDIX 8.2

SPECIFICATION OF "VANILLA" RESIDUAL FUEL OIL

TABLE A-10 FUEL SPECIFICATION

Composition:

Carbon	86.1% wt.
Hydrogen	11.0% wt.
Sulphur	2.4% wt.
Ash	0.083% wt.
Water content	0.21% wt.

Ash composition:

This was determined in an oxygen atmosphere.

OXIDE	% IN ASH	P.P.M. IN FUEL
V_2O_5	78.4	651 (365 as V)
Na_2O	7.0	58 (44 as Na)
NiO	7.2	60
SO_3	7.2	-
Fe_2O_3	1.7	14
Al_2O_3	1.25	10
MgO	1.20	9
SiO_2	0.9	7
CaO	0.85	7
ZnO	0.2	2

ELEMENT	% IN ASH
V	43.9
Na	5.3
Ni	5.7
S	2.9
Fe	1.2
Al	0.7
Mg	0.72
Si	0.42
Ca	0.61
Zn	0.16

The following oxides were also found in the ash, each contributing less than 0.05% : BaO, Cr_2O_3, MNO_2, PbO, SnO_2, SrO, TiO_2, CuO, Co_3O_4.

The analysis, as per cent of ash, totals in excess of 100%. This is to be expected in high vanadium ashes, where during ignition, some dissociation of V_2O_5 to V_2O_4 occurs..

Viscosity:

at 70°F (21°C) 1820 S.R. secs.

at 100°F (38°C) 614 S.R. secs.

at 210°F (99°C) 60 S.R. secs.

Flash Point:

202°F (95°C)

Specific Gravity:

at 60°F (15.6°C) = 0.9635

Distillation:

Initial Boiling Point : 177°C

10% Recovery 257°C

50% Recovery 346°C

Vapour Pressure:

at 100°C = 0.36 m Hg

at 400°C = 245.0 cm Hg

Gross Calorific Value:

42.9 KJ/g (18400 Btu/lb)

Nett Calorific Value:

39.7 $\frac{KJ}{g}$

APPENDIX 8.3

CALIBRATION CURVES FOR ATOMISER

Calibration Curves for atomiser Mark IV No 2 for hoth air and steam were worked out. These curves represent a correlation between atomising fluid mass flow rate and atomising pressure for a particular temperature and atomiser shim size. The calibration curves are presented in Fig. A.1 for air at 50°C and super-heated steam at 200°C using a shim of 7.27 mm (0.2865 ins.). Atomiser cup diameter was 12.7 mm (0.5 ins.) and a zero setting of 6.47 mm (0.2545 ins).

General Principles

The general equation for the adiabatic flow of a compressible fluid across a reduction in cross sectioned area of a conduit is (73):

$$W = \frac{A_2}{\sqrt{1 - n^2}} \sqrt{2g} \sqrt{P_1 \rho_1} \quad \beta \quad \ldots\ldots\ldots\ldots\ldots \quad (8.3.1)$$

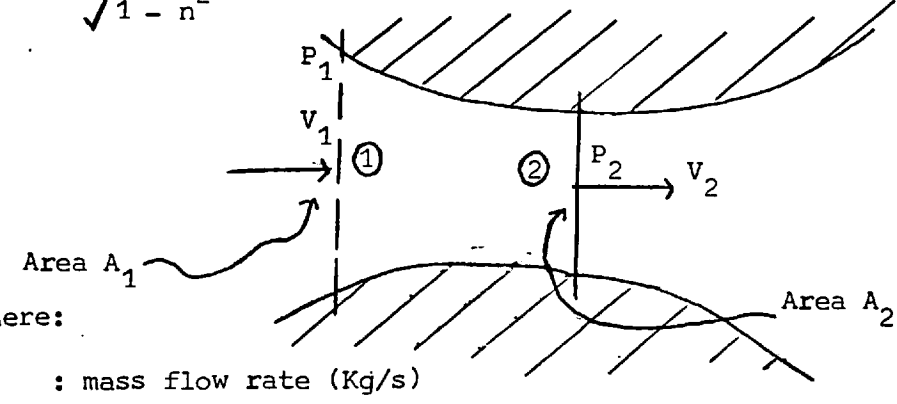

where:

W : mass flow rate (Kg/s)

A_2 : cross sectional area in the throat (m^2)

A_1 : cross sectional area upstream of the throat (m^2)

P_1 : Absolute pressure upstream of the throat (N/m^2)

ρ_1 : Density of the fluid at conditions 1 (Kg/m^3)

γ = Cp/Cv V : mean linear velocity of the fluid (m/s)

$\eta = A_2/A_1$

$$\beta = \sqrt{\frac{\left(\frac{\gamma}{1-\gamma}\right)\left(1 - \{R\}^{\frac{\gamma-1}{\gamma}}\right) R^{2/\gamma}}{\frac{1 - n^2 R^{2/\gamma}}{1 - n^2}}} \quad \ldots\ldots\ldots\ldots (8.3.2)$$

Referring to equation 8.3.1, it can be seen that the maximum flow rate occurs when β is maximum. This maximum value of β happens at a value of R given by differentiating equation 8.3.2 respect to R and equating to zero. The final expression is:

$$\frac{\gamma + 1}{R^{2/\gamma}} - \frac{2}{R^{\frac{\gamma+1}{\gamma}}} - (\gamma-1)\, n^2 = 0 \quad \ldots\ldots\ldots\ldots (8.3.3)$$

In the case of a gas discharging out of a vessel through a nozzle, n can be taken as approximating to zero.

$$R = \left(\frac{2}{\gamma + 1}\right)^{\frac{\gamma}{\gamma - 1}} \quad \ldots\ldots\ldots\ldots\ldots\ldots\ldots\ldots (8.3.4)$$

When this condition is staisfied, the mass throughput the nozzle is maximum and the velocity the fliud V_2 reaches, is equal to that of the sound under the conditions ruling at that point. Any further minimution in the downstream pressure P_2, will not influence the discharge.

Therefore, when operating below the critical ratio, given by equations 8.3.4, it is possible to measure the flow of a given gas through a nozzle by a knowledge of the upstream pressure and temperature.

If the nozzle operates under shocked conditions a simplified equation can be written:

$$W = KA\sqrt{P_1\rho_1} \qquad \ldots\ldots\ldots\ldots\ldots\ldots\ldots\ldots\ldots\ldots \quad (8.3.5)$$

where:

W : mass flow rate through the nozzle (g/s)

K : constant depending upon γ and n

A : area of the throat (m^2)

P_1 : absolute pressure upstream of the throat (N/m^2)

ρ_1 : density of the fluid at upstream conditions (Kg/m^3)

Theoretical values of β and R for n equal to zero have been calculated for steam and air.

TABLE A.11 VALUES FOR γ , β AND R FOR STEAM AND AIR

FLUID	γ	β	R
STEAM	1.31	0.468	0.544
AIR	1.41	0.481	0.527

steam calibration curve.

Applying equation 8.3.1 for both air and steam:

$$Wa = \frac{A_2}{\sqrt{1 - n^2}}\sqrt{2g}\sqrt{P_1\rho_a}\ \beta_a \qquad \ldots\ldots\ldots\ldots\ldots\ldots (8.3.6)$$

a : air
s : steam

$$Ws = \frac{A_2}{\sqrt{1 - n^2}}\sqrt{2g}\sqrt{P_1\rho_s}\ \beta_s \qquad \ldots\ldots\ldots\ldots\ldots\ldots (8.3.7)$$

Dividing eq. 8.3.7 by eq. 8.3.6,

$$\frac{Ws}{Wa} = \frac{\sqrt{\rho_s}}{\sqrt{\rho_a}} \quad \frac{\beta_s}{\beta_a} \qquad \ldots\ldots\ldots\ldots\ldots\ldots\ldots\ldots\ldots\ldots \quad (8.3.8)$$

From Table A, $\beta_s = 0.468$ and $\beta_a = 0.481$, and substituting into eq. 8.3.8

$$\frac{Ws}{Wa} = 0.973\sqrt{\frac{\rho_s}{\rho_a}}$$

Thus,

$$Ws = Wa \times 0.973\sqrt{\frac{\rho_s}{\rho_a}} \qquad \ldots\ldots\ldots\ldots\ldots\ldots\ldots\ldots\ldots\ldots \quad (8.3.9)$$

Equation 8.3.9 enables us to calculate steam mass flow rate through atomiser using air calibration data.

Rotameters for Gases

In the special case of air and similar gases, the equation for a rotameter is expressed as (74):

$$C\,\rho\,A\,v^2 = k \qquad \ldots\ldots\ldots\ldots\ldots\ldots\ldots\ldots\ldots\ldots \quad (8.3.10)$$

where:

C : resistence coefficient

ρ : density of the gas

A : maximum cross sectional area of the float at right angles to the float

v : velocity of the gas

K : constant of the rotameter.

In the general case the resistence coefficient varies with the Reynold number, nevertheless for a conical shaped float this variation has been found to be negligible. Thus, equation 8.3.10 can be reduced to the simple form:

$$Q\sqrt{\rho} = \text{constant} \quad \ldots\ldots\ldots\ldots\ldots\ldots\ldots\ldots\ldots\ldots \quad (8.3.11)$$

where Q is the volumetric flow rate, in terms of which the scale is usually graduated.

Thus if the calibration relates to air density ρ_o and the instrument indicates a volumetric flow rate Q_o when the density is ρ_1 the true value of Q at this density will be given by:

$$Q_1 = Q_o\sqrt{\frac{\rho_o}{\rho_1}} \quad \ldots\ldots\ldots\ldots\ldots\ldots\ldots\ldots\ldots\ldots \quad (8.3.12)$$

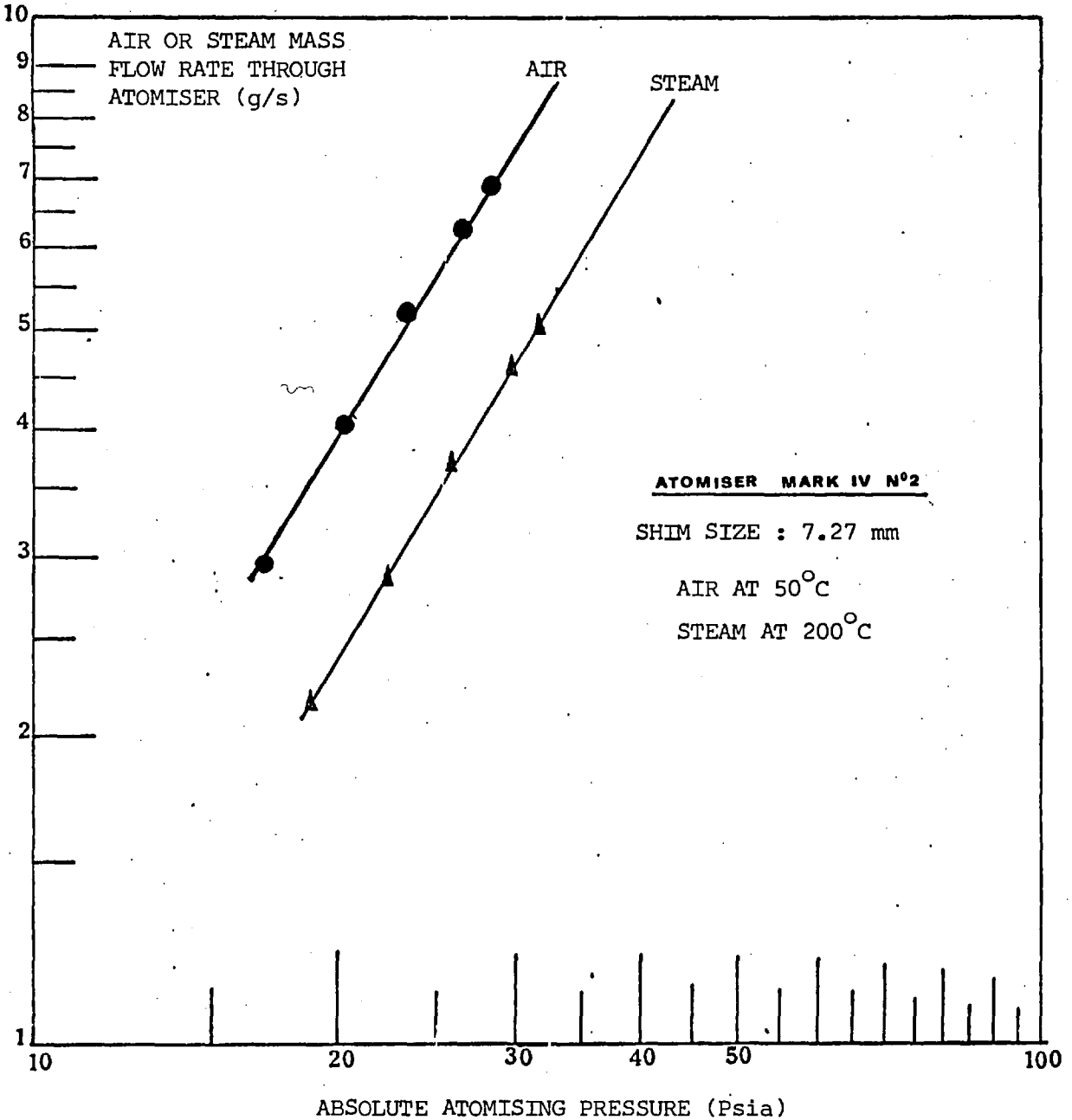

FIG. A.1. CALIBRATION CURVES FOR ATOMISER

APPENDIX 8.4

A.S.T.M. X-RAY DIFFRACTION DATA FOR RELEVANT COMPOUNDS

TABLE A-12, X-RAY POWDER DIFFRACTION DATA FOR COMPOUNDS THAT OCCUR IN SOLID PRODUCTS OF COMBUSTION OF RESIDUAL FUEL OIL. (75)

COMPOUND	A.S.T.M. DIFFRACTION SPACINGS d(A^o) RELATIVE INTENSITIES (I/I_1)				FILE NUMBER REF.(75)
V_2O_5	4.38 100	3.40 90	2.88 65	5.76 40	9-387
V_2O_4	3.20 100	2.43 60	2.14 50	3.31 30	19-1398
V_3O_5	3.29 100	2.86 100	2.63 100	4.64 50	9-148
V_2O_3	1.69 100	2.70 80	3.65 60	3.65 60	1-1293
VO_2	3.25 100	3.15 100	2.44 50	3.44 10	19-1401
$V_2O_5 \cdot 3H_2O$	12.1 100	10.6 60	2.90 50	17.4 30	7-332
$V_2O_5 \cdot H_2O$	3.23 100	5.78 80	2.89 80	5.78 80	11-673
$V_2O_4 \cdot 2H_2O$	2.46 100	6.42 90	5.12 90	6.42 90	13-346
$VO_2 \cdot YH_2O$	3.51 100	2.64 55	2.00 55	6.16 20	18-1445

.../ cont.

COMPOUND	A.S.T.M. DIFFRACTION SPACINGS d(A^o) RELATIVE INTENSITIES (I/I_1)				FILE NUMBER REF.(75)
$V_2O_4 \cdot 6V_2O_5$	1.80 100	2.28 70	3.11 50	3.11 50	15-247
$Na_2O \cdot V_2O_4 \cdot 5V_2O_5$	3.37 100	9.46 80	7.28 80	9.46 80	20-1170
$NaVO_3$	3.18 100	1.79 100	6.80 80	6.80 80	20-1168
α-$NaVO_3$	5.00 100	3.61 100	3.26 100	6.85 10	15-51
$NaVO_3 \cdot H_2O$	5.00 100	2.95 50	3.24 38	7.1 15	1-0246
Na_3VO_4	4.43 100	2.51 100	2.44 80	4.43 100	20-1169
Na_2O	1.97 100	2.78 37	3.21 29		23-528A
Na_2SO_4	2.78 100	4.66 73	3.18 51	4.66 73	5-0631
NiO	2.09 100	2.41 91	1.48 57	2.41 91	4-0835
NiS	1.97 100	2.96 80	1.71 80	2.96 80	2-1280
$NiSO_4$	2.55 100	3.56 80	3.33 50	4.31 40	13-435
NiV	2.16 100	1.96 100	2.31 51	4.11 5	5-0692

APPENDIX 8.5

CARBON AND HYDROGEN ANALYSIS OF SOLIDS

Carbon and hydrogen content of the solids collected were carried out by means of the elemental analyser Mod. 1102, for details see Section 4.3. The procedure employed to obtain the experimental results can be summarozed as follows:

1. Carbon and hydrogen in the solid have been totally oxidised to gaseous CO_2 and H_2O. Their determination from the gaseous phase is done by Gas Chromatography using a Poropax Q column. The peaks obatined for CO_2, H_2O and N_2 are given in Figs. A.2 and A.3, where two standard samples and two experimental solid samples are analysed.

2. Peak heights are used to determine carbon and hydrogen content of the sample, by referring to the values given by the standard sample. In this work the standard sample used was a mass of cyclohexanone 2,4 dinitrophenylhydrazone, whose composition was:

51.79 %W of carbon

5.07 %W of hydrogen

20.14 %W of nitrogen

3. Calculate response factor Y_c and Y_h for carbon and hydrogen respectively as follows:

for carbon:

$$Y_c = \frac{51.79 \times \text{weight of 2,4 dinitro}}{\text{2,4 dinitro peak area } (CO_2)}$$

for hydrogen:

$$Y_h = \frac{5.07 \times \text{weight of 2,4 dinitro}}{\text{2,4 dinitro peak area } (H_2O)}$$

4. Calculate mass per cent of carbon and hydrogen in solid sample as follows:

$$\%W \text{ of carbon} = Y_c \times \frac{\text{peak area of sample } (CO_2)}{\text{weight of sample}}$$

$$\%W \text{ of hydrogen} = Y_h \times \frac{\text{peak area of sample } (H_2O)}{\text{weight of sample}}$$

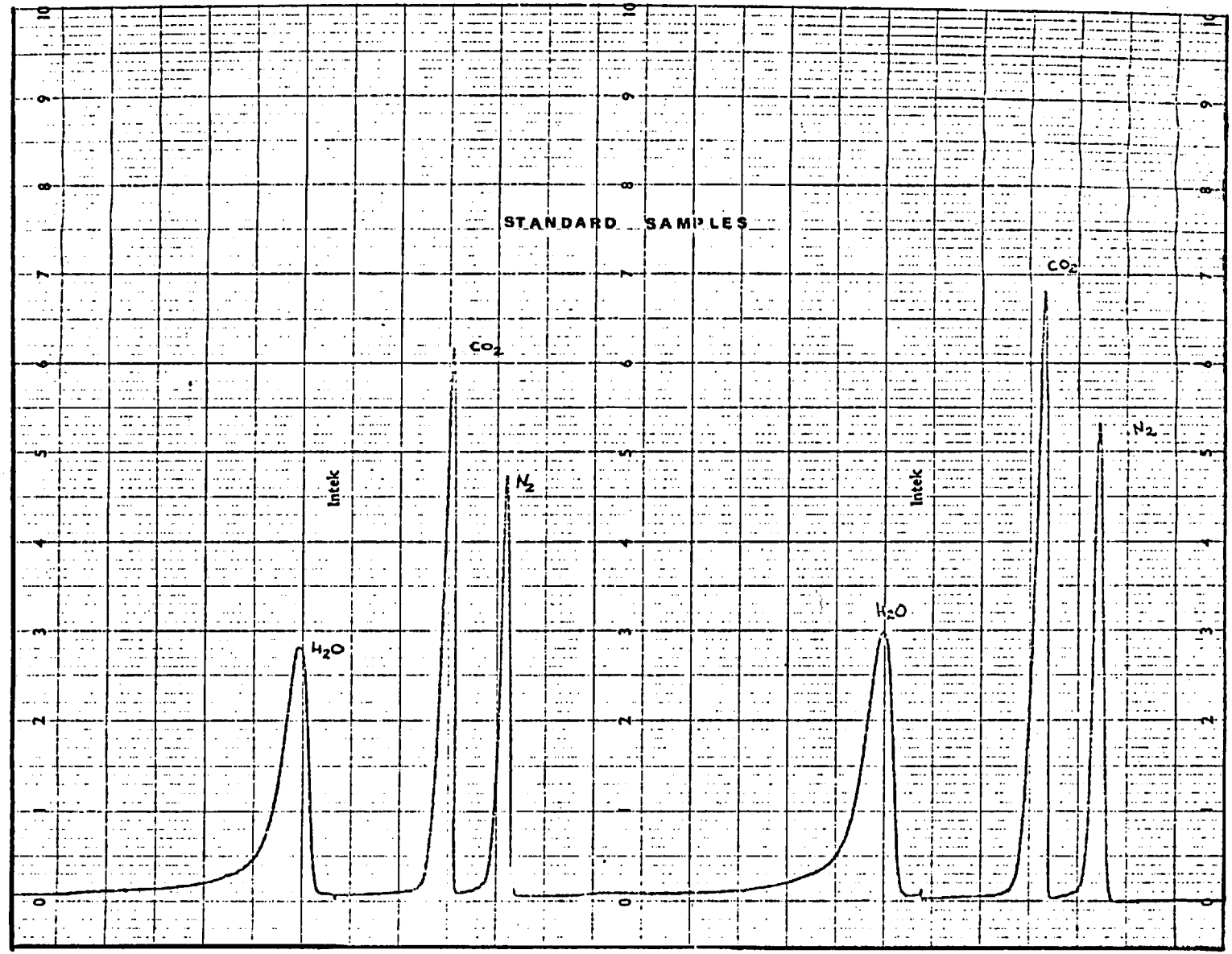

FIG A.2 CARBON, HYDROGEN AND NITROGEN DETERMINATION FOR TWO STANDARD SAMPLES

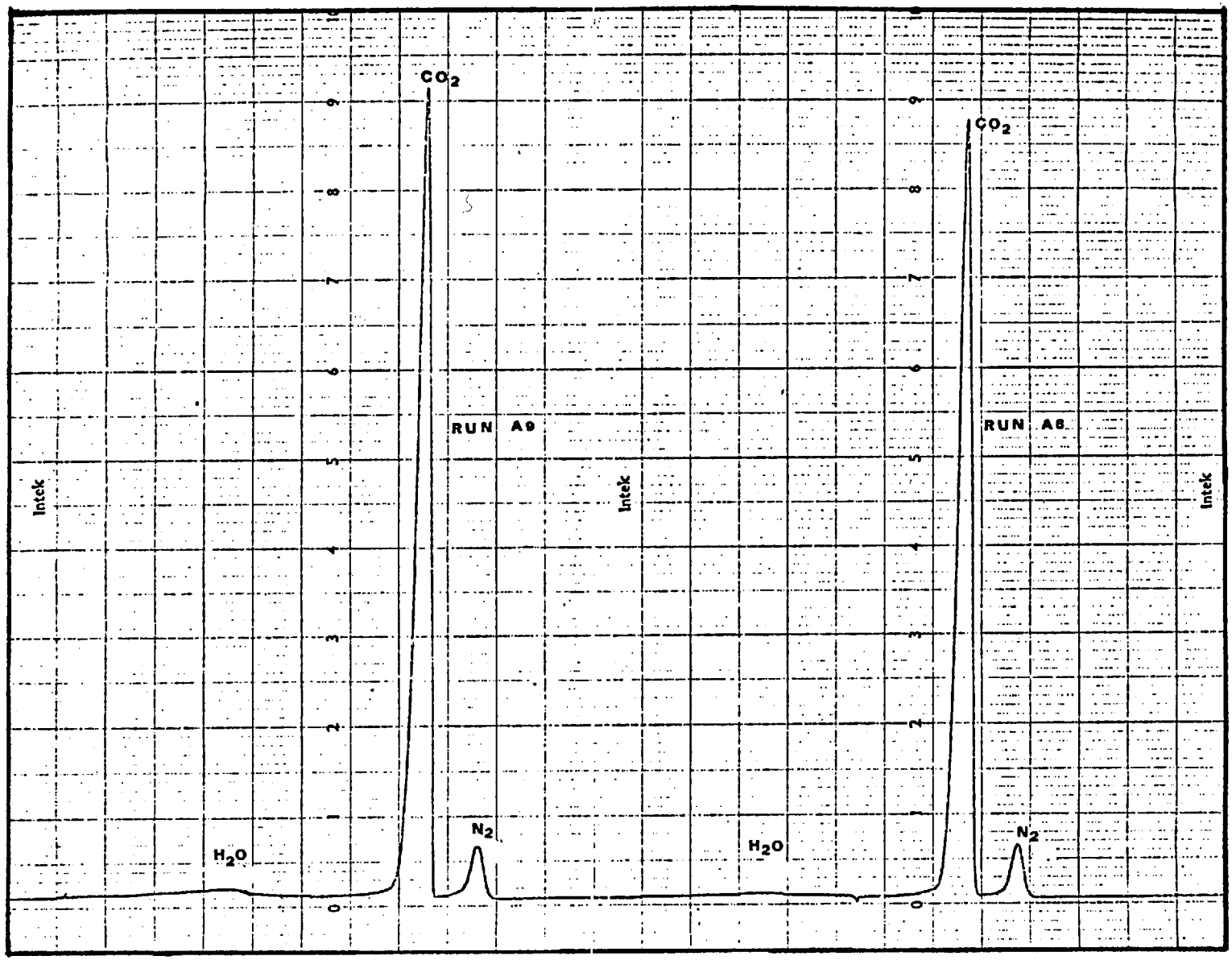

FIG. A.3 CARBON AND HYDROGEN DETERMINATION OF TWO TYPICAL SAMPLES

APPENDIX 8.6

GIBBS FREE ENERGY FOR RELEVANT COMPOUNDS

TABLE A-13 GIBBS FREE ENERGY OF COMPOUNDS THAT OCCUR IN SOLID PRODUCT OF COMBUSTION OF RESIDUAL FUEL OIL (76).

SPECIES		GIBBS FREE ENERGY G°, (Kcal/g-mol)*				
		1100°K	1300°K	1500°K	1700°K	1900°K
V	(gas)	+ 68.3	+ 58.0	+ 47.4	+ 36.7	+ 25.9
VO	(gas)	- 32.0	- 45.3	- 58.8	- 72.6	- 86.6
VO_2	(gas)	-126.7	-142.9	-157.5	-173.4	-189.6
O_2	(gas)	- 58.6	- 70.6	- 82.8	- 95.2	-107.9
V_2O_3	(cond)	-338.2	-351.3	-365.5	-380.6	-396.7
V_2O_4	(cond)	-394.8	-410.7	-427.8	-446.0	-466.4
V_2O_5	(cond)	-432.9	-453.6	-475.6	-498.9	-523.5
Na_2SiO_3	(cond)	-413.7	-429.0	-446.8	-466.2	-486.5
SiO_2	(cond)	-230.1	-236.3	-243.0	-250.0	-257.7
NaOH	(gas)	-119.0	-133.3	-148.0	-163.0	-178.2
$NaVO_3$	(cond)	-323.4	-339.0	-356.3	-375.5	-396.6
Na_2SO_4	(gas)	-374.0	-395.3	-418.1	-442.4	-467.7
Na_2SO_4	(cond)	-399.1	-419.1	-440.8	-463.8	-487.9
NaCl	(gas)	-109.3	-122.8	-136.5	-150.5	-164.7
$NaAlO_2$	(cond)	-305.0	-314.6	-325.0	-336.1	-347.7
Al_2O_3	(cond)	-428.0	-437.7	-448.4	-459.9	-472.1
H_2O	(gas)	-112.8	-124.3	-136.1	-148.2	-160.6
SO_2	(gas)	-143.1	-158.2	-173.7	-189.6	-205.8
Cl_2	(gas)	- 64.0	- 77.1	- 90.5	-104.1	-117.9
HCl	(gas)	- 75.7	- 86.6	- 97.8	-109.2	-120.7
MgO	(cond)	-157.4	-161.6	-166.3	-171.3	-176.6
CaO	(cond)	-169.6	-174.7	-180.3	-186.2	-192.5
MgV_2O_6	(cond)	-599.1	-627.3	-658.9	-693.8	-732.1
CaV_2O_6	(cond)	-634.6	-662.8	-693.1	-725.6	-760.1
$MgSiO_3$	(cond)	-390.8	-401.0	-412.3	-424.3	-437.0
$CaAl_2O_4$	(cond)	-606.8	-622.5	-639.5	-657.8	-677.0

(*) to convert to S.I. units (KJ/g-mol) multiply by 4.1868

(gas) indicated gaseous phase

(cond) indicates solid, liquid, or both, depending on the melting point of the compound.

TABLE A-14. STANDARD GIBBS FREE ENERGY CHANGES, ΔG_T^o OF VARIOUS REACTIONS INVOLVING FUEL OIL IMPURITIES (56)

REACTION	ΔG_T^o = A + BT (Kcal/gmol)*	
	A	$Bx10^2$
$VO(gas) + \frac{1}{2}O_2 = VO_2(gas)$	- 87.95	2.05
$2VO_2(gas) = V_2O_3(cond) + \frac{1}{2}O_2$	-172.68	5.33
$2VO_2(gas) = V_2O_4(cond)$	-218.73	7.03
$VO(g\ s) = VO(cond)$	-130.36	3.76
$NaCl(gas) + H_2O = NaOH(gas) + HCl$	28.78	-0.13
$2NaOH(gas) + V_2O_5(cond) = 2NaVO_3(cond) + H_2O$	-107.45	1.95
$2NaCl(gas) + V_2O_5(cond) + H_2O = 2NaVO_3(con\ ) + 2HCl$	- 48.50	1.60
$2NaOH(gas) + SO_2 + \frac{1}{2}O_2 = Na_2SO_4(gas) + H_2O$	-164.84	8.04
$2NaCl(gas) + SO_2 + H_2O + \frac{1}{2}O_2 = Na_2SO_4(gas) + HCl$	-107.29	7.79
$2NaVO_3(cond) + SO_2 + \frac{1}{2}O_2 = Na_2SO_4(cond) + V_2O_5(cond)$	- 88.04	6.68
$2HCl + \frac{1}{2}O_2 = H_2O + Cl_2$	-13.98	1.63
$2Ni(gas) + O_2 = 2NiO(cond)$	-309.83	10.58
$2Fe(gas) + O_2 = 2FeO(cond)$	-297.08	8.93
$2V(gas) + O_2 = 2VO(cond)$	-437.04	10.64

Temperature range of the equation is 1100 - 1900°K

(continued over)

TABLE A-14.

(gas) refers to gaseous phase.

(cond) refers to solid, liquid or both depending on the melting point of the compound.

(*) to convert to S.I. Units ($KJ/_{g.mol}$) multiply by 4.1868.

TABLE A-15. STANDARD GIBBS FREE ENERGY CHANGES ΔG_T° OF VARIOUS REACTIONS INVOLVING RELEVANT INORGANIC COMPOUNDS (58)

REACTION	$\Delta G_T^\circ = A + BT$ (KJ/g.mol)	
	A	B x 10^2
$2FeS_2(s) = 2FeS(s) + S_2(g)$	+310.24	-29.25
$2FeS(s) = 2Fe(s) + S_2(g)$	+301.04	-10.17
$S_2(g) + 2O_2 = 2SO_2(g)$	-724.88	+ 14.60
$2Fe(s) + O_2 = 2FeO(s)$	-525.72	+13.35
$2NaCl(l) + SiO_2(s) + H_2O(g) = 2HCl(g) + Na_2SiO_3(l)$	+215.06	-8.87
$NaCl(g) + H_2O(g) = NaOH(g) + HCl(g)$	+96.44	+1.05
$2NaCl(g) + H_2O(g) + SO_2 + \frac{1}{2}O_2 = Na_2SO_4(g) + 2HCl(g)$	-409.82	+30.25
$2NaOH(g) + SO_2 + \frac{1}{2}O_2 = Na_2SO_4(g) + H_2O(g)$	-582.62	+26.82

(s), (l), and (g) refer to the solid, liquid and gaseous phases respectively.
Temperature range of the equation is: 500 - 1500°K

APPENDIX 8.7

PHYSICAL PROPERTIES OF RELEVANT COMPOUNDS

TABLE A-16. PHYSICAL PROPERTIES OF COMPOUNDS THAT OCCUR IN SOLID PRODUCTS OF COMBUSTION OF RESIDUAL FUEL OIL (64)

COMPOUND	MELTING POINT (^{o}C)	MOLECULAR WEIGHT	SOLUBILITY IN GRAMS PER 100 cm^3	
			COLD WATER	HOT WATER
V_2O_5	690	181.8	0.8^{20}	-
V_2O_4	1967	165.9	i	i
V_2O_3	1970	149.88	sl.s	s
VO_2	1967	82.94	i	i
VO	ign	66.94	i	i
$Na_2O.V_2O_4.5V_2O_5$	624	1187.4	0.002^{20}	0.015^{70}
$NaVO_3$	630	121.95	21.1	38.8
Na_3VO_4	850	183.9	s	s
Na_2SO_4	884	142.4	s	42^{100}
NiO	1990	74.71	i	i
NiS	797	90.77	0.00036^{18}	-
$NiSO_4$	d848	154.78	29.3^{o}	83.7^{100}
Na_2O	subl 1275	61.98	d	d

Abbreviations used:

i	:	insoluble
s	:	suluble
sl	:	slightly
ign	:	ignites
d	:	decomposes
subl	:	sublimes

REFERENCES

1. HTUN, M.N. Residual fuel oil combustion : The effect of air/fuel ratio on combustion products formed. Ph.D. Thesis, University of London, 1968
2. ARCHER, J.S. An experimental investigation of spray combustion in a two stage system. Ph.D. Thesis, University of London, 1969.
3. GROUT, P.D. Combustion of residual fuel-oil : modelling and optimisation of a two stage system. Ph.D. Thesis, University of London, 1970
4. NELSON, W.L. Questions on technology. Oil and Gas Journal 64, 127. 1966.
5. SKINNER, D.A. Chemical state of vanadium in Santa Maria Valley crude oil. Ind. Eng. Chem. 44, 1159, 1952.
6. DUNNING, H.N., MOORE, J.W. AND MYERS, A.T. Properties of porphyrins in Petroleum. Ind. Eng. Chem. 46, 2000, 1954.
7. BEACH, L.K. AND SHEWMAKER, J.E. The nature of vanadium in petroleum. Ind. Eng. Chem. 49, 1157, 1957.
8. WOLSKI, A.D. AND CHAPMAN, F.W. A study of an intrinsic contaminant in petroleum, the nature of vanadium in asphaltenes. Proc. American Petroleum Inst. 40, 423, 1960
9. REYES, A., HUEBLER, J. AND MATTHEWS, C.W. paper presented at the International Symposium of Metals in petroleum. Maracaibo, Venezuela, August, 1973.
10. PHILMAC OILS LIMITED, North Road, Ellesmere Road, Wirral, Cheshire L65 1AJ. Personal Communications.
11. MCMULLEN, J.J. et al. Boiler problems associated with the use of Bunker C fuel. Combustion 31, 42, 1960.
12. GINNEKEN, A.J.J. et al. Shell process desulfurized resid. Oil and Gas Journal 73, 59, 1975.

13. JOHNSON, G.M. et al. Distribution of sulphur species in the burnt gas of fuel rich propane-air flames. Combustion and Flame 15, 211, 1970

14. BODENSTEIN AND POHL. Gleichgewichtsmessungen an der Kontanktschwefelsaure. Z. Electrochem. 11, 373, 1905.

15. LOWRISON, G.C. and HEPPENSTALL, F. Conversion stage in the manufacture of sulphuric acid by contact process. Brit.Chem. Engng. 3, 252, 1958.

16. LADNER, W.R. AND PANKHURST, K.S. Paper 10. The formation of sulphur trioxide. Proc. of Int. Conference. The mechanism of corrosion by fuel impurities. London, Butterworths, 1963.

17. HEDLEY A.B. Factors affecting the formation of sulphur trioxide in flame gases. J. Inst. of Fuel 40, 142, 1967.

18. HEDLEY A.B. Paper 11. A kinetic study of SO_3 formation in a pilot scale funace. Proc. of Int. conference. The Mechanism of Corrosion by Fuel Impurities, London, Butterworths, 1963.

19. BARRET, R.E., HUMMEL, J,D, AND REID, W.T. Formation of SO_3 in a noncatalytic combustor. Trans. A.S.M.E. J. Engng for Power 88A, 165, 1966

20. CULLIS, C.F. AND MULCAHY, M.F.R. The kinetics of combustion of gaseous sulphur compounds. Combustion and Flame. 18, 225, 1972

21. The Mechanism of Corrosion by Fuel Impurities. proc. of Int. conference. London, Butterworths, 1963

22. HANCOCK, P. Corrosion of alloys at high temperatures in atmosphere consisting of fuel combusiton products and associated impurities. H.M.S.O., London 1968.

23. HART, A.B. AND CUTLER, A.J.B. Editors, deposition and corrosion in gas turbines. proc. of Int. conference. Applied Science Publishers, London 1973.

24. BANCHERO, J.T. AND VERHOFF, F.H. Evaluation and interpretation of vapour pressure data for sulphuric acid aqueous solutions with application to flue gas dew points. J. Inst. of Fuel 48, 76, 1975.

25. BARRET, R.E. High temperature corrosion studies in an oil-fired laboratory combustor Trans . A.S.M.E., J. Engng for Power 89A, 288, 1967.

26. SHAW, J.T. AND GREEN P.D. Oxidation of sulphur dioxide in air at 950°C. Co-operative influence of carbon monoxide and nitric oxide. Nature 211, 1171, 1966.

27. GLAUBITZ. The economic combustion of sulphur-containing heating oil. Combustion 34, 25, 1963.

28. LAXTON, J.W. Paper 13. The influen e of excess oxygen and metallic additives on the formation and deposition of sulphur oxides in the flue gas. Proc. of Int. Conference. The Mechanism of Corrosion by Fuel Impurities. London, Butterworths, 1963.

29. SHAW, J.T. Progress review No. 64: A commentary on the formation, incidence, measurement and control of nitrogen oxides in flue gas. J. Inst. of Fuel 46, 170, 1973.

30. DESOETE, G.G. Overall kinetics of nitric oxide formation in flames. La Rivista dei Combustibili 29, 35, 2975.

31. ZELDOVICH, J. J. Acta Physicochimica URSS 21, 577, 1946.

32. KAUFMAN, J.R. Thermal decomposition of nitric oxide. J. Chem Phys. 23, 1702, 1955.

33. BARTOK, W. et al. Control of NO_x emissions from stationary sources. Chem. Eng. Progress 67, 64, 1971.

34. FENIMORE, C.P. 13th Symp. on Combustion. The Combustion Inst. Pittsburgh, 1971.

35. ARCHER, J.S. On line analysis of wet combustion gases by gas chromatography. J. Inst. of Fuel 43, 56, 1970.

36. FLINT, D. A method for the determination of small concentrations of SO_2. J. of Soc. Chem Ind. 67, 2, 1948.

37. CORBETT, P.F. A phototurbidimetric method for estimation of SO_3 in the presence of SO_2. J. of Soc. Chem. Ind. 67, 227, 1948.

38. CORBETT, P.F. The determinsation of SO_2 and SO_3 in flue gases J. Inst. of Fuel 24, 247, 1951.

39. FIELDER, B.A., JACKSON P.J., RAASK, E. The determination of SO_3 and SO_2 in flue gases. J. Inst. of Fuel 33, 84, 1960.

40. SEIDMAN, E. Determination of sulphur oxides in stack gases. Anal. Chem. 30, 1680, 1958.

41. BERTOLECINI, R. BARNEY, J. Colorimetric determination of sulfate with barium chloranilate. Anal Chem. 29, 281, 1957.

42. GOKSØYR, H., ROSS, K. The determination of sulphur trioxide in flue gases. J. Inst of Fuel. 35, 177, 1962.

43. LEIBRAND, R.J. Atlas of gas analyses by gas chromatography. J. of Gas Chromatography 5, 518, 1967.

44. APPLEBURY, T.E. AND SCHAER, M.J. Analysis of Kraft pulp mill gases by process gas chromatography. J. of Air Pollution Control Ass. 20, 83, 1970.

45. BIRK, J.R. et al. Gas chromatographic determination of sulfide, sulfite, and carbonate in solidified salts. Anal. Chem 42 (2), 273, 1970.

46. OBERMILLER, E.L. AND CHARLIER, G.O. Gas chromatographic separation of bitrogen, oxygen, argon, carbon monoxide, carbon dioxide, hydrogen sulfide and dulfur dioxide. J. of Gas Chromatography 6, 446, 1968.

47. OBERMILLER E.L., AND CHARLIER, G.O. Gas chromatographic separation of nitrogen, oxygen, argon, carbon monoxide, carbon dioxide, hydrogen sulfide and sulfur dioxide. J. of Gas Chromatography 7, 580, 1969.

48. CASTELLO, G. AND MUNARI, S. Analisi di inquinanti atmosferici gassosi per via gascromatografica. La Chimica e L'Industria (Milan) 51, 469, 1969.

49. FONTIJN, A., SABADELL, A.J. AND RONCO, R.J. Homogeneous chemiluminescent measurement of nitric oxide with ozone. Anal. Chem. 42, 575, 1970.

50. ALLEN, J.D. A review of methods of analysis for oxides of nitrogen. J. Inst. of Fuel 46, 123, 1973.

51. ALLEN, J.D., BILLINGSLEY, J. AND SHAW J.T. Evaluation of the measurements of oxides of nitrogen in combustion products by the chemiluminescence method. J. Inst. of Fuel 47, 275, 1974.

52. GILLS, B.C. Production and emission of solids, SO_x and NO_x from liquid fuel flames. Paper presented at first Nat. Conv. of the Inst. of Fuel on combustion and environment. June 1972.

53. ARCHER, J.S. and EISENKLAM, P. Multistage combustion of residual fuel oil, Part I. J. Inst. of Fuel 43, 397, 1970

54. ARCHER, J.S., GROUT, P.D. AND EISENKLAM P. Multistage combustion of residual fuel oil, part II. J. Inst. of Fuel. 43, 451, 1970

55. HALSTEAD, W.D. Progress review No. 60. Some chemical aspects of fire side corrosion in oil fired boilders. J. Inst. of Fuel 43, 234, 1970.

56. HALSTEAD, W.D. Thermodynamics of fuel oil ash constituents in combustion systems. J. Inst. of Fuel 42, 419, 1969.

57. GRIMLEY, R.T. et al. Thermodynamics of the vaporization of nickel oxide. J. Chem. Phys. 35, 551, 1961.

58. HALSTEAD W.D. AND RAASK, E. The behaviour of sulphur and chlorine compounds in pulverized-coal-fired boilers. J. Inst. of Fuel 42, 344, 1969.

59. MACFARLANE, J.J. The relationship between combustion conditions and the corrosion of metal surfaces by fuel oil ash deposits. Paper 16. Int Conference, proc. The Mechanism of Corrosion by Fuel Impurities, Lon on, Butterworths, 1963.

60. FOSTER, W.R. The oil ash corrosion problem. Research (Applied in industry) 12, 189, 1959.

61. COATS, A.W. The chemistry of deposits in oil fired boilers: the $Na_2SO_4 - V_2O_5 - SO_3$ system. J. Inst. of Fuel, 42, 75, 1969.

62. DE SANTIS, R. Some aspects of the problem: "Fireside corrosion in oil fired boilers". La Rivista dei combustibili, Milan 27, fas (4-5), 1973.

64. HANDBOOK OF CHEMISTRY AND PHYSICS. The chemical rubber Co. 1972-73.

65. PALMER, H.B. AND BEER, J.M. Conbustion Technology : some modern developments. Academic Press, London 1974.

66. JOHNS, W.R. Residual fuel-oil combustion: the effect of air/fuel ratio on the temperature of combustion. Ph.D. Thesis, University of London, 1965.

67. ADMUNDSON, N.R. Mathematical Methods in Chemical Engineering. Prentice hall Inc. Englewood Cliffs. N.J. 1966

68. BALZHISER, R.E., SAMUELS, M, RAND ELIASSEN, J.D. Chemical Engineering thermodynamics. Chapters 11 and 12. Englewood cliffs, N.J. 1972.

69. JANAF THERMOCHEMICAL TABLES. Second Edition June 1971. National Standard Reference Data System. Washington.

70. GROUT, P.D. AND EISENKLAM, P. The modelling of two stage combustion reactors. I. Chem. Eng. Symposium Series No. 43 (June 1975)

71. MUNZ, NATHAN Personal Communications. Imperial College,

72. KISER, R.W. Introduction to mass spectrometry and its applications. Englewood cliffs, N.J. Prentice hall, 1965.

73. LINFORD, A. Flow measurements and meters SPON London 1961.

74. OWER AND PANKHURST. The measurement of air flow Pergamon Press, 1966

75. A.S.T.M. X-ray POWDER DIFFRACTION FILE 1973. Publisher : Joint Committee on powder diffraction Standards. Pennsylvania, U.S.A.

76. HALSTEAD, W.D. The chemical behaviour of fuel oil impurities in combustion systems. Central Electricity Generating Board. C.E.R.L. Report No. RD/L/N84/67 1967.

77. EDWARDS, J.A. Fire-side Deposits and Corrosion Associated with Boiler and Superheater Tubes. Literature Survey. B.P. Research Centre, Sunbury. 1964.

78. SHAW, H. and MAGEE, E.M. Evaluation of pollution control in fossil fuel conversion processes. U.S. Environmental Protection Agency EPA-650/2-74-009-c Washington July 1974

79. BEER, J.M. Combustion Aerodynamics. Applied Science Publishers London 1972.

80. LEWIS, B., PEASE, R.N., TAYLOR, H.S. Combustion Processes. Oxford University Press 1956.